DISSERTATION

RADIOLOGICAL CHARACTERIZATION OF RADIOACTIVE WASTE AT CERN

ausgeführt zum Zwecke der Erlangung des akademischen Grades eines Doktors der Technischen Wissenschaften unter der Leitung von

Ao.Univ.Prof. Dipl.-Ing. Dr.techn. Helmuth Böck

E141

Atominstitut der Österreichischen Universitäten

eingerichtet an der Technischen Universität Wien

Fakultät für Physik

von

Matteo Magistris

Matr. Nr.: 0627366

CERN, CH-1211 Geneva 23, Switzerland

Wien, 19. March 2008

Diese Dissertation haben begutachtet:
Prof. Dr. H. Böck Prof. Dr. N. Vana

Zusammenfassung

Die Europäische Organisation für Teilchenphysik (CERN) betreibt seit 50 Jahren zahlreiche Teilchenbeschleuniger für Forschung im Bereich der Hochenergiephysik. Der Betrieb dieser Beschleuniger führt zur Produktion radioaktiver Abfälle. Für die Entsorgung dieser Abfälle ist die Erfassung des Nuklidvektors - einer Liste aller Nuklide und deren spezifische Aktivität - erforderlich.

Zur Zeit gibt es keine einzelne Methode zur Bestimmung des Nuklidvektors von allen radioaktiven Abfällen aus beliebigen Beschleunigern. Die Entwicklung einer Methode zur radiologischen Charakterisierung von Beschleunigerkomponenten des CERN - des grössten Elementarteilchenphysiklabors Europas - ist das herausforderndes Ziel der vorliegenden Arbeit.

Der Nuklidvektor von CERN Abfällen hängt von verschiedenen Faktoren ab, die in dieser Dissertation erläutert werden. Diese Faktoren umfassen die französischen und schweizer Gesetze hinsichtlich der Entsorgung radioaktiver Abfälle, die charakteristischen Merkmale von jedem CERN-Beschleuniger, die nuklidspezifischen Aktivitätsverteilungen innerhalb eines Gebindes, die durchgeführten Experimente und die Erfahrung von anderen Forschungszentren.

Fünf verschiedene Methoden werden hier vorgestellt, die die Eigenschaften der verschiedenen Kategorien von CERNs radioaktiven Abfällen berücksichtigen. Zu diesen Methoden gehören stationäre automatische Messanlagen und Monte Carlo Simulationen der erzeugten Radioaktivität. Wenn die chemische Zusammensetzung der Materialien und ihre radiologische Historie bekannt sind, kann die Aktivität durch die *Matrix Methode* berechnet werden. Gemischte Abfälle und Gebinde mit unbekannter radiologischer Historie können mit der *statistischen Methode* charakterisiert werden, die auf Wahrscheinlichkeitsverteilungen und Fehlerfortpfianzung beruht. Die *Fingerprint Methode* schätzt den Nuklidvektor durch eine Kombination von Berechnung und Probennahme ab. Durch die erfolgreiche Anwendung der *Fingerprint Methode* wurde der Nuklidvektor der CERN ISOLDE-Targets bestimmt.

Die beschriebenen Methoden besitzen generelle Gültigkeit und können auf die radiologische Charakterisierung von Komponenten jedes beliebigen Beschleunigers angewendet werden.

Abstract

The European Laboratory for Particle Physics (CERN) has been operating a number of particle accelerators for fundamental and applied research for more than 50 years. The operation of these accelerators has lead to the unavoidable production of radioactive waste. The elimination of an item of radioactive waste towards final repositories requires the radionuclide inventory, i.e. a list of nuclides with their specific activity.

At present there is no single method for the radiological characterization which can be applied to all items of waste from any particle accelerator. The development of a characterization method to meet the needs of CERN - the largest accelerator's complex in Europe - is the challenging task of this thesis.

The characterization of CERN waste is based on a number of factors, which are covered in the present study. These aspects include the legal requirements for Swiss and French radioactive waste, the characteristics of each CERN accelerator, the nuclear models describing the activation process, the detectors available on the market, activation experiments and the experience from other Research Institutes.

Five different methods are proposed to address the specificities of the different categories of CERN waste. These methods range from an automated system for gamma-spectroscopy measurements to Monte Carlo predictions of induced radioactivity. If the material composition and radiological history are known, the activity can be calculated analytically with the Matrix method. Mixed waste and items with unknown radiological history can be characterized with the Statistical method, which is based on probability distributions and error propagation. The Fingerprint method combines Monte Carlo predictions with gamma-spectroscopy. This method has been successfully applied to the characterization of the targets irradiated in the ISOLDE experiment.

The methods described in this thesis are of general validity and can be applied to any particle accelerator.

Contents

1 Introduction **2**
- 1.1 Material activation in particle accelerators . . . 2
- 1.2 The French legislation . . . 3
  - 1.2.1 Radioactive waste zoning . . . 4
  - 1.2.2 Removal of controls for radioactive waste . . . 4
  - 1.2.3 Overview of legal documents . . . 5
  - 1.2.4 Overview of relevant institutions . . . 6
- 1.3 The Swiss legislation . . . 6
  - 1.3.1 Switzerland: Free release . . . 6
  - 1.3.2 Overview of legal documents . . . 7
  - 1.3.3 Overview of relevant institutions . . . 8
- 1.4 Elimination pathways and final repositories . . . 9
  - 1.4.1 Switzerland: interim storage at ZWILAG . . . 9
  - 1.4.2 France: final repositories . . . 10
  - 1.4.3 Reuse of radioactive material . . . 10
  - 1.4.4 Treatment of metal waste by melting . . . 11
  - 1.4.5 Nuclear transmutation . . . 11
- 1.5 Motivation for a radionuclide inventory . . . 12

2 The production of radioactive waste at CERN **13**
- 2.1 Machines at CERN . . . 13
  - 2.1.1 Linac 2 . . . 14
  - 2.1.2 Linac 3 . . . 14
  - 2.1.3 PS Booster (PSB) . . . 15
  - 2.1.4 PS . . . 15
  - 2.1.5 n_TOF, the neutron facility . . . 15
  - 2.1.6 AD, the antiproton decelerator . . . 15
  - 2.1.7 LEAR and LEIR . . . 16
  - 2.1.8 SPS . . . 16
  - 2.1.9 LEP . . . 16
  - 2.1.10 CNGS . . . 16
  - 2.1.11 LHC . . . 17
  - 2.1.12 Areas of validity of the Swiss and French legislations . . . 17
- 2.2 Beam losses . . . 17

2.2.1 Beam dynamics: emittance and acceptance 17
2.2.2 Mechanism and impact 19
2.3 Particle spectra 20
2.3.1 Hadron and electromagnetic spectra 20
2.3.2 Ratio between hadron fluxes 20
2.3.3 Angular distribution of secondary particles 21
2.4 Radioactive waste from CERN accelerators 21
2.4.1 Radioactive waste presently stored at CERN 21
2.4.2 Future production of waste 22
2.5 Management of radioactive waste 23
2.5.1 Sorting and pre-conditioning 23
2.5.2 The radioactive waste project 23

3 State of the art of radiological characterization 25
3.1 Detectors for gross monitoring and free-release available on the market 25
3.1.1 Monitoring system for characterization of waste with low activity 25
3.1.2 Clearance measuring system with scintillating chambers . . 26
3.1.3 Clearance measuring system with gamma spectroscopy . . 27
3.1.4 In situ gamma spectroscopy 27
3.2 Present status of the characterization at CERN 28
3.2.1 Laboratory Ge detectors 29
3.2.2 In Situ Gamma spectroscopy: ISOCS 29
3.2.3 A software for data processing: Genie2000 29
3.2.4 NaI scintillator: MICROSPEC-2 30
3.2.5 FLUKA simulations 30
3.2.6 MicroShield 31
3.2.7 Empiric formulae 31
3.3 The characterization at Paul Scherrer Institute 31
3.3.1 Accelerator complex and characterization strategy 32
3.3.2 The PWWMBS code system 32
3.3.3 Cross-sections 33
3.3.4 Representative spectra 33
3.3.5 Representative materials 33
3.3.6 Validation 34
3.3.7 Application of the PSI method to CERN waste 34
3.4 The radiological characterization at ISPRA 35
3.4.1 Radioactive waste characterization system 36
3.4.2 Conditioning facilities 37

4 Nuclear interactions: physics, data and computational tools 38
4.1 Nuclear Interactions 38
4.1.1 The Intranuclear Cascade Model 39

4.1.2 Glauber cascade and formation zone . . . 39
4.1.3 Pre-equilibrium . . . 40
4.1.4 Evaporation . . . 40
4.1.5 Photonuclear reactions . . . 42
4.1.6 Nuclear interactions of ions . . . 42
4.2 Libraries with evaluated cross-sections . . . 44
4.2.1 The ENDF format . . . 44
4.3 Codes for the calculation of cross-sections . . . 46
4.3.1 TALYS . . . 47
4.3.2 Silberberg . . . 47
4.3.3 MCNPX . . . 48
4.3.4 FLUKA . . . 50
4.3.5 Conclusions on the codes . . . 51
4.4 Reaction channels of interest . . . 51

5 The fingerprints method **54**
5.1 Hypotheses . . . 54
5.1.1 Known irradiation geometry . . . 55
5.1.2 Known material composition . . . 55
5.1.3 Known weight fraction of subcomponents . . . 55
5.2 The mathematical model . . . 55
5.2.1 Definition of classes . . . 56
5.2.2 Calculation of the fingerprints . . . 57
5.2.3 Choice of the representative samples . . . 57
5.2.4 Normalization of the fingerprints to the sample activity . . . 57
5.3 Application of the fingerprint method . . . 59
5.3.1 The ISOLDE targets . . . 59
5.3.2 Elimination campaign . . . 60
5.3.3 FLUKA simulations and definition of classes . . . 60
5.3.4 Calculation of the fingerprints . . . 63
5.3.5 Induced radioactivity in the Al components . . . 63
5.3.6 Induced radioactivity in categories "Other Metals" and "Ceramics" . . . 64
5.3.7 Induced radioactivity in the target core and container . . . 67
5.3.8 Induced radioactivity in the source . . . 68
5.3.9 Corrections for the presence of extraneous bodies . . . 69
5.3.10 Off-line calculation of the radionuclide inventory . . . 69
5.4 Validation . . . 70
5.4.1 Direct prediction: activity in the target container . . . 70
5.4.2 Scaled prediction: Activity in the Al, Cu and other metals 71
5.5 Conclusions on the fingerprint method . . . 73

6 The matrix method **75**
6.1 Hypotheses . . . 75
6.1.1 Uniform irradiation profile . . . 75
6.1.2 Known irradiation cycle . . . 76
6.1.3 Uniform particle spectrum . . . 76
6.1.4 Known particle spectrum . . . 76
6.1.5 Uniform material composition . . . 77
6.1.6 Known material composition . . . 77
6.1.7 Absence of heavy (Z>82) elements . . . 77
6.1.8 No contamination . . . 77
6.1.9 Representative dose rate measurement . . . 77
6.2 Activation formula and additive rule . . . 78
6.3 Definition of activation matrix . . . 79
6.4 Normalization with dose rate measurement . . . 80
6.5 Requirements for the implementation of the matrix method . . . 80
6.6 Fields of application . . . 81
6.6.1 Waste from large areas with uniform spectrum . . . 82
6.6.2 Small-size waste . . . 82
6.6.3 Components with well known radiological history . . . 82
6.6.4 Future machines . . . 82
6.7 Corrections and extensions . . . 82
6.7.1 Extension to waste with non-uniform radiation intensity . 83
6.7.2 Extension to waste with non-uniform material composition 83
6.7.3 Completion with contamination assessment . . . 83
6.7.4 Correction for volatile nuclides . . . 83
6.8 Disadvantages . . . 84

7 Dependence of induced radioactivity on the irradiation cycle **85**
7.1 The activation formula . . . 86
7.2 Definition of time variables . . . 86
7.3 Information available on the radiological history . . . 87
7.3.1 Scenario a: t_{in} is known, t_{out} is unknown . . . 88
7.3.2 Scenario b: t_{out} is known, t_{in} is unknown . . . 88
7.3.3 Scenario C: $t_{irr} = \mu$ is known, t_{in} and t_{start} are unknown . 89
7.4 Calculation of the uncertainty of the time build-up . . . 89
7.5 Categories of nuclides . . . 90
7.5.1 Time build-up for nuclides with $T_{1/2} < 1$ year . . . 90
7.5.2 Time build-up for nuclides with 1 year $< T_{1/2} <$ 30 years . 91
7.5.3 Time build-up for nuclides with 30 years $< T_{1/2} <$ 100 years 92
7.5.4 Time build-up for nuclides with $T_{1/2} > 100$ years . . . 93
7.6 Correction for non-uniform irradiation cycles . . . 94
7.7 Conclusions . . . 96

8 Further methods for the radiological characterization **97**
8.1 The direct FLUKA calculation 97
8.1.1 Relevant settings 97
8.1.2 Off-line treatment of time build-up 98
8.1.3 On-line treatment of time build-up 99
8.1.4 General considerations on the FLUKA method 99
8.2 Gamma spectroscopy measurements 100
8.3 The statistical method 101
8.3.1 Bayes 101
8.3.2 Probability distributions 102
8.3.3 Uncertainty propagation 105
8.3.4 Detection limit and decision threshold 105
8.3.5 Considerations on the statistical method 106

9 Conclusions **108**
9.1 A challenging task 108
9.2 Methods for radiological characterization 109
9.2.1 The matrix method 110
9.2.2 The fingerprint method 110
9.3 Project planning 111
9.4 Final considerations 115

A Comparison between two scintillators for gamma ray spectroscopy **118**

Bibliography **120**

Acknowledgements **129**

List of Figures

2.1 Schematic layout of the CERN accelerator's complex 14
2.2 Phase space ellipse, $\beta < 1$ and $\alpha > 0$. 18
2.3 Phase space ellipse, $\beta > 1$ and $\alpha < 0$. 18
2.4 Photograph of the treatment centre at CERN, building 573 24

3.1 Photograph of a Monitoring System for Characterization of Radioactive Waste DMS, Beznau NPP (Switzerland) 26
3.2 Photograph of the clearance measuring system RADOS RTM644Inc, PSI, Villigen (CH) 27
3.3 Photograph of the release measurement system (NUKEM) for packed waste at the research centre Ispra. 28
3.4 Schematic layout of the PSI accelerator complex. 34

5.1 Photograph of the inner parts of an ISOLDE target unit. The vacuum vessel was removed to show the target core and the direction of the incoming beam (black arrow). 60

6.1 Example of constant irradiation profile. 76
6.2 Example of irregular irradiation profile. 76

7.1 Line of time with start and end of the machine operation (squares), introduction and removal of the object (triangles) and present (circle). 87
7.2 Line of time with start and end of the machine operation (squares), and integrating variable x (circle). 94

8.1 Probability distribution of the true value η ($\hat{x}$ in the text) given in equation 8.3 for a non-negative measurand y (x in the text). . . . 103
8.2 Triangular probability distribution with a=0, c=0.5 and b=1.0. . 104
8.3 Curvilinear trapezoid, probability distribution with inexact lower and upper limits. 104
8.4 Illustration of the decision threshold y^* and the detection limit η^*. 106

List of Tables

4.1 List of the most frequently identified radionuclides with half-life longer than one year. 53

5.1 Results from FLUKA simulations for Cu, targets 70, 71, 82 and 146. The specific activities are normalized to 1 Bq g^{-1} of ^{60}Co. . . 62
5.2 Specific activity (Na-22) of all the Al elements with respect to the Al samples for a selection of target. Average ratio ϵ_{Al} to be used for the normalization. 64
5.3 Specific activity (Co-60) of all the Cu elements with respect to the Cu samples for a selection of target. Average ratio ϵ_{Cu} to be used for the normalization. 65
5.4 Comparison between the specific activity in "Other Metals" as measured by ISOCS and calculated with the preliminary fingerprint method. 65
5.5 Weight fraction of elements in different sources. The sum over all fractions is 1.0 for every source family. 68
5.6 Specific activity (kBq/g) of the Ta bar in target 183 as measured with gamma spectroscopy (average and maximum values) and estimated with FLUKA. 72
5.7 Specific activity (Bq/g) of "aluminium" of target 146 as measured with gamma spectroscopy (ISOCS) and estimated with FLUKA. The symbol "-" means that the activity is below the detection threshold. 73
5.8 Specific activity (Bq/g) of "Other Metals" of target 47 as measured with gamma spectroscopy (ISOCS) and estimated with FLUKA. The symbol "-" means that the activity is below the detection threshold. 73

A.1 Direct comparison of Inspector1000 and BNC935 119

Chapter 1

Introduction

1.1 Material activation in particle accelerators

Particle accelerators are useful for both fundamental and applied research in the sciences. Among the main uses of primary and secondary beams one could mention [1]:

- research in basic subatomic physics;
- analysis of physical, chemical and biological samples;
- modification of the physical, chemical and biological properties of matter.

The other face of the medal of such useful applications, is that the interaction of particle beams with matter might lead to the activation of the accelerator structure and its surroundings. The induced radioactivity is either due to direct interactions of the primary beam or to secondary particles produced in a multitude of nuclear processes. At the end of their operational lifetime and depending on the irradiation conditions, some of the accelerator components must be treated as radioactive. The production of radioactive waste is therefore an unavoidable aspect of the operation of particle accelerators.

Most of the radioactive material produced in accelerators ranges from pumps to cables and magnets and it is of metallic nature [2]. One of the main differences between waste produced in nuclear power plants and in accelerators is that in accelerator waste there is:

- little probability of producing long-lived alpha activity;
- little probability of producing contamination (except for special targets and activation of dust);
- large spectrum of radioactive nuclides.

The level of induced radioactivity varies considerably depending on the type of acclerator, on the location of the item with respect to beam losses and on the waiting time following activation. Recycling within the nuclear industry is certainly a reasonable elimination pathway for at least a fraction of this material. For the majority of waste items, the activity is indeed very low and there is neither contamination nor alpha emitters [2]. There is nevertheless a fraction of waste which has detectables and - in a limited number of cases - high levels of radioactivity. This waste must be eliminated towards final repositories respecting the laws imposed by the national authorities.

The European Laboratory for Particle Physics (CERN) has been operating a number of accelerators for fundamental and applied research for more than 50 years (cf. chapter 2). The machines, located near Geneva on both French and Swiss territory, are designed to accelerate particles to energies of 33 TeV (lead ions), 7 TeV (protons) and 100 GeV (electrons, positrons).

In operational radiation protection CERN has its own rules based on legislation in the host states Switzerland and France. With respect to radioactive waste, it is the legislation of the host state where the material has been activated which applies. This is layed down in the CERN Safety Code [3]:

> As a general rule, radioactive waste activated on the Swiss part of the CERN site shall be disposed of in Switzerland; radioactive waste activated on the French part of the CERN site shall be disposed of in France. CERN shall not dispose of radioactive waste towards any other country without prior agreement of the receiving country and of the Host State involved.

The French and Swiss legislations have quite different approaches to the treatment of radioactive waste, as described in the sections 1.2 and 1.3.

1.2 The French legislation

The French national system for waste elimination is based on the principle that the so-called "nuclear waste" [1], waste prone to have been contaminated or activated, shall be segregated from "conventional waste" using a system involving successive lines of defence. The goal is to build a very high level of confidence that no "nuclear waste" will be eliminated without control in conventional waste eliminators or recycling facilities.

The first line of defence is provided by the "zoning" of the facility (cf. section 1.2.1) based on a functional analysis and history of the facility; the second line of defence is provided by implementation of measurement procedures, which aim at the validation of the *a priori* zoning study but that cannot be the unique basis for the decision on the radioactive characteristics of a material. The definition of these

[1] At CERN the words 'radioactive waste' are used instead of 'nuclear waste'

lines of defence is under the responsibility of the operator. The "nuclear waste" is eliminated in dedicated facilities or repositories; recycling is only permitted within the nuclear industry (cf. section 1.2.2).

1.2.1 Radioactive waste zoning

In the French legislation, a legislative process is required to obtain a permit to build and run a nuclear installation. The definition of a nuclear installation, called 'Basic Nuclear Installation' (INB) is based on the radioactivity inventory.

CERN is equiparated to an INB, even if its international status allows and requires that the national definition is not automatically applied. The INB regulation (cf. section 1.2.3), among other requirements, foresees the establishment of a waste study prior to the commission of the installation. The aim of such a study is to establish a "zoning" of the facility, i.e. a classification of materials which may or may not have been activated. To demonstrate that a given component or material is "non-radioactive", i.e. "conventional", one has to prove that all activation mechanisms can only produce insignificant amounts of radioactivity [4].

The general purposes in the establishment of a waste study are:

- The improvement of the management of radioactive waste and in particular the attempt to decrease their overall production;
- The full knowledge of the production of waste and of the evolution of their radiological and physical characteristics;
- The establishment, where possible, of a recycling or revalorization of radioactive waste. Where this is not possible, the follow-up of their disposal towards the national final repository;
- The survey of the conditioning of the waste and their temporary storage on the site.

The structure of a waste study, which shall include 5 chapters, is defined in the directive [5].

1.2.2 Removal of controls for radioactive waste

A major constraint imposed by the French legislation is that material or equipment classified as "radioactive" in the waste study cannot be declassified as "conventional" by means of a measurement, no matter how accurate the latter is in showing no traces of induced radioactivity. The French regulation does not foresee any waste release from a nuclear zone based on measurements only because any set of release criteria is liable to inconsistencies and ambiguities [6].

This approach is developed from the following considerations:

- The way the materials are recycled has an impact on the committed dose and thus on the release criteria. Although it is possible to base the estimates on current national practice, exceptional uses might lead to exposures above the average.

- Experience has shown that safety can be improved by implementing several lines of defence. Measurements shall represent a second line of defence (the first line is calculations), and not the only line.

- When decommissioning a nuclear power plant, the radioactivity of a large fraction of waste actually comes from contamination. Any system to detect contamination is prone to failure when applied to large objects. This argument is not valid in the case of particle accelerators, where the contamination concerns a very small fraction of the waste and induced radioactivity in large objects can be easily detected.

Material can be "declassified" only by revising the zoning of its area of origin. The revision must be based on a combination of measurements and calculations. If the zoning study is too pessimistic, one may end up with handling as radioactive a large amount of material, which would actually pose no radiological risk if released. On the other hand, an over-optimistic waste study would lead to anomalies (*écarts* in French), i.e. material classified as conventional but found to be radioactive by measurement. If too many anomalies are found the French authorities can intervene and stop operation. The waste study has therefore to be as realistic as possible [4].

1.2.3 Overview of legal documents

Nuclear legislation in France does not derive from one general-framework act. It has developed in successive stages in line with technological advances and growth in the atomic energy field.

Although French nuclear law is characterised by its variety of sources, the original features of this legislation derive from international recommendations or regulations. For example, radiation protection standards are derived from the Recommendations of the International Commission on Radiological Protection (ICRP) and directives issued by the European Union.

Concerning the INB installations, the obligations that the operator has to implement during decommissioning are described into the the decree of 11^{th} december 1963. The article 6, issued on 19^{th} january 1990, modifies the procedure for decommissioning of the INB.

The legal basis for the waste study is to be found in the Law of july 15^{th}, 1975 about waste elimination and the Ministerial Order of december 31^{st}, 1999. Two administrative notes (9^{th} November 1990 and 17^{th} February 2003) were issued to explain in details the procedure.

Further information on the French legislation can be found in the NEA report [7].

1.2.4 Overview of relevant institutions

In France, radiation protection is under the responsibility of the Health and Labour Ministries. The main authority in safety of nuclear installations is the ASN (Authorité de Sureté Nationale), a governmental authority which reports both to the Ministries in charge of the Environment and in charge of Industry.

The Radiation Protection and Nuclear Safety Institute (IRSN) provides technical support to the ASN.

The role of ASN, the French Nuclear Safety Authority, is to regulate nuclear safety and radiation protection in order to protect workers, patients, the public and the environment from the risks involved in nuclear activities. It also contributes to informing the citizens.

The French radioactive waste management agency ANDRA is a public organisation created in 1991. It is in charge of the studies and the operation of waste disposal centres.

The CEA is the French Atomic Energy Commission. It is a public body established in 1945 to lead technological research and ensure that the nuclear deterrent remains effective in the future. Among other projects, CEA is presently working on final waste containment systems and reversible geological disposal of radioactive waste.

In addition to the above mentioned institutions, various organizations play an active part in waste management: the carriers (Cogema Logistic, BNFL SA), the processing contractors (SOCODEI, COGEMA), the interim storage (CEA, COGEMA, ANDRA) or disposal centre operator (ANDRA), the organizations responsible for research and development to optimise these activities (CEA, ANDRA).

1.3 The Swiss legislation

According to the Swiss legislation [8], the responsibility for radioactive waste management lies with the waste producers. The Swiss waste must be disposed of in Switzerland, although the option of a multilateral project is not ruled out.

The legislation requires that all final repositories for radioactive waste must be located in suitable geological formation and not near the surface. Two repositories are foreseen, one for high level waste (typically spent fuel) and one for short-lived low and intermediate level waste. All radioactive waste is presently stored in interim storage facilities because there is no repository available.

1.3.1 Switzerland: Free release

According to the recommendations from the IAEA [9], the material can be cleared from regulatory control as long as the following requirements are fulfilled:

- maximum individual dose: 10 μSv per year

- maximum collective dose: 1 $manSievert$ per year

As a general remark, there is a fundamental difference between *clearance* and *exemption*. A practice is *exempted* from regulatory control whilst a material is *cleared*, i.e. is no longer to be considered as radioactive. As a matter of fact, clearance levels are numerically smaller than exemption limits [2]. The reason is that radioactivity which falls below the exemption limits might still present a relatively high radiation risk in the case of large amounts of material. Therefore such material should meet more severe requirements in order to be cleared. On the other hand, practices which involve radioactive sources below the exemption limits will seldom produce large amounts of potentially radioactive material. As a result, these sources can be free-released without further requirements on their activity.

The international Basic Safety Standards contain tables with radionuclide specific exemption limits but do not make recommendation with respect to the clearance of radioactive material. Studies have been performed by different national Authorities to obtain clearance values. The results depend on the specific scenario which was considered and on a number of assumptions about the possible uses of the material and the environmental conditions. [10].

In Switzerland, the exemption limits for solid waste laid down in the Radiation Protection Ordinance [8] are at the same time clearance levels if an additional condition is fulfilled: the dose rate at 10 cm distance from the surface of the item must not exceed 100 nSv/h [2].

1.3.2 Overview of legal documents

The peaceful use of nuclear energy was first regulated by the Swiss Confederation in the form of a Federal Order, dated 18^{th} December 1946, encouraging research in the field of nuclear energy. Due to the complexity of the issues raised by the use of nuclear technology, the jurisdiction is divided between federal and cantonal authorities, as sanctioned at tribunal level in decisions of 1973 and 1977.

The main governmental regulations and ordinances for the handling of radioactive waste are:

- Swiss regulation n. 815.50 Strahlenschutzgesetz, Art.25-27;
- Swiss ordinance n. 814.501 Strahlenschutzverordnung, Art. 79-87;
- Swiss ordinance n. 814.557 Verordnung ueber die ablieferungspfiichtigen radioaktiven Abfaelle, Art.1-10.

[2]Until 1976, in Switzerland the specific activity limit below which material was not considered to be radioactive was 74 Bq/g. In 1976 this limit was further relaxed to 740 Bq/g for beta and gamma emitters in order to include also substances containing natural radioactivity [11]. In the Ordinance of 1994, radionuclide specific exemption limits are defined in conjunction with the dose rate limit of 100 nSv/h at 10 cm distance [8].

Among the HSK (cf. section 1.3.3) directives for the later storage of radioactive waste into the final repository we mention:

- HSK Directive B05, Requirements for conditioning of radioactive waste
- HSK Directive R13-d, Inactive clearance of material from control zones
- HSK Directive R21-d, Requirements for the final repository
- HSK Directive R29-d, Requirements for the interim storage
- HSK Directive R52-d, transport and storage containers for interim storage

More information can be found in the NEA report [12].

1.3.3 Overview of relevant institutions

The Federal Office of Public Health (OFSP/BAG) takes over the responsibility for the management of the radioactive waste generated by the use of radioisotopes in research, industry and medicine. The producers of radioactive waste, i.e. the Federal State and the nuclear power plans, formed the National Co-operative for the Disposal of Radioactive Waste (NAGRA), which is responsible for the disposal of all kinds of radioactive waste.

ZWILAG Zwischenlager Wuerenlingen AG is one of the Swiss nuclear power plant operating companies. The purpose of the company is the construction and operation of storage and treatment facilities for radioactive waste from Switzerland (cf. section 1.4.1). The responsibility for conditioning and interim storage of radioactive waste at the nuclear power plants remains with the operators.

There are two authorities and one company in Switzerland that are involved in safety aspects in nuclear installations:

- Federal Office of Public Health (BAG);
- Federal Nuclear Safety Inspectorate (HSK);
- National Accident Insurance Fund (Suva).

The BAG is part of the Federal Department of Internal Affairs. The overriding aim of the BAG is to promote the health of all people living in Switzerland. Its mission covers the increase of awareness of health-related matters, desease prevention and health protection campaigns.

Suva is an independent, non-profit company under public law. In 1918, Suva opened its doors as the Swiss Accident Insurance Fund. Suva's business activities are based on the accident insurance law. It mainly insures companies in the secondary business sector, i.e. industrial, trading and commercial enterprises. SuvaPro and SuvaLiv stand for services in the safety and health protection sector and include occupational and leisure-time safety as well as the promotion of health in the workplace.

The HSK is part of the Federal Office of Energy. It is the competent authority for supervising the nuclear facilities, namely the nuclear power plants. HSK also has the tasks to specify the detailed safety requirements and to review license applications.

1.4 Elimination pathways and final repositories

In France the unconditional clearance is not allowed. Very low level radioactive material can only be disposed of via predefined and approved elimination pathways (*filières*) where the traceability of the material must be fully assured. The free-release in Switzerland is certainly a convenient elimination pathway for waste whose radioactivity is very low (cf. section 1.3.1). In the case of metals, this can be achieved by homogenisation of induced radioactivity by means of melting (cf. section 1.4.4).

The Swiss waste that cannot be free-released and the French waste from a nuclear zone (cf. section 1.2.1) must be eliminated towards the appropriate final repositories in the respective countries. In Switzerland there is no repository at present. Radioactive waste must be temporarily stored onsite or shipped to the interim storage at ZWILAG (cf. section 1.4.1). According to the Swiss regulations from the Federal Office for Public Health, CERN participates in the annual collection of radioactive waste organised by BAG. The collected waste is then delivered to the Paul-Scherrer Institute which conditions and temporarily stores it until a final repository is available. In France there exist final repositories, which are described in section 1.4.2.

A promising elimination pathway is the reuse of radioactive material within the nuclear facility where it has been produced (cf. section 1.4.3). The option of nuclear transmutation has been the object of a recent study in Ukraina and is briefiy presented in section 1.4.5.

1.4.1 Switzerland: interim storage at ZWILAG

The Central Storage Facility in Wuerenlingen is operated by the company ZWILAG (Zwischenlager Wuerenlingen AG). In this facility, radioactive waste from nuclear medicine is decontaminated, reduced to small pieces, compacted and packed in the conditioning plant. In addition, ZWILAG has the capability to process low-level radioactive waste with a plasma oven. The waste is melted or thermally disintegrated and becomes chemically resistant, i.e. suitable for permanent disposal without further treament.

One of the main advantages of the plasma technology is that a single process can deal with virtually any type of waste, including organic solids and liquids. Nevertheless, safe and uniform operation of the plasma facility requires that the quantity and type of materials composing the waste stay within well-defined acceptance criteria. It is therefore the responsibility of the client to prepare waste packages which fulfil the above requirements [13].

The interim storage consists of a hall for highly radioactive waste, mainly from spent fuel elements, and several halls for low and medium radioactive waste [14].

1.4.2 France: final repositories

The organization responsible for the long-term management of radioactive waste produced in France is ANDRA, the French National Agency for Radioactive Waste Management (cf. section 1.2.4).

There are presently three waste disposal facility:

- the Manche facility in Beaumont-Hague (Manche), which received waste packages between 1969 and 1994 and is now in the surveillance phase;
- the Aube facility in Soulaines (Aube), which receives short-lived, low- and intermediate-level radioactive waste;
- the VLLW disposal facility in Morvilliers (Aube), which receives very-low level radioactive waste.

In addition, there is an underground research laboratory in Bure (Meuse) to study the feasibility of a deep geological waste repository in clay for high-level and long-lived intermediate-level radioactive waste.

Most of the French radioactive waste produced at CERN will fall in the category very-low-level and be eliminated towards the repository in Morvilliers.

1.4.3 Reuse of radioactive material

The possibility of reuse in a radiation environment is often stressed in the literature but in practice is rather limited. In the case of accelerators, one possibility would be to reuse radioactive metal for radiation shielding [15]. Recycling has been successfully used at CERN at various occasions:

- activated iron shielding blocks were reused in the PS for the ocillating neutrino experiment (1983), the wall between EPA and PS (1984), LIL (1982) and the ISOLDE complex (1991);
- transformation in 1997 of 68 ISR magnet yokes into LHC beam dump shielding blocks and
- reuse of about 200 t of activated concrete in the shielding of the ISOLDE complex.

Certain components can be reused in different accelerators if the underlying technology is not obsolete. As an example, a superconductive module from the LEP experiment at CERN has been recently shipped to an Indian laboratory for reuse [16]. At CERN a heated hall of 800 m^2 is dedicated to proper storage of radioactive items to be reused.

1.4.4 Treatment of metal waste by melting

In the last years, the management of metal waste arising from the nuclear industry has been addressed careful examination because of the large volumes involved [17]. Various countries (namely Germany, Sweden and France) have developed strategies for metal management which include metal melting facilities. The benefits of melting of metal are volume reduction of waste and homogenisation of induced radioactivity and contaminants within the bulk metal.

In the case of metals from particle accelerators, characterized by a non-uniform activation, homogenisation opens the possibility to free-release metals which are not activated on the whole, but present small sources of radioactivity in the areas directly exposed to the beam. It is important to note that the homogenisation is different from dilution, where conventional material is mixed with radioactive material with the sole purpose of reducing the specific activity [3].

At present, there are three commercial facilities in Europe which are specialised in segmentation, decontamination, melting and transport of radioactive metal: Socodei (France), Siempelkamp (Germany) and Studsvik (Sweden).

1.4.5 Nuclear transmutation

Recent studies have shown that it is possible to obtain nuclear transmutation via electron beam, laser and neutron irradation. As an example, it is here mentioned the experiment on nuclear transformation which was carried out at the EDL (ElectroDynamics Lab) in Kiev, Ukraine [4]. The decrease in activity is proportional to the number of radioactive nuclides in the target which undergo transmutation.

At present there is no operating facility for eliminating radioactive waste via nuclear transmutation. Nevertheless, the transmutation offers many possible future applications. In particular, it would be appropriate for material with very high and concentrated radioactivity, e.g. spent fuel from nuclear power plants.

At CERN almost the totality of the radioactive waste produced has relatively large volumes with low or very low radioactivity. The transmutation of this waste would be very expensive because only a small volume can be treated in any one irradiation cycle. In addition, the transmutation could produce heavy and long-lived nuclides which are undesirable for final storage. Nevertheless, a facility operating nuclear transmutation might be an interesting elimination pathway for high energy proton targets.

[3] The specific activity is the activity per unit mass

[4] In the Proton-21 experiment a $1kJ$ electron beam pulse is sent to a Cu target. The energy, deposited in a $0.5\ mm^3$ volume, compressed the material up to $10^{26} atoms\ cm^{-3}$. The target exploded and the explosion products precipitated on a special screen. During explosion there was a rearrangement of neutrons among the target nuclei. Some target elements generated lighter nuclides whilst others combined to form heavier nuclides. Evidence of the transmutation was given by the radiochemical analysis of the explosion products. [18]

1.5 Motivation for a radionuclide inventory

One of the requirements for the elimination of radioactive waste towards french and swiss repositories is the knowledge of the radionuclide inventory. At CERN there are difficulties in eliminating accelerator waste along the argument that, contrary to waste coming from nuclear industry, its radionuclide inventory is not well known. In particular, the national repositories claim that unknown radionuclides as the result of high-energy spallation reactions will add to the normal radioisotope inventory due to classical neutron- and gamma-capture reactions.

CERN and the Paul-Scherrer Institute (PSI) have started a pioneering collaboration for the establishement of the radionuclide composition in activated accelerator material. The radionuclide inventory of CERN waste will depend on the characteristics of CERN machines (cf. chapter 2) and on the nuclear processes at the basis of material activation (cf. chapter 4). The state of the art of radiological characterization at CERN and in other laboratories is described in chapter 3.

The so-called *fingerprint method*, presently used in nuclear power plants, is here presented after significant changes with its first application in an accelerator context (cf. chapter 5).

Chapter 6 presents the method developed and used in PSI: the so-called *matrix method*. It is for the first time described in a mathematical formulation and with a complete list of underlying hypotheses. The matrix method allows calculating the production rate of radioactive nuclides but not the time build-up. The latter aspect is investigated in chapter 7, where various irradiation scenarios are studied with a statistical approach.

Last, an overview of other possible methods is given in chapter 8, which includes direct Monte Carlo calculations, gamma-spectroscopy measurements and a statistical development of the matrix method.

Chapter 2

The production of radioactive waste at CERN

CERN is the European Laboratory for Particle Physics. It was founded in the years following the Second World War, when the claim for an international collaboration gave birth to the United Nations with its agencies. In 1944, the French physicist Louis de Broglie first proposed the creation of a European science laboratory. This suggestion led, in 1952, to the creation of a provisional Council, the *Conseil Européen pour la Recherche Nucléaire* (CERN). In 1953 the Council decided to build a central laboratory astride the Franco-Swiss border west of Geneva at the foot of the Jura Mountains.

Over the last 50 years, particle accelerators of increasing energy have been designed, built and put into operation at CERN. However, due to the interaction of particle beams with matter, part of the accelerator structure and its surrounding has now become radioactive. The activation process depends on the characteristics of the radiation environment, which is determined by the energy and type of particle used in the various machines of the accelerator's complex. This chapter begins with a description of the most important machines at CERN (cf. section 2.1), it continues with a section dedicated to particle spectra and beam loss mechanisms and concludes with an overview of the radioactive waste produced at CERN in the last 50 years.

2.1 Machines at CERN

The accelerator's complex of CERN is a succession of particle accelerators. Each accelerator increases the energy of a particle beam, which can be directly used for experiments or injected into the next machine for further acceleration. A schematic layout of the accelerator's complex is shown in Figure 2.1. Protons are obtained from hydrogen atoms by removing electrons and are accelerated via the linac2 (cf. section 2.1.1), the PS Booster (cf. 2.1.3), the SPS (cf. 2.1.8) and the LHC (cf. 2.1.11).

Lead ions for the SPS are produced by a source of vaporised lead and are

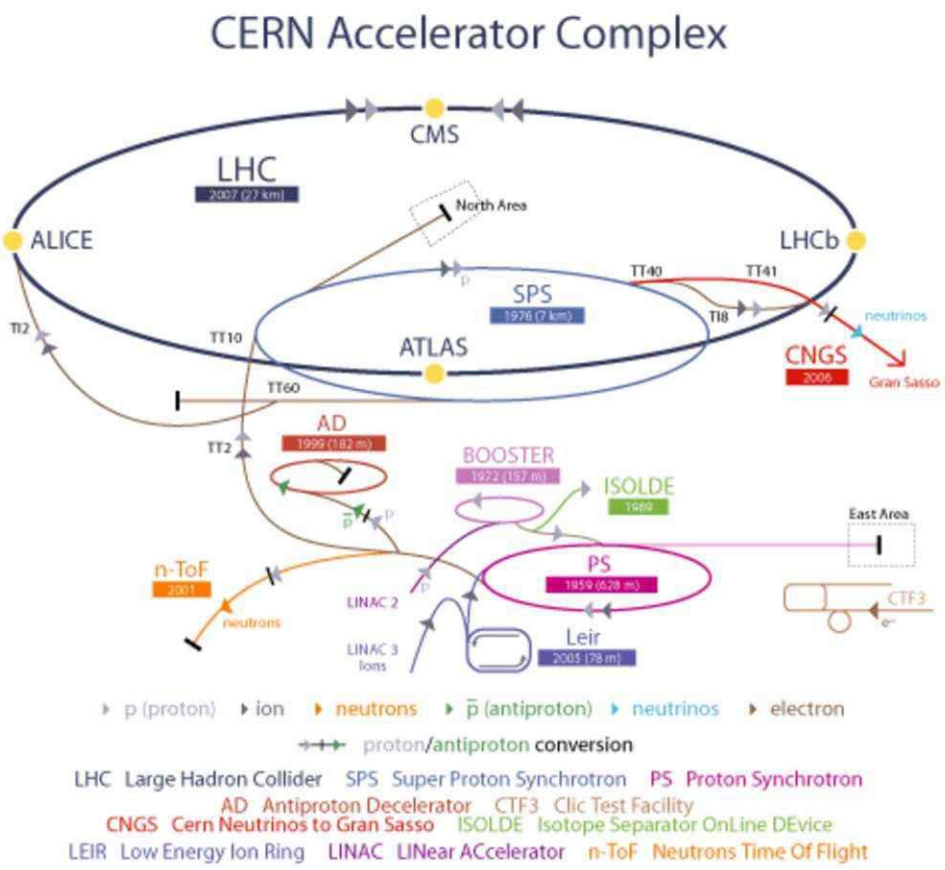

Figure 2.1: Schematic layout of the CERN accelerator's complex

accelerated in linac3 (cf. section 2.1.2) and in the Low Energy Ion Ring (cf. section 2.1.2).

2.1.1 Linac 2

Linac 2 is an Alvarez linear accelerator which delivers protons at 50 MeV. In the first section of the machine, protons are generated in a source and enter a 2 m long radiofrequency quadrupole (RFQ) for transversal focussing and acceleration up to 750 keV.

The last section consits of three tanks, where protons are accelerated under a longitudinal 1.5 MV m^{-1} electric field. Every tank is 10 m long and 1.5 m in diametre. The transverse focussing is obtained with magnetic quadrupoles located around the drift tubes [19].

Proton beams from this linac are injected in the PS booster at 50 MeV energy.

2.1.2 Linac 3

This linac, commissioned in summer 1994, presently provides beams of 208Pb to the PSB. Although intended for 170 GeV/u experimental physics in the SPS, the

lead beam was regularly injected into LEAR/LEIR for cooling experiments. In 2003, beams of Indium were accelerated for the SPS [19].

2.1.3 PS Booster (PSB)

The proton synchrotron booster receives protons from Linac2 at 50 MeV and accelerates them up to 1.4 GeV by using four concentric rings. The four beams are ejected sequentially either to the PS or directly to ISOLDE for nuclear physics.

The booster ring is made of 16 periods. Each period contains a group of basically identical main magnets (bending magnets and quadrupoles). The straight sections contain kickers, septa, RF cavities and beam monitoring.

2.1.4 PS

With a circumference of 628 m (100 m diameter), the Proton Synchrotron (PS) accelerates protons delivered by the PS Booster or heavy ions from the Low Energy Ion Ring. It became operational in 1959 and was for a brief period the world's highest energy particle accelerator. Now it delivers protons to the SPS and n_TOF facilities.

The PS has 277 electromagnets, including 100 bending dipoles and it operates up to 25 GeV. As for all circular accelerators, the arcs consist of a regular cell structure that is repeated many times around the ring. In addition to protons, it has accelerated alpha particles, oxygen and sulphur nuclei, positrons and electrons [19]. It was also used to decelerate antiprotons, to be injected into the LEAR machine.

2.1.5 n_TOF, the neutron facility

The neutron time-of-fiight facility, n_TOF, is a neutron source that has been operating at CERN since 2001. Neutrons are produced in a wide range of energies and in very intense beams. Neutron production is accomplished by spallation reactions in a massive Pb target. A solid block of Pb is hit by a 20 GeV proton beam provided by PS. Each proton produces a few hundred neutrons which may reach the experimental area after traversing two collimators at about 130 and 180 m from the spallation target.

2.1.6 AD, the antiproton decelerator

The Antiproton Decelerator provides low-energy antiprotons for studies of antimatter, in particular for creating anti-atoms.

At the end of the 70's CERN built an antiproton source (the Antiproton Accumulator, AA). The antiprotons were decelerated in the PS and further decelerated in the LEAR. In 1986 a second ring, the Antiproton Collector (AC) was built around the existing AA in order to improve the antiproton production rate.

The AC is now being transformed into the AD, which will perform all the tasks that the AC, AA, PS and LEAR used to do with antiprotons: produce, collect, cool, decelerate and eventually extract them to the experiments.

2.1.7 LEAR and LEIR

LEAR is the Low Energy Antiproton Ring, a machine which has been in operation between 1982 and 1996. It could decelerate the antiprotons coming from the PS to different intermediate energies, down to a few MeV. The machine has 78.5 m diameter, four magnetic dipoles and 20 quadrupoles. Today antiprotons are decelerated in the AD machine.

The Low Energy Ion Rings (LEIR) project aims at modifying the LEAR machine for its new role as an ion accumulator for LHC. The main feature of the future LEIR is the electron cooling, which allows reducing the transversal emittance and the energy dispersion. The ions will be directly injected into the PS for further acceleration.

2.1.8 SPS

The Super Proton Synchrotron is the second largest machine in CERN accelerator's complex. Measuring nearly 7 km in circumference, it takes particles from the PS and accelerates them to provide beams for the LHC (450 GeV [20]), the COMPASS experiment and the CNGS project (400 GeV).

It was switched on in 1976 to investigate the inner structure of protons and lead to the Nobel-prize-winning discovery of W and Z particles, made with the SPS running as proton-antiproton collider.

The SPS has 1317 conventional electromagnets, including 744 bending dipoles, and it operates at up to 450 GeV.

2.1.9 LEP

With 27 km, LEP is the largest accelerator yet built. LEP accelerated electrons and positrons in opposite directions before inducing them to collide head-on. It started operation in 1989 and stopped in 2000 and operated at a maximum energy of 105 GeV per beam. It had four intersection regions, each surrounded by a particle detector to measure the properties of the secondary particles created from the electron-positron collision.

2.1.10 CNGS

The CNGS (CERN Neutrinos to Gran Sasso) project aims at investigating the oscillation of neutrinos. The proton beam produced at the SPS interacts with a graphite target in a dedicated tunnel to produce muon-type neutrinos. The neutrinos interact very rarely with matter and can therefore pass underground to

their destination, the Gran Sasso National Laboratory of the INFN in italy, 730 km from CERN.

The first beam extracted to CNGS target was in September 2007.

2.1.11 LHC

The Large Hadron Collider (LHC) is a proton collider which will start operation in 2008. Fed by the SPS, it is installed in the 27 km LEP tunnel and is designed to accelerate protons up to 7 TeV. In addition to protons, the LHC can collide beams of heavy ions such as lead with a total collision energy in eccess of 1250 TeV.

The LHC has eight straight sections and eight arcs. Four straight sections are dedicated to experimental detectors, where the beams will collide. The remaining four straight sections are used by systems for the machine operation: beam dumps, beam cleaning, RF-cavities etc. Each arc consists of 23 regular cells with six dipole magnets and two quadrupoles.

2.1.12 Areas of validity of the Swiss and French legislations

A convention stipulated at CERN in 2000 assimilates the future LHC as well as the SPS (considered as its injector) and the CNGS to a French "Installation Nucléair de Base" (INB) (cf .section 1.2). The underground tunnels and surface areas of LHC, CNGS and SPS and some areas of the CERN sites are therefore submitted to the regulations fixed by ASN for the INB installations. The LHC experiments (CMS, ATLAS, LHCb, ALICE, TOTEM) are part of the so called "INB perimeter" and are submitted to the INB regulations [21]. The remaining machines are submitted to the Swiss regulations.

2.2 Beam losses

During machine operation, the consequences of beam losses are prompt radiation and induced radioactivity. This section provides an introduction to beam dynamics and an overview of the mechanisms which lead to beam losses in any accelerator complex.

2.2.1 Beam dynamics: emittance and acceptance

In any kind of accelerator there is exactly one curve, the design orbit, on which ideally all particles should move. If this design orbit is curved, bending forces are needed.

In reality, most particles of the beam will deviate slightly from the design orbit. In order to keep these deviations small on the whole way, focusing forces are required. Both bending and focusing forces can be accomplished with electromagnetic fields.

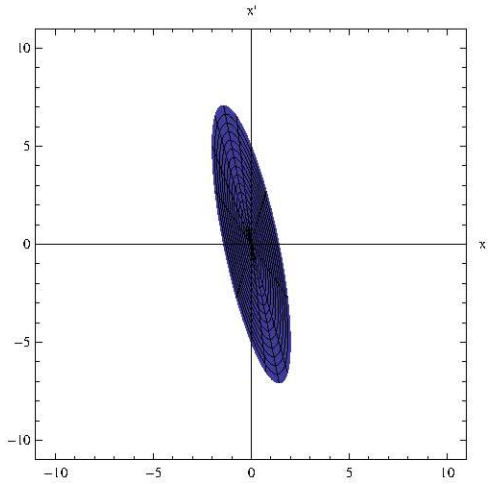

Figure 2.2: Phase space ellipse, $\beta < 1$ and $\alpha > 0$.

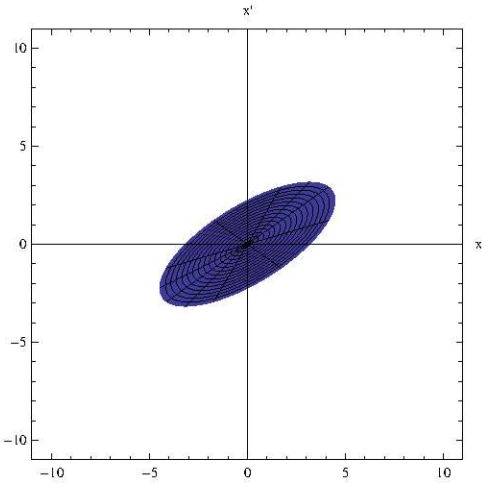

Figure 2.3: Phase space ellipse, $\beta > 1$ and $\alpha < 0$.

This type of deviations from the design orbit (also calle *oscillations*) forms the basis of all transverse motion in an accelerator and is called *Betatron* [22]. The betatron oscillations exist in both horizontal and vertical planes. They are described by the so-called *Hill's equation*:

$$\frac{d^2x}{ds^2} + K(s) \cdot x = 0 \tag{2.1}$$

where x is the displacement, s is the position along the longitudinal motion and K is the restoring force. The solution to the equation 2.1 is:

$$\begin{cases} x = \sqrt{\epsilon\beta}cos\phi \\ \dot{x} = -\alpha\sqrt{\frac{\epsilon}{\beta}}cos\phi - \sqrt{\frac{\epsilon}{\beta}}sin\phi \end{cases} \tag{2.2}$$

where α and β are parameters set by the design of the machine and the transverse emittance ϵ is determined by the initial beam conditions. If we plot $\dot{x}$ versus x as ϕ goes from 0 to 2π we get an ellipse, which is called the *phase space ellipse*. The projection of the ellipse on the x-axis gives the physical transverse beam size. As the beam moves around the machine, the shape of the ellipse will change because β changes under the influence of the magnets. Figures 2.2 and 2.3 show two ellipses with the same emittance but different design parameters.

The area of the ellipse - the emittance - is practically defined as the region of space which contains 95% of primary particles. The acceptance is the maximum area of the ellipse, which the emittance can attain without losing particles. Machine components, where the emittance is close to (e.g., septum magnets) or larger than (e.g., collimators) the acceptance, experience significant beam losses. In addition, a small fraction of primary particles are anavoidably lost through nuclear interactions with residual gas molecules.

2.2.2 Mechanism and impact

The distribution and magnitude of losses depends on the operation mode of the machine. Every experiment has specific requirements in terms of beam intensity, energy and time-structure. These requirements have an impact on the beam dynamics, which in turn infiuences the loss mechanisms. An estimate of beam losses in a machine must necessarily take into account the schedule of experiments in the year of interest. If this information is missing, conservative assumptions can be made. In particular, it can be assumed that most of the time the machine has been running under the worst beam-loss scenario.

In addition to the operation mode, also the total number of particles accelerated is important. Even the most unfavourable operation mode leads to negligible losses if the machine is working at low intensity. Some examples of nominal intensities are [23]:

- CNGS: $4.5 \cdot 10^{19}$ particles per year (ppy)
- Fixed target: $1.37 \cdot 10^{19}$ ppy
- LHC: $0.33 \cdot 10^{19}$ ppy
- nTOF: $1.5 \cdot 10^{19}$ ppy
- AD: $0.13 \cdot 10^{19}$ ppy
- ISOLDE: $23 \cdot 10^{19}$ ppy

The energy of the primary particles determines the number and energy of secondary particles produced in the interactions with the beam components. This infiuences, in turn, the total amount of induced radioactivity. The total number N_{sec} of spallation interactions produced or initiated by a proton of energy E in GeV is [24]:

$$N_{sec} \propto E^{0.92} \text{ stars per proton} \tag{2.3}$$

which is an increasing function of energy. In addition to the spallation reactions, also low energy neutrons contribute to the material activation. This is more complex to estimate, but under the assumptions that less than 20% of thermal neutron capture reactions will result in a relevant radioactive isotope and that on average 2.5 evaporation neutrons are emitted per spallation reaction [25], the the total activity S per 1 W of beam loss is [24]:

$$S \propto E_0^{-0.08} ln[\frac{(T+t)}{t}] \; GBq \cdot W^{-1} \tag{2.4}$$

where T is the irradiation time and t is the waiting time.

To summarize, the radiological impact of beam losses is determined by:

- the number of primary particles delivered every year for a given beam operation;

- the relative beam loss magnitude;
- the energy of the primary particle.

2.3 Particle spectra

Due to the heterogeneity and complexity of CERN accelerator complex, it is not possible to find one single representative radiation field which can be applied to all machines.

On the other hand, FLUKA can calculate the particle spectrum for any specific area and its associated beam loss mechanism. Although technically feasible, the calculation of all possible spectra is impractical. It would lead to a very large number of spectra without necessarily improve the prediction of induced radioactivity. From the point of view of radiological characterization, two different particle spectra which lead to the same production rate of a given nuclide are at all effects equivalent.

A preliminary study based on FLUKA simulations of the collimation area IR7 of LHC is dedicated to the calculation of particle spectra in hundreads different locations [26]. All these spectra have been effectively reduced to a few representative ones, which suggests that the same study can be successfully repeated for other CERN accelerators.

2.3.1 Hadron and electromagnetic spectra

The relative presence of hadrons and electromagnetic (EM) particles is governed by the propagation of hadron and electromagnetic showers.

As a general rule, losses in proton and ion machines at CERN involve reactions above 290 MeV, which is the threshold for pion production. In the presence of a significant pion production, an increasing fraction of the energy is transferred from the hadronic to the electromagnetic sector due to production of mesons which quickly decay into EM particles [27]. This is the main mechanism which determines the equilibrium between hadron and EM spectra.

2.3.2 Ratio between hadron fluxes

The ratio between the thermal and high energy hadron fiuxes near an accelerator can vary widely with the layout and energy of the machine as well as with the position and the nature of the surrounding environment [24]. For example, experimental data suggest that 1 to 4 thermal neutrons will be formed per high energy neutron incident on concrete [28]. The spectrum of thermal neutrons mainly depends on the moderating properties of the material. For higher energies, the spectrum mainly depends on the angular position with respect to the beam line.

2.3.3 Angular distribution of secondary particles

The fiuxes of particles formed at different stages of a nuclear reaction (see subsection 4.1.1) can be distinguished by their energy and angular distributions. The cascade stage is characterized by high-energy nucleons fiying mostly forward. Nucleons of the pre-equilibrium stage have considerably lower energies and their angular distribution is close to the isotropic distribution. The same holds true to even a greater extent for evaporating nucleons.

2.4 Radioactive waste from CERN accelerators

The production of radioactive material in an accelerator environment is a continuous process. Normally items of small dimensions are replaced during short-time periods of maintenance and bigger items (like magnets) are only delivered to the radioactive waste storage in longer shutdown periods.

Obsolete activated vacuum chambers or radioactive cables are delivered for radioactive storage at any time whilst bigger parts like whole activated magnets usually come in during longer shutdown periods. Generally the material requiring some radioactive cooling prior to any further handling is left in pre-storage near the production place.

From the point of view of material activation, it is during the machine operation that the accelerator components become radioactive. However, it is only at the time of dismantling that an item is regarded to as radioactive waste.

2.4.1 Radioactive waste presently stored at CERN

A constant amount of material is sent to the treatment and storage centre during operation of the accelerator complex but the largest fraction of radioactive waste arises from special decommissioning projects. The major projects, which are described in reference [29], can be summarized as follows:

- the SC improvement program, with important modifications of the SC vacuum chamber, the RF system and the ISOLDE facility connected to it in 1973;
- the ACOL project which required the complete dismantling and modification of the AA target area in 1984;
- the cleaning operation of the neutrino cavern of the SPS in 1992;
- the dismantling of the magnets of the former ISR in 1993;
- the decommissioning of the SC complex (work in progress);
- the decommissioning of LEP.

The resulting waste has been partially eliminated over the years and partially stored in dedicated buildings and old experimental tunnels. The CERN storage area includes the TT1 and TT7 tunnels and part of the former ISR tunnel.

The TT1 tunnel, which is the transfer tunnel to the former ISR, is used for the storage of activated electrical signal cables. The TT7 tunnel, which was used in the past for the PS oscillating neutrino experiment, is filled with activated metals, mainly steel and iron.

In the former ISR tunnel (a ring with 1 km diameter) there are three areas in used for the predisposal storage of radioactive scrap materials: the areas I5, I6 and I7. These areas currently host:

- ANDRA containers filled with radioactive scrap from the dismantling of the old neutrino tunnel;
- irradiated ISOLDE targets (cf. section 5.3.1);
- superconductive modules from the LEP experiment;
- miscellaneous items, including elements from PS, SPS and ISR machines.

In addition, a shielded area was created to store the few highly radioactive, including SPS targets and items coming from the former neutrino tunnel.

2.4.2 Future production of waste

At present, the Radioactive Waste Section of the Radiation Protection Group conditions and temporarily stores about 400 m^3 of radioactive per year of waste which come from installations, laboratories and experiments [30].

The first accelerators to be decommissioned are the Linac 2 (which will be replaced by the Linac4), the PS Booster and the PS. A large fraction of components of these machines will have to be disposed of as radioactive waste. Moreover, in the near future also the LHC will produce radioactive waste (namely electronic cards, magnets and other accelerator components) as unavoidable consequence of maintenance and repair.

It is clear that when CERN closes its activities a large amount of activity will be left in the accelerator components. Eventually, all waste which has been accumulated until the decommissioning of CERN must be shipped to the appropriate elimination pathways. Already in 1994 CERN was asked by the Swiss federal authorities to provide information on the amount of radioactive waste Switzerland could expect to receive from CERN in the next century for disposal in its planned final repository. The answer partially depends on the efficiency of CERN in the free-release process, where the performance of the radiological characterization plays an important role.

2.5 Management of radioactive waste

One of the first steps of waste management at CERN is the traceability of the waste during the whole process, from the dismantling of the components to the elimination. In Switzerland, the traceability is a legal requirement [8]. The computer-based database used at CERN for this purpose is *ISRAM*, "Information System for Radioactive Materials".

The next step is the separation of the components based on their chemical properties and level of activity. The separation is performed in the treatment centre *Centre Anneau*, as described in section 2.5.1. This operation is not a legal requirement but it is performed in order to reduce the waste volume.

A delicate step is the radiological characterization, which allows assessing the radiation risk and complying with the radiation safety requirements associated to conditioning, transport and storage.

2.5.1 Sorting and pre-conditioning

As from 1980, at CERN the radioactive waste is sorted and preconditioned. In particular, the volume is reduced by several procedures like stripping the inactive insulation of the electrical power cables and compressing the aluminium and copper conductors with a press. After sorting of activated items and volume reduction, $1m^3$ containers are usally used for predisposal storage of small items.

Volume reduction of bulky activated accelerator components is mainly carried out in the Centre Anneau in building 573 (see picture 2.4) with the following tools:

- a scrap baling press for metallic and non-metallic waste, which produces compressed blocks of 30 cm x 30 cm;
- a 22 kW hydraulic shear device (MBH model H-F-30 Senior) to cut tubes of up to 50 cm diameter and plates of 60 cm x 2.5 cm;
- a cable cutting machine (Swiss prototype) which can cut electrical power cables with a diameter of up to 5 cm into piece of 1 m length
- a cable stripping machines which can remove the insulation from electrical power cables.

All machines in which small amounts of aerosols may be produced are linked to an air extraction system equipped with an absolute filter unit.

2.5.2 The radioactive waste project

The steady increasing amount of radioactive waste in the last years, together with the reduction of disposal campaigns, is determining a critical situation in the CERN storage areas that are now close to saturation. In 2003, this resulted in the definition of a project for the implementation of a new policy in the radioactive waste management with the following main goals [30]:

Figure 2.4: Photograph of the treatment centre at CERN, building 573

- enlargement of the current interim storage facility to the entire ISR;
- establishment of a new waste treatment centre and
- establishment of new waste elimination pathways.

The pre-condioning centre described in section 2.5.1 will be converted in a fully operational and officially authorized conditioning centre, according to the legal requirements set by the competent authorities of the two Host States.

The basic step for the implementation of this project is the complete knowledge of the types of waste, radioactivity level, amount of materials and their history, the legally required handling and the expected disposal pathways. This is part of a comprehensive management system for the radioactive waste that considers the life of a waste from the source to its final elimination.

The Radioactive Waste Project includes the establishment of methods for the radiological characterization, which is the subject of the present study.

Chapter 3

State of the art of radiological characterization

3.1 Detectors for gross monitoring and free-release available on the market

Radioactive or potentially radioactive waste may come in a variety of forms, from simple shapes like steel supports to complex shapes like magnetic dipoles or vacuum pumps. In spite of the geometrical complexity, gamma-ray measurement is a reliable technique to assess the material activation because gamma rays are penetrating particles, can pass through the waste and interact with the detector. For this reason most of the measuring systems used during operation and dismantling of nuclear facilities are based on gamma detectors.

Section 3.1.1 describes a typical system of monitoring of slightly radioactive material based on gross gamma counting. Sections 3.1.2 and 3.1.3 present the most common systems for free-release measurements.

3.1.1 Monitoring system for characterization of waste with low activity

The characterization of waste for interim storage, transportation or final disposal requires values of average and maximum dose rate and a quantitative determination of gamma emitters. This information can be obtained by one measuring system which consists of ionization chambers and one Ge detector, with the necessary mechanics and software to handle the waste and analyse the data.

The technical specification of such a measuring system will depend on the purposes of the characterization and on the characteristics of the waste. Typical requirements include the dose rate distribution over the surface and at one metre distance. These values can be obtained by turning the waste drum during the measurement and registering the countings of fixed Geiger detectors as a function of time. Repeating the measurement at different drum heights leads to the

Figure 3.1: Photograph of a Monitoring System for Characterization of Radioactive Waste DMS, Beznau NPP (Switzerland)

localization of the hot spot. In addition, the gamma emitters are determined by positioning the Ge detector at a specified height and measuring the gamma emissions while the drum is rotating. The radionuclide inventory (gamma emitters only) is then estimated by taking into account the source distance and density distribution within the drum.

The measurement range of a typical monitoring system is 0.5 microSv/h - 20 mSv/h. In the case of a 200 l drum with 10 microSv/h contact dose rate, the measuring time is about 2 minutes. Figure 5.1 shows a measuring system produced by the company NUKEM (UK) with proportional counters, a Ge detector, a turnable table and a working station.

3.1.2 Clearance measuring system with scintillating chambers

Clearance measurements can be performed by using scintillating chambers to detect gamma rays emitted by the waste. The first free-release measurement facility (RMF) of this kind was developed and built by the company RADOS with the support of the European Commision in 1991 [31].

The system is based on the so-called *gross gamma activity measurement*, where all the energy deposited by any photon in the detector contributes to the response [32]. This includes photons which deposit a fraction of their energy via Compton interactions. Gamma spectroscopy, on the contrary, is concerned by the few photons whose energy is fully absorbed by the detector and thus requires longer measurement time.

Although the technical details vary from one model to the other, in general a detector consists of a measuring chamber with scintillators and lead shielding, a movable cart for transport of the waste from and to the chamber and a control panel with a pc, as shown in Figure 3.2. The scintillators cover a large solid angle and the because gamma radiation is relatively penetrating, the measurement is only slightly affected by the geometry of the waste. This system is particularly appropriate for large amounts of bulk material like, for example, concrete from

Figure 3.2: Photograph of the clearance measuring system RADOS RTM644Inc, PSI, Villigen (CH)

radiation shielding.

3.1.3 Clearance measuring system with gamma spectroscopy

In a clearance measuring system with gamma spectroscopy, the first part of monitor consists of large area scintillation panales in the form a of a tunnel, which the waste package has to pass by moving on a conveyor system. This system performs a gross gamma anlysis like the one described in section 3.1.2.

In addition, the monitor has a HPGe detection system for identification of isotopes and a more precise inventory determination with lower sensitivity compared with the plastic scintillation array.

An example is given by the release measurement system for packed waste (Figure 3.3) which was installed at the Joint Research Centre of Ispra (cf. section 3.4) by the company NUKEM.

3.1.4 In situ gamma spectroscopy

By *in situ* gamma spectroscopy it is meant gamma measurements performed with a portable Ge detector, which can be placed near the object to be measured. This technique has proven to be cost-effective in almost all applications where field sampling and laboratory analyses are the baseline technologies. Results can be obtained immediately following field acquisitions, thereby reducing the time delays incurred by physical sampling and laboratory analysis.

When analysis by an independent laboratory is required prior to free release of materials, one can define a guideline value of gamma emissions above which the item is certainly not a candidate for free-release.In this case, in situ measurements serve as a screening technique, eliminating the unnecessary analysis of samples

Figure 3.3: Photograph of the release measurement system (NUKEM) for packed waste at the research centre Ispra.

above the guideline level. The errors arising from non-homogeneity can be reduced by performing measurements under a small angle of view.

An example of detector for in situ measurements is ISOCS (produced by Canberra, France), which is described in the section 3.2.2 dedicated to CERN instrumentation.

3.2 Present status of the characterization at CERN

At present the radiological characterization at CERN relies on a combination of gamma spectroscopy measurements, semi-empirical formulae and Monte Carlo calculations.

The gamma spectroscopy measurements are performed with laboratory Ge detectors and with the portable detector ISOCS, which are described in sections 3.2.1 and 3.2.2. The data analysis is done with the CANBERRA software Genie2000 (section 3.2.3).

CERN is also equipped with a scintillator (MICROSPEC, section 3.2.4). This detector will be soon replaced by a new LaBr scintillator (cf appendix A), which has been tested as part of this study. A scintillator does not allow performing accurate gamma-spectroscopy but its precision is good enough to distinguish the gamma rays of the dominant radioactive nuclide. This information can be then used for normalization purposes in the matrix and fingerprint methods (chapters 6 and 5, respectively).

Detectors are certainly effective for radiological characterization of existing waste. For future machines, the predictions of material activation are usually done with the Monte Carlo code FLUKA (cf. section 3.2.5). In addition to this code, a large number of Windows-based softwares (e.g., MicroShield) and user-written routines are used to make specific studies like calculating the geometry factors and the dose rate near a source.

To complements these tools, semi empirical formulae based on educated guess and experience have been developed over the years.

3.2.1 Laboratory Ge detectors

Specific and total activity measurements of waste samples are made with high-purity Ge detectors. In addition to the detector itself, each gamma-ray spectrometer consists of a liquid-nitrogen refrigerated cryostat, a preamplifier, a detector bias supply, a linear amplifier, an analog-to-digital converter (ADC) and a multi-channel storage of the spectrum. A lead shield surrounds the detector to reduce the counting rate from room-background radiation.

At CERN there are three gamma-ray spectrometers with relative efficiency between 20% and 40%: CANBERRA models GX2018, GX6022 and GX4020. These detectors are coaxial with a thin Be cryostat window, which extends the useful energy range down to 3 keV.

The spectra analysis and reports are made with the software Genie2000 (cf. section 3.2.3).

3.2.2 In Situ Gamma spectroscopy: ISOCS

The In Situ Object Counting System (ISOCS) is a gamma spectroscopy system which relies on a Ge detector (40% efficiency at 1.33 MeV). In addition to the detector itself, it consists of a portable liquid-nitrogen cryostat, lead shielding, a portable spectroscopy analyzer and laptop for data processing. Thanks to its relatively small size, the system fits on a push cart and can be used for in situ measurements.

ISOCS has a calibration software which combines the detector characterization (produced with MCNP), a collection of predefined geometries and physical parameters. The efficiency calibration is calculated on the basis of the geometry description given by the user, without need of calibration samples. The spectra analysis is performed with Genie2000 (cf. section 3.2.3).

CERN has purchased the system in order to perform the radiological characterization of waste, including free-release measurements. There is a large fraction of waste which cannot be easily moved (e.g., SPS bending dipoles) nor does it fit in the laboratory Ge detector. With this respect, the advantage of having a transportable Ge detector is evident. Nevertheless, it is a fragile instrument which requires careful handling during transport. Therefore, ISOCS has been installed in a dedicated room, where most of the measurements and the weekly quality assurance checks are performed.

3.2.3 A software for data processing: Genie2000

Genie2000 is a Canberra software for acquiring and analyzing spectra from Multichannel Analyzers (MCA) [33]. Its functions include MCA control, spectral dis-

play and manipulation, spectrum analysis and reporting.

Presently all Ge detectors at CERN run under Genie2000. The main reasons why the software Genie2000 was chosen are:

- straightforward sample processing;
- neat graphical user interface (GUI);
- Software stability;
- modern data transmission (1997 Ethernet, now USB).

The spectrum analysis relies on libraries of radiactive nuclides which allow the automated identification of gamma lines. The analysis is a delicate step in the radiological characterization because - if the library is not adequate - it can lead to erroneous conclusions on the radionuclide inventory. The creation of specific libraries in Genie2000 is an important middle-term goal of the waste management at CERN.

3.2.4 NaI scintillator: MICROSPEC-2

Accurate dose rate measurements are carried out with a portable NaI-based system called MICROSPEC-2 developed by BTI Canada. This system uses a 50x50 mm cylindrical scintillator to measure both the ambient dose equivalent and the gamma spectrum. For the analysis of the gamma spectrum it contains a library of 71 radionuclides. The dose rate is evaluated from the gamma spectrum with a rather fiat energy between 80 keV and 3 MeV. This detector will be soon replaced by the LaBr detector Inspector1000 (cf. appendix A).

3.2.5 FLUKA simulations

One of the method used at CERN to predict induced radioactivity, especially for operational radiation protection, is Monte Carlo simulations with FLUKA. The production of radionuclides in FLUKA results directly from the description of hadronic interactions. It can therefore be modelled for any incoming hadron, target nucleus and energy. Interactions of low-energy neutrons ($E < 19.6$ MeV) form the only exception, for which pre-tabulated cross sections are used. If such cross sections are not available for a certain target element, radionuclides are not generated in interactions on that element by default [26]. For all other reactions, radionuclides follow directly from the last step of the interaction and results are thus infiuenced by all previous stages.

Just to mention one its many applications, the radioactive waste zoning of LHC and CNSG is based on FLUKA simulations. More information on its capabilities can be found in section 8.1.

3.2.6 MicroShield

MicroShield, v.4.2 is a commercially available (Grove Engineering, Inc) code to calculate dose rates near homogeneous sources with a given geometry, containing radioactive nuclides with a given activity. The code performes a numerical calculation which includes the build-up factor. MicroShield was strongly recommended by the specialists of ANDRA for the evaluation of the activity in radioactive waste containers [29].

An evident limit of this software is that it assumes that the radioactivity is homogenous, a condition which is hardly met by accelerator components. Nevertheless, it is very useful to obtain a quick and rough estimate of dose rate for a calculated radionuclide inventory, which can be obtained by FLUKA simulations. It is also a convenient tool to study the impact of geometry and material density in gamma ray transmission. MicroShield can also be used to calculate the afterheat, that is the heat deposited by gamma and beta particles emitted in the decay of radioactive nuclides [34].

3.2.7 Empiric formulae

The radioactivity level expected in an accelerator facility depends on a variety of factors which cannot be reduced to a handful of algebric expressions. Nevertheless, experience has shown that at least an appreciation of the magnitude of radioactivity is still achivable without the need of detailed calculations. Some literature works provide guidelines on how to perform educated guess, especially in the domain of radiation protection in particle accelerator. An outstanding example is the guide written by Sullivan [24].

As an example of a semi-empiric formula established at CERN, Y. Donjoux in his work as a student [35] has worked out a relationship between dose rate at 10 cm and specific activity of 22Na in compressed cable blocks being 0.17 microSv/h/(Bq/g). This result, which was found with the NaI detector MICROSPEC-2 (cf. section 3.2.4), shows that in this case the limiting factor for unsrestricted release (in the absence of other radionuclides) is the dose rate limit of 0.1 microSv/h and not the specific activity.

These formulae are not accurate enough to provide a radiological characterization which is acceptable for the purposes of transport and elimination. Nevertheless, they are a valid support in the choice of the most appropriate method and in the setting up of the final calculations.

3.3 The characterization at Paul Scherrer Institute

The Paul Scherrer Institute (PSI) is a multi-disciplinary research centre for natural sciences and technology (*http://www.psi.ch*). In national and international

collaboration with universities, other research institutes and industry, PSI is active in solid state physics, materials sciences, elementary particle physics, life sciences, nuclear and non-nuclear energy research, and energy-related ecology.

The Paul Scherrer Institute operates four major laboratories: an X-ray synchrotron source (SLS), a continuous spallation neutron source (SINQ), the world's most powerful continuous-beam μSR facility (SμS) and a meson factory for fundamental nuclear and elementary particle physics (LTP).

3.3.1 Accelerator complex and characterization strategy

In terms of particle accelerators, the PSI complex consists of:

- two 72 MeV cyclotrons for isotope production: one for a variety of applications and research, one as injector for the 590 MeV proton accelerator and for isotope production;
- 590 MeV proton accelerator with 2 meson-production target stations, a spallation neutron source (SINQ) and (starting in 2009) an ultracold neutron source (UCN);
- 250 MeV proton accelerator for medical applications (PROSCAN);
- 2.4 GeV electron accelerator with a synchrotron light source (SLS).

The operation of these accelerators leads unavoidably to material activation. The radioactive waste from the accelerator complex consists of a fairly large number of different materials with a very wide range of induced radioactivity. A scheme for obtaining a nuclide inventory for any piece of waste removed from the complex has been developed over the last few years [36]. While directly irradiated components are simulated exactly with the Monte Carlo transport program MCNPX, components from secondary irradiation fields are treated with a simplified method. The basis of this method is to calculate the inventory using a representative material composition and secondary irradiation spectrum and to normalise to a measured surface dose rate. The calculations are carried out by the PWWMBS code system which provides the nuclide inventory for a waste package on a specified date [37]. The system solves the Bateman equation, based on an adapted version of the code ORIHET [38]. The decay data used by the Bateman code come from the NUBASE library [39].

3.3.2 The PWWMBS code system

The PWWMBS system is a self-contained PC code package for the classification and characterization of all the radioactive waste produced by the PSI-West accelerator complex destined for repository disposal. The system is the result of a study programme, whose goal was the estimate of the nuclide inventory with an accuracy sufficient for the needs of safety assessment of the radioactive

waste repository, while minimizing the dose to PSI personnel and allowing a rapid throughput of radioactive waste from removal to packaging.

3.3.3 Cross-sections

The PWWMBS relies on a library of neutron cross sections from 2 to 800 MeV for 72 stable isotopes of 24 chemical elements [40, 41, 42]. Below 100 MeV the cross sections are calculated using ALICE, above 100 MeV with MECC and EVAPX. These cross-sections have been benchmarked with experimental values and are regularly updated.

3.3.4 Representative spectra

The strategy in calculating the representative secondary neutron spectra consists in the calculation of the source term, followed by the transport of secondary particles through the shielding. The result is a set of spectra per source-term and per material-shielding as a function of depth into the shielding.

Representative spectra of the 590 MeV regions in PSI were calculated in 1994 [43] with the code ONEDANT [44]. The selection of spectra and materials was completed in 2001.

Extensions to cover the 72 MeV areas were done using Monte-Carlo in 2004 [45]. The source spectra have been calculated with the code ALICE95, which takes into account both the pre-equilibrium emission and the Weisskopf-Ewing evaporation.

An important step of this work is the sensitivity analysis to quantify the variation of inventory with spectrum. The investigation of spectral differences which lead to significant variations in the characterization allows reducing the number of representative spectra. The 590 and 72 MeV areas are divided into direct or secondary irradiation zones, the latter being represented by appropriate secondary neutron spectra [46]. Picture 3.4 presents a schematic layout of part of the PSI accelerator complex with its division into irradiation zones.

3.3.5 Representative materials

As a general remark, it should be noted that in the radiological characterization the materials play a dual role:

1. they become the active waste
2. they shape the irradiation spectra.

The majority of the material in the PSI complex is shielding in large blocks. Materials of construction mainly come from industry and have compositions based on industrial norms. However, the most difficult problem for characterising radioactive waste is how to take material impurities into account. More information on the approach adopted by PSI on this subject can be found in [37].

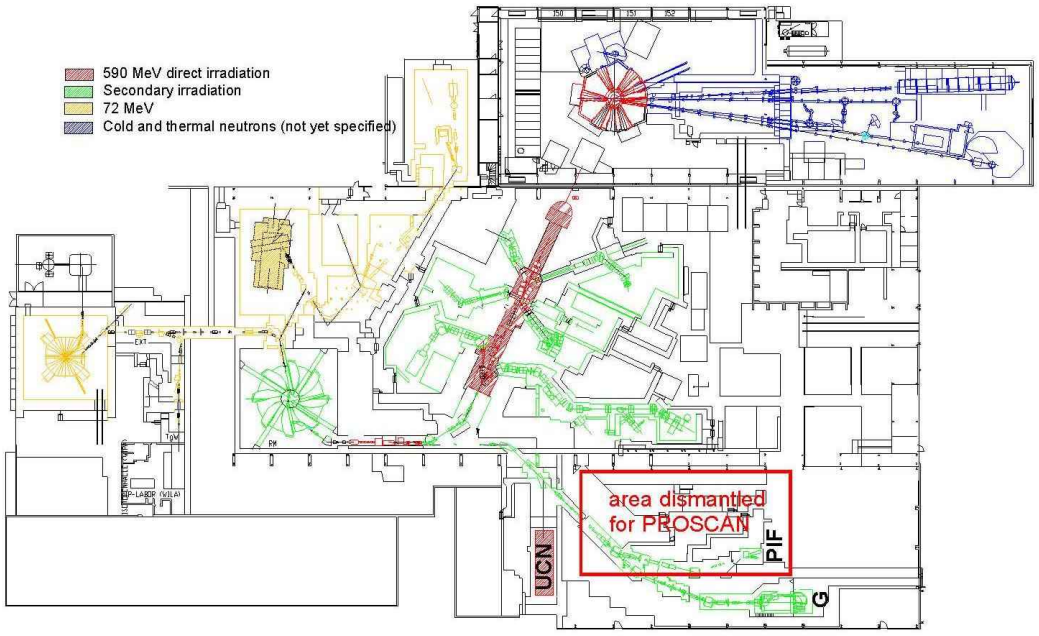

Figure 3.4: Schematic layout of the PSI accelerator complex.

There are presently 11 representative materials in PWWMBS including steel, iron, aluminium, copper and lead. The material compositions are calculated as average values from measured assays of samples. They are stored in a database, which develops with the waste stream.

3.3.6 Validation

The PWWMBS code, which at present is fully operational, has been validated in a number of experiments [47]. The validation consists in collecting material samples from various irradiated components, predict the radionuclide inventory with PWWMBS and compare the predictions with the measurements. The measurements are in part peformed with gamma-spectroscopy techniques. Additional nuclides (e.g. H-3, Be-10, C-14, Al-26, Cl-36, Mn-53, Fe-55, Fe-60 Ni-59, Ni-63) are determined after chemical separation using liquid scintillation counting (LSC), accelerator mass spectrometry (AMS) and inductively coupled plasma spectrometry (ICPMS). In particular, a collaboration is established between the radiochemistry laboratory of PSI and the AMS laboratories of the ETH Zurich and the TU Munich.

3.3.7 Application of the PSI method to CERN waste

The method described above has been conceived and developed at PSI as a result of about 15 years of research. Its successful application to the radioactive waste

from PSI suggests that it might be used also for CERN waste. However, the PWWMBS code cannot be used at CERN as it is because:

- the study is limited to neutrons (protons, photons and pions needed);
- the cross-sections are limited to 800 MeV (up to 7 TeV needed);
- the point losses are very localised (at CERN they are distributed over the accelerator);
- it implies good traceability for a large fraction of historic waste;
- the limited number of materials and machines keeps the system to a manageable size.

Nevertheless, the idea of calculating representative materials and representative spectra - to be folded with calculated cross-sections - can be applied to a large fraction of CERN waste, as it is described in chapter 6. The actual development of such a method still requires several years of research.

3.4 The radiological characterization at ISPRA

The mission of the Joint Research Centre Ispra Site (JRC-Ispra), an integral part of the European Commission, is to provide scientific and technical support for the conception, develpment, implementation and monitoring of EU policies. Among the research projects lead by the centre it should be mentioned the long-term safe operation of Western and Russian type of nuclear power plants and the environmental impact of nuclear waste management.

To date, the policy for managing the obsolete nuclear installations in the Ispra Site has been one of keeping them in a state of safe conservation. In a Communication of 1999, the Commission says that the current strategy of continued surveillance is expensive and that faster decommissioning would make better use of resources. The Commission therefore envisages a Decommissioning and Waste Management Programme which will last for about 20 years. The aim of the programme is the progressive elimination of the historical liabilities of the centre, namely those installations for radioactive waste management and nuclear R&D facilities which are no longer part of the mission of JRC.

In Italy there are no guidelines for conditioning. Only site-specific levels have been given by the National Agency for Environmental Protection and Technical Services (APAT), as for the case of the nuclear power plant of Caorso. The design and construction of a radioactive waste treatment centre for the dismantling of the Ispra facilities has required a great effort in terms of project management and control over the external companies and different work packages, as well as handling the uncertainties on cost estimates and the delays related to licensing. A description of the future treatment centre is given in section 3.4.2.

The treatment centre also includes a system for the automated radiological characterization of radioactive waste (cf. section 3.4.1). Ideally, the characterization could be done by measuring the items of waste as they are (non-destructive analysis). However, destructive measurements [1] are required due to the non-uniform activation. The disadvantages of destructive measurements are that they are expensive both in terms of time and money.

3.4.1 Radioactive waste characterization system

The radioactive waste characterization system used in Ispra is composed by two main stations:

- a gamma measurement station to quantify the activity distribution of gamma emitters (Figure 3.3);
- a neutron measurement station to evaluate the activity of alpha-emitting radionuclides.

Both stations are designed to measure heterogeneous waste drums of 35 to 400 litres and are equipped with a personal computer and a software for the data acquisition, analysis, reporting and storage of measurements.

In addition, the system comprises an integrated station to read the bar-code, determine the weight and measure the dose rate of the drum.

Gamma measurement station

The station uses detectors with high purity Ge with a detection efficiency of 40%. The detectors are fixed whilst the drum can rotate by means of a turntable system.

The calculation of the spatial distribution of radioactivity depends on the density distribution of the material. The determination of the waste matrix attenuation at different energies is performed by a transmission source system. The correction coefficients of matrix attenuation are automatically calculated and included in the data analysis.

A typical measurement of a 200 l drum containing low-level waste (about 10 Bq/g of gamma emitters) with a matrix density of 2000 kg/m^3 requires about one hour.

Neutron measurement station

The neutron measurement station is based on the so-called *active interrogation principle* for the quantification of the fissile isotopes. The principle of operation is the following:

[1] A destructive measurement involves cutting and extracting small samples from the waste item, mainly for radiochemical analysis.

- the drum of waste is surrounded by a neutron moderator;
- a neutron generator located outside the moderator emits *interrogating* neutrons with a fixed frequency, which are thermalized in the moderator before reaching the drum;
- the thermal neutrons interact with the fissile isotopes inside the drum inducing fission;
- the fission reactions produce prompt and delayed; neutrons. After thermalization in the moderator, these neutrons reach the detectors and are measured.

The operations above are repeated as many times as needed to obtain sufficient measurement data. A typical measurement of a 200 l drum with long-lived low level waste (about 100 Bq/g of alpha-emitting nuclides) and a density of $1500 kg/m^3$ requires about one hour.

3.4.2 Conditioning facilities

The so-called *Area 40* was designated as the location for the future centre for waste treatment which will include:

- a radioactive liquid waste effiuent treatment plant;
- a decontamination plant with an abrasive blasting unit;
- a radioactive waste characterization system (cf. section 3.4.1);
- an interim store for temporary storage of radioactive waste.

From the experience of the European project for the dismantling of obsolete facilities in Ispra it is possible to obtain some ideas which could be applied to the CERN radioactive waste. In particular, attention should be paid to the potential sources of cost and delay, e.g. licences from the Authorities, validation of the fingerprints, study of the attenuation matrix inside the containers, security aspects, public opinion and progressive loss of knowledge about the stored waste.

Chapter 4

Nuclear interactions: physics, data and computational tools

4.1 Nuclear Interactions

From a physical point of view, the events responsible for material activation are the nuclear interactions. In nuclear reactors all interactions are neutron-induced and take place at relatively low energy (<10 MeV). In particle accelerators the palette of possible reactions is much larger and also includes protons, photons and pions with energy range from a fraction of eV (netrons) to a few TeV (protons). Charged particles trigger electromagnetic reactions like Compton, photoelectric effect and pair production. The electrons and photons extracted can trigger further reactions and lead to a *electromagnetic shower* (EM shower). As soon as the energy of the projectile particle exceeds 10 MeV, secondary particles have enough energy to trigger further nuclear interactions, giving rise to a *hadronic shower*.

There are two basic differences between hadronic and EM showers [27]

- while energetic hadronic showers are always giving rise to significant EM ones, EM showers develop independently without further hadronic particle production, a part for the small probability of electron and photonuclear interactions.
- EM interactions are in principle well understood and described by QED [48]. This is not the case for hadronic nuclear interactions where such a complete theory does not exist and one has to resort to suitable models to have some insight into the physics of the processes.

There actually exist a large number of models to describe the nuclear interactions and predict quantities of interest. An exhaustive list and a detailed description of these models are beyond the scope of the present study. Nevertheless, it is essential to understand the basic aspects in order to choose the appropriate computational tools for the radiological characterization.

In this section the most commonly used models are mentioned and special attention is paid to their field of validity. The models are selected based on the particles and energy range of interest of CERN machines.

4.1.1 The Intranuclear Cascade Model

The *INC* (Intranuclear Cascade Model), which was for the first time proposed by Serber [49] and Goldberger [50], describes the intermediate-energy nuclear reactions and is based on the classical description of a collision between a particle and a nucleus. It is intrinsically a Monte Carlo model and no analytical expression can be derived without severe approximations. Therefore INC models spread rapidly with the evolution of computers.

In the INC model the target is assumed to be a cold Fermi gas of nucleons in their potential well [51]. The Fermi motion is taken into account when considering elementary collisions, both for the purpose of computing the interaction cross-section and of producing particles in the final state. The hadron-nucleon cross sections are those of free nucleons and the only quantum mechanical effect included is the Pauli principle. More information can be found in [52].

Concerning the validity of the model, the most important requirements are that the wavelength associated to hadron motion is much shorter than the hadron mean free path inside the target nucleus and much shorter than the average distance among two neighbouring nucleons. These conditions are fulfilled only starting from 200 MeV [27]. Admittedly, the Pauli principle reduces the number of possible final states and therefore increases the particle mean free paths. Nevertheless, the physical foundations of INC are not sound below a few hundreds of MeV/c. In addition, starting from 1 GeV there are important phenomena (e.g., multiple primary collisions) which are not included in the INC.

Below 200 MeV the most appropriate nuclear model is pre-equilibrium. The validity of INC can be extended above 1 GeV by including the Glauber cascade and the formation zone.

4.1.2 Glauber cascade and formation zone

Experiments show that there are at least two physical phenomena which distinguish the hadron-nucleus interactions above a few GeV projectile energy. The first phenomenon is the increasing number of shower particles produced with increasing mass number of the target (Glauber cascade). The second one is the apparent reduced probability of reinteraction of the projectile inside the nucleus (formation zone) [53], [54], [55].

According to the Glauber cascade model, one primary particle can simultanously interact with several nucleons with a probability which increases with the target mass number.

The formation zone is a mechanism which limits high energy reinteractions in nuclei. It can be understood by considering that the typical zone of strong

interactions is about 1 fm. If one thinks of hadrons emerging from an inelastic interaction, it requires them some time to be able to undergo further interactions, namely the time needed to travel the formation zone. If the formation zone exceeds the nucleus radius, reinteraction within the same nucleus is forbidden.

4.1.3 Pre-equilibrium

The physical foundations of the intranuclear cascade model become approximate at low energies [56]. Moreover, the INC calculations can be time consuming if nucleons are followed down energy much lower than 100 MeV. For these reasons, in most Monte Carlo codes the nuclear reactions in the energy range between evaporation and INC are treated with the theory of pre-equilibrium.

The leading approach to pre-equilibrium is the exciton model, which relies on statistical assumptions. The main principles can be explained as follows. After the intranuclear cascade, several excited nucleons with relatively low energy remain inside the nucleus. Nucleons knocked out during the cascade leave *holes* in the nucleus. Moving in the nucleus, these excited nucleons and holes reach its boundary. They are reflected from it, as a rule, and continue to move in the nucleus, interacting with other nucleons and exchanging energy. To leave the nucleus with a noticeable probability, a nucleon must acquire a corresponding energy. The larger the number of nucleon interactions, the lower the probability that one single nucleon acquires sufficient energy to escape. Hence, the mean time of the nucleon (mainly neutron) emission is considerably larger at pre-equilibrium than at the intranuclear cascade. If the energy of an incident particle is not very high ($<$ 50-80 MeV), the intranuclear cascade may not take place and the pre-equilibrium emission becomes the initial stage of the process.

The pre-equilibrium can also be explained by means of the quantum-mechanical multistep model [57]. However this model, which has a very good theoretical background, is rather complex and is not accurate in the description of multiple nucleon emission [27].

4.1.4 Evaporation

At the end of the pre-equilibrium stage the nucleus is left in an equilibrium state, in which the excitation energy is shared by a large number of nucleons. The probability that a nucleon accumulates the energy sufficient to escape from the nucleus decreases progressively with the number of exciton collisions and the process of particle emission gradually takes on the features of evaporation. If the excitation energy is higher than the Coulombian wall, during evaporation also light fragments can be emitted. The evaporation follows a sequential scheme, i.e. one nucleon or one fragment per emission. More information on the evaporation model can be found in [58]. It is interesting to note that the spectrum of emitted neutrons is a Maxwellian distribution with temperature proportional to the square root of the nucleon excitation energy.

The evaporation model is valid for nuclei with atomic mass > 16 and excitation energy below 2-3 MeV per nucleon. For light nuclei ($A < 16$) the dominant emission process is Fermi break-up.For intermediate-heavy nuclei ($A>70$) the evaporation is in competition with fission. Nuclear fragmentation is relevant for heavy nuclei ($A > 100$) and projectile energy > 1 GeV.

Fission

The evaporative process is in competition with another equilibrium process, that is fission [59]. A fraction of the excitation energy may be spent to induce a collective deformation. As the nucleus shape departs from sphericity, the potential energy increases and reaches a maximum at a deformation stage which is called *saddle point*. The height of the potential energy over the ground state is the fission barrier. Once a nucleus reaches the saddle point, fission occurs and the nucleus separates - most of the times into two heavy fragments.

Fission for nuclei with $Z < 70$ can be neglected in any practical calculation [27].

Fermi Break-up

For light nuclei, the sequential emission scheme underlying the classical evaporation model is not appropriate because the mass of the evaporated fragment can be comparable to or even larger than the mass of the residual nucleus. The physical basis of the Fermi break-up is the assumption that the nucleus undergoes an explosive break-up into a final state. The final state (break-up channel) represents a set of particles (nucleons and fragments) in the phase space [60], [61].

A break-up into a definite number of particles begins from a certain threshold energy necessary to detach at least a particle from a nucleus. As the excitation energy increases, new break-up channels open and the break-up into a larger number of particles becomes more probable. The dependence of the probability of formation of a definite fragment on the excitation energy has a threshold character and changes dramatically with increasing energy.

This model is valid for relatively light nuclei ($10 < A < 20$) and excitation energy below 100 MeV.

Nuclear fragmentation (multifragment break-up)

A process similar to Fermi break-up occurs in medium-heavy nuclei and becomes important at reactions induced by protons > 1 GeV and heavy ions. It is called *nuclear fragmentation* and is characterized by the emission of low energy fragments with $A > 4$ from a thermalized nucleus [62], [63].

The equations governing nuclear fragmentation have the Van der Waals form [64] characteristic of systems undergoing the liquid-gas phase transition [65]. For mean density of nucleons $< \rho_0 = 0.15 fm^{-3}$ and at temperature lower than the

critical temperature $15 - 20MeV$, a uniform distribution of matter is thermodynamically unfavourable, and it must split into a liquid (dense) and a gaseous (rarefied) phase. This phase transition is a consequence of the fact that nucleon-nucleon interaction is attractive at large and repulsive at small distances. It is the balance between the attractive and repulsive forces that determines the equilibrium at the value of density equal to ρ_0. If the mean density is lower than ρ_0, the situation is dominated by attractive forces. This leads to an increase in density fiuctuations and a clusterization of matter. In addition, Coulomb and surface energy affect the phase transition.

At sufficiently low densities, surface tension and Coulomb interaction result in a disintegration of the liquid phase into a multitude of drops of different sizes. These drops of nuclear liquid are actually nuclear fragments.

The instant of break-up corresponds to the situation when the mean distance between nuclear fragments is equal to the range of nuclear forces and strong interaction does not play any significant role. At this point, separate fragments move apart under the action of long-range Coulomb interaction and undergo de-excitation through evaporation or Fermi break-up, depending on their masses.

The nuclear fragmentation model is valid if the excitation energy per nucleon exceeds about 3 MeV [66] and nuclei have mass A $>$ 100.

Nuclear fragmentation will not infiuence the development of a shower or the average energy deposition. However, it is the only one which can produce residual nuclei far away both from the target mass and from the fission product distribution. It must be therefore taken into account for a detailed analysis of residual nuclei.

4.1.5 Photonuclear reactions

The photonuclear reactions at low and intermediate energies are initiated by three types of resonance processes: giant resonance, quasi-deuteron resonance, and (3,3) resonance. These initial interactions of photons with nuclei are purely electromagnetic and are quite different from that of hadron-induced reactions, which are initiated by the strong interaction between the projectile and a nucleon in the target nucleus [67]. The high-energy photon reactions can be described with the Vector Meson Dominance [68] and the Delta Resonance [69].

4.1.6 Nuclear interactions of ions

The extension of the intranuclear cascade model to very light nuclei is relatively straightforward, at least for energies well above the binding energy. Interactions between nuclei with high Z and low energy are more complex. Little information exists in the literature both because of the lack of experiments and because of the few technological applications - with the exception of cancer therapy [70].

The three standard models of ion interactions are the BME (up to 100 MeV per nucleon), the RQMD (from 100 MeV per nucleon to a few GeV per nucleon)

and DPMJET (for high energy reactions).

RQMD

In the INC model the incident particle is transported inside the nucleus assuming a constant nuclear field. This *mean-field* approximation [71] is not accurate when both the projectile and the target are nuclei. The situation is similar the one of adjacent molecules, where each atom is infiuenced by the charges of other atoms from adjacent molecules. Chemists have described this phenomenon with the quantum molecular dynamics (QMD) [72]. The RQMD is the (relativistic) quantum molecular dynamics tailored to the specific features of nuclear interactions [73]. In particular, the nuclear field is not constant - as it is in INC - but it is recalculated at each time step to account for the time-dependent position of nucleons in the target and projectile nuclei.

The energy range of validity of RQMD is from 100 MeV per nucleon to about 5 GeV per nucleon. The model can in principle describe the interaction down to the final state. However, unavoidable approximations in the recalculation of the field lead to non-accurate values at lower energy. In event generators, the evolution is usually stopped at an intermediate point and is continued by separate models for pre-equilibrium and evaporation.

BME

The Boltzmann Master equation (BME) theory is a nucleon transport model based on nucleon-nucleon collision processes in the nuclear potential. This theory unifies the description of ion-induced interactions from about 100 MeV down to equilibrium [74].

The initial state is created by either the complete or the partial fusion of the projectile and target ions. During the interaction the nucleons exchange energy and generate a *nuclear friction* which damps the relative motion of the two ions. In the course of this thermalization unbound particles may be emitted, which greatly reduces the excited nucleus energy. The thermalization ends - and the integration of the BME stops - when the probability of emission of fast particles becomes negligible. The BME calculations might in principle be continued to predict the emission of low energy particles and fragments [75], however the necessary readjustments of the mean nuclear field would be very time-consuming. The thermal equilibrium states which are produced at the end of the thermalization phase further de-excite by evaporation of particles and gamma-ray emissions until a residual nucleus is formed, which can be described by standard evaporation models [76].

DPM

High energy ion interactions can be described by a combination of the Glauber formalism (cfr section 4.1.2 and the Dual Parton Model (DPM) [77]. In DPM

hadrons are considered as open strings with quarks, antiquarks or diquarks sitting at the ends [78]. At sufficiently high energies the interactions can be explained in terms of a string exchange - the so-called *Pomeron exchange* - and the subsequent splitting of the string system into two separate *chains*. The chains produced in an interaction are then hadronized, that is they are converted into product particles. Further information can be found in [79].

4.2 Libraries with evaluated cross-sections

In the literature there are many cross-section sets available for reactions induced by neutrons below 20 MeV. These cross-sections have been measured in dedicated experiments or they are predicted by nuclear models. Measurements in different experiments and use of different parameters in the nuclear model lead to different values for the same cross section.

An evaluated nuclear data set is produced by analyzing experimentally measured cross sections and combining those data with the predictions of nuclear model calculations in an attempt to extract the most accurate interaction description.

4.2.1 The ENDF format

The Cross Section Evaluation Working Group, formed in the USA in the 60s, standardized the ENDF format, which is now the internationally agreed upon format for dissemination of evaluated nuclear data.

Tapes, materials, files sections

In the ENDF-format, nuclear data are sorted in different levels: tapes, materials (MAT), files (MF) and sections (MT). Every level is identified by one numerical identifier.

An ENDF "tape" is a file that contains one or more target materials.

The material is the target nuclide (element, isotope and isomeric state) and is identified by a 4-digit integer. The first two digits are the atomic number. The last two digits are the isotope/isomer. They start from 25 (the lightest common isotope) and step by 3 to allow for isomers. For example, 6152 is Pm-148 and 6153 is Pm-148m.

Files are identified by a 2-digit integer (MF) which ranges from 1 to 36:

1. descriptive and miscellaneous data,
2. resonance parameter data,
3. reaction cross sections vs energy,
4. angular distributions,

5. energy distributions,
6. energy-angle distributions,
7. thermal scattering data,
8. radioactivity data
9. nuclide production data (multiplicities),
10. production of radioactive nuclides.

The remaining files contain photon production data (MF=12-15) and covariance data (MF=30-36).

The identifier of sections is a 3-digit integer. One section corresponds to one specific reaction. For example, MT=1 is the total cross section, MT=2 is elastic scattering and MT=16 is the (n,2n) reaction.

An ENDF tape contains one or more materials in increasing order by MAT. Each material contains several files in increasing order by MF. Each file contains several sections in increasing order by MT.

Pre-processing of the ENDF files

The information on the cross-sections is spread over different files. Special processing is needed to obtain complete cross-sections. The International Atomic Energy Agency distributes a set of 16 codes which are called PREPRO [80]. Only the codes relevant for radionuclide-production are here mentioned.

Cross sections are represented as tables of data points. Depending on the energy range, these data must be interpreted using a special interpolation law which is provided at the beginning of the section. The code *Linear* uses the recommended interpolation law to produce a new table, where values can be linearly interpolated.

In the ENDF format the resonances can be given by means of resonance parameters and tabulated background corrections. The code *Recent* merges this information into one single set of complete cross-sections ad 0 Kelvin.

The cross-sections at 0 Kelvin can be recalculated for any other temperature with the Doppler-broadening formula [81]. This is done by the code *Sigma1* for 300 Kelvin temperature.

The neutron interaction cross-sections (differential in energy) are contained in file 3. Whenever there is a certain probability that the product nuclide is left in an excited state (isomer), the branching ratio is provided in file 3. The cross-section for the production of the product nuclide in a certain energetic level (i.e. the partial cross-section) is therefore the product of the total cross-section (file 3) and the branching ratio (file 9). The code *Activate* makes this multiplication for all reactions where branching ratios appear and writes the partial cross-sections in file 10.

The tabulated distributions and Legendre coefficients are converted to linearly interpolable tables by the code *Legend*. This code checks and corrects negative angular distributions, which could otherwise lead to unreliable results if used in applications.

A number of tests are perfomed by the code *Fixup* to check if the data are perfectly consistent. For example, one test aims at verifying that the total cross-section is equal to the sum of its parts at all energies. It should be noted that Fixup requires linearly interpolable tables (cfr the code Linear).

After running these codes in sequence the nuclear data file contains complete cross-sections for product nuclides in the ground state (file 3) and in the isomer state (file 10), linearly interpolable and at room temperature. Data are still in ENDF format.

The JEFF library

There are several libraries written with ENDF format:

- the ENDF/B-VII in the United States,
- the JEFF in Western Europe,
- the JENDL in Japan,
- the CENDL in China and
- the BROND in Russia.

These libraries are all complete in terms of target nuclides and nuclear reactions. For consistency with other studies at Cern [82] and after discussion with experts [83] it was decided to use the library JEFF3.1.

A script in Python [84] was specifically written to run the PREPRO codes in sequence and to extract the required cross-sections from the library JEFF3.1.

4.3 Codes for the calculation of cross-sections

There exists a huge and accurate body of experimental information on neutron interactions below 20 MeV (cf. section 4.2). Due to the lack of experimental values above 20 MeV, nuclear models and codes are needed to predict those cross-sections which are not available in literature.

The cross-sections can be estimated by codes which perform the calculations analytically or based on Monte Carlo. Monte Carlo can be used to simulate a statistical process (such as the interaction of nuclear particles with materials) and is particularly useful for complex problems that cannot be modeled by computer codes that use deterministic methods. The individual probabilistic events that comprise a process are simulated sequentially. The probability distributions governing these events are statistically sampled to describe the total phenomenon.

In general, the simulation is performed on a digital computer because the number of trials necessary to adequately describe the phenomenon is usually quite large. The statistical sampling process is based on the selection of random numbers - analogous to throwing dice in a gambling casino - hence the name *Monte Carlo.*

One of the fundamental requirements for a model describing nuclear interactions to be applied in Monte Carlo codes is computational speed. There are two possible approaches to improve the speed. The first approach is to develop accurate and sophisticated models, which require time-consuming calculations, and use them to produce comprehensive tabulations of energy-angle spectra of all emitted particles for a fine mesh of energies of possible projectiles. The second approach is to use approximated models and simulate at run time every interaction.

There are several reasons why the second approach is used by the vast majority of Monte Carlo codes for interactions above 20 MeV projectile energy. One important reason is that comprehensive tabulations would require large dynamic memory even for a rough energy mesh. Another reason is that a large amount of information would be lost in producing tabulations, namely the correlation between angle and energy of particles emerging from the same collision [27].

These sections present a short list of available codes: analytical (TALYS, Silberberg) and Monte Carlo (MCNPX and FLUKA).

4.3.1 TALYS

The nuclear-reaction program TALYS was created at CEA (Bruères-le-Châtel, France) and at NRG (Petten, the Netherlands) to provide a complete simulation of nuclear reactions in the $1\ keV - 200\ MeV$ energy range for neutrons, protons and light ions (deuteron, tritium, 3He) and α [85].

The code is written in Fortran77 and it consists of about 250 routines. Values of discrete levels, masses, resonances etc are taken from the Reference Input Parameter Library [86]. The results depend on 150 parameters which should be specified by the user. Nevertheless, a complete set of approximated cross-sections can be obtained with a minimum of four parameters (i.e. the target mass and number, the projectile type and energy).

4.3.2 Silberberg

The first studies of activation of accelerator components were done with semi-empirical systematics for proton cross-sections. The first formulae were developed by Rusdtam in the middle of the 60s and fail to accurately predict deep spallation processes [1].

The Rudstam formulae were improved in the 90s by Silberberg [87] , who implemented them in the code YIELDX. The Silberberg formulae are valid for

[1] *Deep* spallation processes are those which involve large differences of atomic weight between the target and product nuclide.

energies above 50 MeV, although they are not accurate near reaction threshold.

The YIELDX code is freely available for application in research from the GSI website of CHARMS (collaboration for high-accuracy experiments on nuclear reaction mechanisms with magnetic spectrometers).

4.3.3 MCNPX

MCNP is a general-purpose Monte Carlo code that can be used for neutron, photon and electron transport. The MCNPX represents an expansion of the MCNP code, putting in place the ability to track high energy particles - a major requirement for simulation of particle accelerators.

MCNPX offers options based on three physics packages; the Bertini [88] [89] and ISABEL models taken from the LAHET Code System, and the CEM package [90], which has been specially adapted for MCNPX. All the three codes include the preequilibrium and evaporation stage.

HETC

The Bertini model is incorporated into MCNPX through the LAHET implementation of the HETC Monte Carlo code developed at Oak Ridge National Laboratory [91]. The nuclear density is represented by 3 density steps. Projectiles particles are protons, neutrons and pions. The energy range of validity is from 20 MeV to 3.5 GeV.

ISABEL

ISABEL is an INC model which allows hydrogen, helium and antiprotons as projectiles. ISABEL is derived from the VEGAS INC code [CHE68]. It allows for interactions between particles both of which are excited above the Fermi sea. The nuclear density is represented by up to 16 density steps, rather than the three of the Bertini INC.

The running time is generally 5-10 times greater per collision than with the Bertini model. The energy range of validity is from 20 MeV to 1 GeV.

CEM

The Cascade-Exciton Model (CEM) of nuclear reactions was proposed initially at the Laboratory of Theoretical Physics, JINR, Dubna [92] to describe intermediate-energy spallation reactions induced by nucleons and pions. It is based on the Dubna IntraNuclear Cascade (INC) [93] and on a special pre-equilibrium model (cf. section 4.3.3.

The incident particles can be neutrons, pions and protons. The target nuclei can be carbon or any heavier element. The energy range of validity is from 100 MeV to 5 GeV.

MPM

Subsequent de-excitation of the residual nucleus after the INC phase may optionally employ a multistage, multistep preequilibrium exciton model, or MPM [94]. The MPM is invoked at the completion of the INC, with an initial particle-hole configuration determined by the outcome of the cascade.

When the ISABEL intranuclear cascade model is invoked, it is possible to determine explicitly the particle-hole state of the residual nucleus, thus providing sound initial conditions for MPM calculations. In the case of Bertini and CEM this is not true and the interface between their output and MPM is based on heavy approximations.

MEM

The pre-equilibrium model implemented in the code CEM is based on the exciton model EM (crf section 4.1.3) and it is called the Modified Exciton Model (MEM) [95]. The main assumption in MEM is that in the pre-equilibrium stage of a reaction only the the last filled nuclear shell is involved. The model also includes the emission of alpha particles [96].

Evaporation and Fermi Break-Up

MCNPX, when used with the Bertini or ISABEL options, employs the Dresner evaporation model, based on work originally due to Weisskopf [58]. Although the Dresner model can emit 19 different particles from a nucleus, only those with Z up to 2 are implemented in MCNPX, which means that the multifragmentation model - which is very important for residual nuclei predictions - is not included. In the LAHET/MCNPX implementation, Fermi break-up considers only two- and three-body break-up channels. This is an abbreviated form of a more extensive implementation which includes up to 7-body simultaneous break-up, used previously for cross section calculations on light nuclei [97].

In the case of CEM, the evaporation and fission models are specific to the CEM code and different from those in HETC and ISABEL.

High energy interactions

MCNPX contains an early version of the FLUKA high-energy code, which consists of the Dual Parton Model event generators HADEVT and NUCEVT [98] for hadron-hadron and hadron-nucleus collisions as implemented in the form of EVENTQ in the FLUKA-87 hadron cascade code. Major improvements have been done in the DPM event generator of FLUKA in the last 20 years and which have not been implemented in MCNPX.

4.3.4 FLUKA

FLUKA is a Monte Carlo code which is being developed within Italian National Institute for Physics (INFN) since 1989, in strict collaboration with CERN and The University of Houston further information can be found in the FLUKA web site (http://www.fiuka.org). In 2003 FLUKA has become a joint INFN-CERN project to share the responsibility of developing, maintaining and distributing the FLUKA code.

FLUKA can transport particles with kinetic energies of several TeV down to thermal energies. The nuclear interactions of neutrons below 19.6 MeV are simulated by using tabulated cross-sections. The neutron interactions above 19.6 MeV and those from pions, protons and photons are calculated online by means of physical models.

It can also make predictions about induced radioactivity produced in hadronic and electromagnetic showers. In particular, it can calculate the time evolution of the radionuclide inventory with an exact analytical implementation of the Bateman equations. Furthermore, FLUKA can generate and transport the decay radiation for any irradiation profile and for arbitrary decay times.

The nuclear interactions are first modelled probabilistically based on total cross-sections. If an interaction occurs, an event generator is then employed to simulate the details of the interaction. This section provides a list of the most important event generators used in FLUKA.

PEANUT

The intermediate energy hadronic model of FLUKA is called PEANUT [99]. PEANUT handles interactions of nucleons, pions, kaons, and rays from a few GeV down to reaction threshold (or 20 MeV for neutrons). The reaction mechanism is an explicit Generalized INtranuclear Cascade (GINC) followed by statistical (exciton) preequilibrium emission (cf. section 4.1.3). At the end of the GINC and exciton chain, the evaporation of nucleons and light fragments is performed, following the Weisskopf treatment (cf. section 4.1.4). Further deexcitation includes fission, evaporation and the Fermi Break-up model for light nuclei.

Evaporation

The evaporation treatment in FLUKA was first developed in 1990 based on Weisskopf's theory. The model was improved in the following years to include fision, Fermi break-up and gamma competition. These physics improvements allow a more accurate description of the production of residual nuclei. In 2003, also the production of fragments up to mass 24 (cf. section 4.1.4) was introduced and benchmarked [100].

RQMD

The version of RQMD that is included in FLUKA is a modified version of the code developed by Sorge [73]. The fundamental code has not been changed, but some modifications were made to insure absolute energy conservation [71].

DPMJET-3

DPMJET-3 [101] is a high energy hadron-hadron, hadron-nucleus and nucleus-nucleus interaction model which describes interactions from 5 GeV per nucleon up to the highest cosmic ray energies [102] for all possible ion comibanations. The interactions are treated by DPMJET-3 with the DPM model and the excited reaction products are passed back to the FLUKA evaporation/fission/break-up routines for the final de-excitation.

Photohadron production

The photonuclear reactions below 770 MeV are treated by Peanut according to the Vector Meson Dominance Model. FLUKA can also predict quasideuteron interactions and calculate the giant dipole resonance [102].

4.3.5 Conclusions on the codes

At present there is no analytical code which can evaluate cross-sections for all particles and energy of interest at CERN. In particular, the code YIELDX is designed for quick estimation of cross sections and the results are not suited for physical interpretation. In addition, the code does not account for the decay of fragments. Also the code TALYS would be incomplete because it does not include photons, pions and particles above 200 MeV. Moreover, the evaporation of fragments is not implemented, which represents a severe limitation to the prediction of isotope production.

MCNPX is using the 1990-version of the high energy event generator of FLUKA for interactions above a few GeV (see below). This old model does not conserve energy and quantum numbers on an event basis and uses parametrized expressions for excitation energies. It is therefore not recommendable to use MCNPX for predictions of isotope production in high energy interactions [103]. On the other hand, hadronic interactions below few GeV are described by modern state-of-the-art models including pre-equilibrium, emission, evaporation and fragmentation. These considerations suggest that FLUKA is the most appropriate tool for the radiological characterization at CERN.

4.4 Reaction channels of interest

In the last forty years it has been acquired a relatively large experience in material activation. A number of publications have been written about the properties of

induced radioactivity in high energy particle accelerators. This section gives an overview of the radioactive nuclides which are commonly found in accelerator components.

The importance of a reaction channel is determined by the frequency of occurence and the half-life of the product nuclide. The radioactive nuclides which are of relevance for the radiological characterization have a half-life longer than one year. The present study does not concern nuclides whose activity has decreased to negligible levels by the time the waste is eliminated. The frequency of occurrence depends on the production rate, which is the product of the reaction cross-section (cf. section 4.2), the particle spectrum (section 2.3) and the material composition. It is only by considering these three factors together that one can judge the importance of the nuclear processes presented in section 4.1 on a case-by-case basis.

The most important pathways of inducing radioactivity in accelerators are:

- neutron capture (n,g), which produces a nuclide with the same atomic number as the target nuclide;
- spallation reactions, which produces nuclides with lower or much lower atomic number than the target nuclide;
- inverse reactions g,n, which usually have small cross-sections but are important in electron accelerators.

The connection between this rather short list of reactions and the relatively long list of physical models presented in section 4.1 is that the calculations of cross-sections for spallation reactions require different models depending on the projectile type and energy.

The typical materials which are used for the construction of particle accelerators are:

- iron and zinc, especially for magnets and cable trays;
- copper, used for the coils of the magnets and for electric cables;
- normal and stainless steel, used for supports, pipes for water cooling systems and machine components;
- aluminium for power cables and pipes;
- plastics and resins, used as insulator of electric cables;
- graphite, for collimator jaws;
- concrete, used for walls and as biological shielding from radiation;
- earth, which is exposed to radiation in the case of underground facilities.

The heaviest element which can be encountered is lead: it is seldom used in hadron accelerators but it is an important shielding material against photons and high-energy electrons. The most remarkable difference with respect to nuclear power plants is the quasi absence of fissile elements.

The list of materials given above covers the vast majority of CERN solid waste. However, within the same family (e.g., steel) there are actually many different types of material which differ in density and presence of traces. The trace elements are particularly important for neutron capture where the high cross-section can compensate for the small content.

Taking into account materials, cross-sections and spectra and from the experience gathered in the last years [104], it can be concluded that the radioactive nuclides given in table 4.1 represent the dominant contribution to the radionuclide inventory of CERN waste.

Plastics	H-3	12.2 y	Spallation
	Cl-36	3.E5 y	Cl-35(n,g)
Aluminium	H-3	12.2 y	Spallation
	C-14	5730 y	N-14(n,p); O-17(n,a); Spallation
	Na-22	2.6 y	Na-23(g,n); Spallation
	Al-26	8.E5 y	Al-27(g,n)
Steel	H-3; C-14; 22-Na		Spallation
	Ti-44	48 y	Spallation
	Mn-54	312 d	Fe-54(n,p); Mn-55(g,n)
	Fe-55	2.94 y	Fe-54(n,g)
	Co-60	5.27 y	Co-59(n,g); Ni-60(n,p); Cu-63(n,a)
	Ni-63	92 y	Ni-62(n,g)
Copper	H-3; Ti-44; Ni-63; Co-60; Zn-65	245 d	Cu-65(p,n); Zn-64(n,g)
Lead	As above plus		
	Ag-108	127 y	Ag-107(n,g)
	Ag-110m	254 d	Ag-109(n,g)
	Tl-204	3.8 y	Tl-203(n,g)
Earth	Eu-152	12.7 y	Eu-151(n,g)
	Eu-154	16 y	Eu-153(n,g)
Concrete	Ba-133	10.5 y	Ba-133(n,g)
	Cs-134	2.1 y	Cs-133(n,g); Ba-134(n,p)
	Cs-137	30 y	Ba-137(n,p); Ba-138(g,n)

Table 4.1: List of the most frequently identified radionuclides with half-life longer than one year.

Chapter 5

The fingerprints method

The fingerprint method is currently used in nuclear power plants, where a predefined radionuclide inventory (the so-called *fingerprints*) is scaled to the measured dose rate to obtain the final radionuclide inventory. The method is here adapted to the requirements of particle accelerators. In particular, the fingerprints are calculated with Monte Carlo simulations and the normalization is based on gamma spectroscopy measurement of samples. The mathematical formulation here presented allows defining formulae for correction factors. The underlying hypotheses and fully described, in order to clearly define the field of validity and the requirements. The application to a real case (the ISOLDE targets at CERN) provides a validation of the method and suggestions on how to handle technical difficulties in the implementation.

The Monte Carlo calculations are performed with the code FLUKA. A description of the nuclear models implemented in the code can be found in section 4.3.4 and an overview of its capabilities to predict induced radioactivity is in section 8.1.

5.1 Hypotheses

The fingerprint method can be applied to any item of waste which fulfils the following requirements.

Known irradiation cycle

The irradiation cycle and the waiting time (i.e., the time elapsed from the end of the irradiation) should be known with an uncertainty which is equal to or better than T_{min}, where T_{min} is the half life of the most short-lived nuclide of interest which for the requirements of a final repository is about one year. In principle the irradiation cycle can be arbitrarily complex. However, the longer the waiting time is, the less the characterization depends on the exact irradiation profile.

5.1.1 Known irradiation geometry

If the fingerprints are calculated with a Monte Carlo code, the waste geometry must be known with a precision comparable to the size of the smallest component of interest. Moreover, the simulations require the exact position of the beam losses - or the spectrum of the radiation environment. If this information is missing, other methods (e.g. radiochemical analysis and gamma spectroscopy) are necessary to estimate the fingerprints.

5.1.2 Known material composition

The material composition must be known, possibly including trace elements (i.e., elements with weight fraction $> 0.1\%$). It might be very difficult to predict the induced radioactivity in trace elements with Monte Carlo. Depending on the distance from the source of radiation, large CPU time is required to simulate a statistically significant number of nuclear reactions with the trace elements. In addition, the weight fraction of trace elements cannot be fictitiously increased in the simulations without altering the neutron spectrum, especially if the element has high resonances. Nevertheless, the radionuclides can be measured and included in the fingerprints. Radioactive nuclides produced from impurities (i.e. present at ppm levels) cannot be included in the fingerprints because they vary largely and unpredictably among different items, whilst the fingerprints apply to a whole family of items (cf. section 5.2.1.

5.1.3 Known weight fraction of subcomponents

The fingerprints are given per material and per family of items. The radionuclide inventory of an item is obtained by averaging the fingerprints of different materials/subcomponents over their weight fractions, which must be known.

5.2 The mathematical model

The fingerprint method is based on the calculation of the fingerprints, which are here defined as the complete list of radioactive nuclides with the specific activity normalized to one unit activity of the dominant gamma emitter. The radionuclide inventory is the complete list of radioactive nuclides with their specific activity, which implies that the fingerprints must be normalized to the actual activity of the dominant gamma emitter.

The number of radioactive nuclei of isotope b per gram of target element e produced per unit time under the radiation environment Φ is:

$$n_b(\Phi) = I\frac{N_{Av}}{M_e}\sum_{i=p,n,\pi,pho}\int \Phi_i(E)\sigma_{i,e,b}(E)\,dE \tag{5.1}$$

where N_{Av} is Avogadro's number, M_e is the atomic weight of the target element e, $\Phi_i(E)$ is the fiuence of particle i (proton, neutron, pion or photon) and $\sigma_{i,e,b}(E)$ is the cross-section for the projectile i leading from the target nucleus e to the desired isotope b. The fingerprints calculated for a given irradiation cycle followed by the waiting period t_{wait} are:

$$F_b(t_{wait}) = \frac{\sum_e x_e n_{b,e}(\Phi) g_b(irradiation) e^{-\lambda_b t_{wait}}}{\sum_e x_e n_{B,e}(\Phi) g_B(irradiation) e^{-\lambda_B t_{wait}}} = \frac{S_b}{S_B} \tag{5.2}$$

where λ_b is the decay constant of the isotope b, x_e is the weight fraction of the element e in the material, B is the dominant gamma emitter, S_b is the specific activity of a generic nuclide b, S_B is the specific activity of B and g(irradiation) is the time build-up function - for continuous irradiation over the time t_{irr}, $g_b = (1 - e^{-\lambda_b t_{irr}})$.

The fingerprints depend on the radiation environment, the material composition and the irradiation cycle. In particular, they change in time because of the exponential dependence on twait. The latter dependence can be removed by using the *generic fingerprints*, which are here defined as F_b calculated for a given reference waiting time t_{ref}. The actual fingerprints at the time t_{wait} are then obtained with the formula:

$$F_b(t_{wait}) = F_b e^{(t_{wait} - t_{ref})(\lambda_B - \lambda_b)} \tag{5.3}$$

By using generic fingerprints with t_{ref} 3 years the nuclides with half-life shorter than 6 months are automatically not included in the list, which simplifies the data analysis. In addition, the use of generic fingerprints significantly reduces the number of classes (as defined hereafter).

It should be noted that there is no direct dependence on the material density and on the radiation intensity. Nevertheless, the material density can modify Φ inside bulk materials and indirectly affect the fingerprints.

5.2.1 Definition of classes

The first step in the application of the method is the definition of classes. A class is a collection of items which have the same generic fingerprints and therefore the same material composition, radiation environment Φ and radiological history, i.e. the same g(irradiation). If one item of waste is made by several components and each component has a different material composition, there will be one generic fingerprint per component.

Apart from the material composition, the components will differ among each other also on a series of details. Preliminary Monte Carlo simulations must be performed to study the impact of these differences on Φ and assess whether they impose additional classes. For example, the presence of steel screws in a large piece of copper will not affect Φ and therefore items with different number of screws belong to the same class. However, items which are identical but were placed at different positions with respect to the beam loss might belong to different classes.

5.2.2 Calculation of the fingerprints

In principle the generic fingerprints can be calculated directly with Expression 5.1, with the matrix method, with gamma- and beta- measurements or with Monte Carlo. Expression 5.1 requires the explicit calculation of Φ, which for complex radiation fields can only be calculated with Monte Carlo. The matrix method only applies if there is a representative particle spectrum. If Φ varies significantly in space, which is the case near the beam-line, the representative spectrum and the matrix should be calculated ad hoc for each single component. As this is not practical, accurate and extensive beta- and gamma- measurements are a valid option, although they might turn out to be expensive both in terms of money and time, especially if there are a large number of classes. The most efficient way to calculate the fingerprints for objects irradiated in a space-dependent radiation field with a complex irradiation cycle is with Monte Carlo simulations. Indeed, the fingerprints of all components can be calculated with one single set of simulations.

The efficiency of the Monte Carlo calculations can be improved by merging all components of the same material into one single representative region. If the particle spectrum changes with the position inside the item, the representative region might be split into more subregions in order to obtain the average induced radioactivity. The material composition should be as detailed as to include trace elements. Depending on the desired level of accuracy, classes with similar generic fingerprints can be merged into one single class.

After the classes have been defined and the generic fingerprints calculated, Formula 5.3 must be applied to each item of waste to obtain the actual fingerprints.

5.2.3 Choice of the representative samples

At least one representative sample must be collected from each item of waste. If the item is not uniformly radioactive, the samples of different items must be taken from the same geometrical position. The fingerprint method requires that the activity of one reference radioactive nuclide - and always the same - is measured in each sample, e.g. the dominant gamma emitter B.

5.2.4 Normalization of the fingerprints to the sample activity

It is first assumed that one sample per class is available. The extension to the case of one sample for two or more classes is described at the end of this section.

The activity of B usually varies among components of the same class. The average specific activity of B (S_B) is therefore different from the specific activity of B in the sample (s_B). The normalization to s_B requires the determination of the ratio $\epsilon = S_B/s_B$ which can be estimated by measurement of both S_B and s_B on a limited number of items:

$$S_{b,a} = \frac{S^F_{b,a}}{S^F_{B,a}} \left\langle \frac{S_{B,a}}{s_{B,a}} \right\rangle_{Selecteditems} \times s_{B,a} = F_{b,a}(t_{wait})\epsilon_a s_{B,a} \tag{5.4}$$

where a is a generic class and S_F is the specific activity predicted by FLUKA. The error of the radionuclide inventory S_b will depend on the errors of the fingerprint (statistical error, systematic errors in FLUKA, simplifications, fiuctuations among items from the same class), the error on ϵ and the error in the measurement of s_B in a rather complex way, because these values are all correlated. Because of the correlation the total error is less than the sum of all these errors.

It is possible to implement the sample in the FLUKA geometry and normalize F_b to the expected activity in the sample:

$$S_b = \frac{S^F_b}{s^F_B} s_B = F_b(t_{wait}) s_B \tag{5.5}$$

so that there is no need to estimate ϵ. However, the total error is increased in spite of the absence of ϵ because the error on s^F_B is much larger than the error on S^F_B, which is an average over a larger volume. It is therefore recommended to use Expression 5.4.

If it is unpractical to take one sample per class, the same sample and the same ϵ can be used for more classes (e.g., class $a1$ and class $a2$) if the relative fingerprints are normalized to the same $S^F_{B,a1}$. In this case, it is important that the proportion between the activity of class $a1$ and class $a2$ is correctly predicted by FLUKA, that it is to say:

$$\frac{S^F_{b1,a1}}{S_{b1,a1}} = \frac{S^F_{b1,a2}}{S_{b1,a2}} = k \tag{5.6}$$

for all nuclides b ($b = b1, b2...$) within an acceptable error. This will give:

$$S_{b,a1} = F_{b,a1}(t_{wait})\epsilon_{a1} s_{B,a1} \tag{5.7}$$

and

$$S_{b,a2} = F_{b,a2}(t_{wait})\epsilon_{a1} s_{B,a1} \tag{5.8}$$

where $F_{b,a2} = S_{b,a2}/S_{B,a1}$.

Condition 5.6 is likely to be met if the FLUKA geometry is accurate enough. If this is not the case, a correction term ϵ_{corr} should be used:

$$\epsilon_{corr} = \left\langle \frac{S_{b,a2}/S_{B,a1}}{S^F_{b,a2}/S^F_{B,a1}} \right\rangle_{All\ b} \approx \frac{S_{B,a2}/S_{B,a1}}{S^F_{B,a2}/S^F_{B,a1}} \tag{5.9}$$

The characterization then becomes:

$$S_{b,a1} = F_{b,a1}(t_{wait})\epsilon_{a1} s_{B,a1} \tag{5.10}$$

and

$$S_{b,a2} = F_{b,a2}(t_{wait})\epsilon_{a2}s_{B,a1} \tag{5.11}$$

where $F_{b,a2} = S_{b,a2}/S_{B,a1}$. If condition 6 is met, Expression 5.9 leads to $\epsilon_{corr} = 1$ and Expressions 5.7, 5.8 and 5.10, 5.11 are identical.

5.3 Application of the fingerprint method

The fingerprint method was applied to the characterization of the irradiated ISOLDE targets. The ISOLDE targets meet all the requirements presented in Section 5.1 and have very well known radiological history. The objective of the radiological characterization is the estimate of the total activity per nuclide, per target and per material. The exact distribution of induced radioactivity within a massive component or among components of the same category and from the same target is beyond the scope of the present study.

5.3.1 The ISOLDE targets

ISOLDE is an on-line isotope mass separator facility at CERN, where a 1.4 GeV proton beam is sent to different targets to generate radioactive ions from spallation reactions. It operates two spallation targets coupled to magnetic mass separators in order to produce a wide range of radioisotopes for experiments in nuclear, atomic and solid-state physics. The thick production targets from different materials are bombarded with a pulsed 1.4 GeV proton beam with an average current of 2 μA. The spallation products are diffusing out of the target material to an ion source, they are ionized, accelerated to 60 keV and transported to experimental stations. A target is irradiated with about 10^{18} protons in a relatively short time (about one week) and before transfer to the CERN temporary storage centre it is stored in a provisional waste storage close to the mass separators.

A target unit (Figure 5.1) is characterized by a target core of a certain material (from C to Ta for the targets of interest) and a certain thickness (from 5 to 200 g cm^{-2}). The target core is inside a thin Ta container which is connected to an ion source. These components, together with connections for services, are enclosed in an Al vessel under vacuum.

One reason why the ISOLDE targets were chosen for the first application of the fingerprint method is that their radiological history is well documented and includes the number of primary protons and the irradiation time. Moreover, they all have the same size and structure and were irradiated by protons of the same energy. These common aspects meet the requirements for validity of the fingerprint method and reduce the number of required Monte Carlo simulations with respect to the number of targets to be characterized. In addition, this method is fiexible enough to account for minor differences between the targets (e.g., target-core thickness).

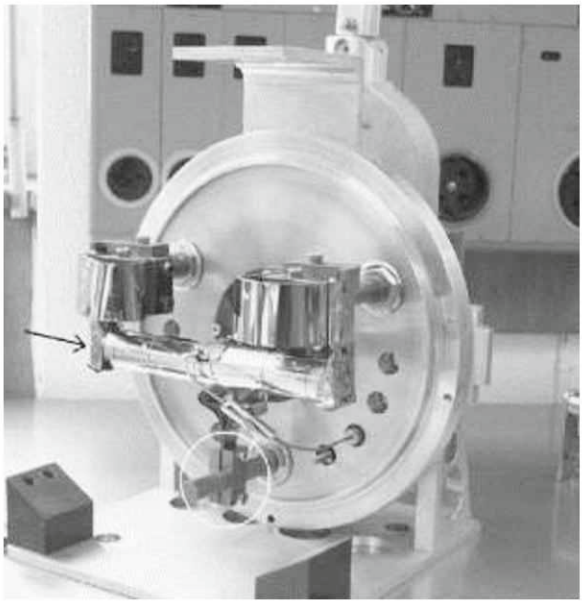

Figure 5.1: Photograph of the inner parts of an ISOLDE target unit. The vacuum vessel was removed to show the target core and the direction of the incoming beam (black arrow).

5.3.2 Elimination campaign

Two elimination campaigns took place in the last year and concerned about 60 ISOLDE targets. The targets were dismantled at CERN following a well-defined step-by-step procedure to reduce the dose to operators during handling and optimize the trial of different materials. The target components were sorted into 5 different categories: "Aluminium", "Other Metals", "Ceramics", "target container" and "target source". Two samples (Al and Cu) were systematically taken from the same position inside the targets and measured by gamma spectroscopy. Together with the weight of each category of material, the target characteristics (namely core material and source type) and the radiological history (number of primary protons, year of irradiation), this information is the basis of the radiological characterization. The gamma spectroscopy measurements were performed with the Ge detector ISOCS (Canberra, In-Situ Ge Object Counting System, see paragraph 3.2.2) using the Genie-2000 Software (Canberra).

5.3.3 FLUKA simulations and definition of classes

The first step in the implementation of the method is the definition of classes. Preliminary FLUKA simulations were performed to identify the parameters which have an impact on the estimate of the fingerprints [105].

Each target differs from the other ones in number of small components (e.g., number and position of steel screws, copper connections, rings of ceramics...). Although these components are very important for the target operation, their

exact number and location does not affect the induced radioactivity due to their relatively small mass. In the modeling of a representative FLUKA target these elements were replaced by larger samples of materials (Cu, C, W, steel and ceramic) placed around the target core. The error introduced by this artifact is well compensated by the reduction of the FLUKA statistical error, which for very small regions (e.g., a screw) would otherwise reach unacceptable levels.

The representative samples were assigned pure C, pure Ta, pure W, pure Cu, stainless steel of grade ANSI 316L (Fe 66.97%, Ni 13.5%, Cr 17%, Mo 2.5% and C 0.03%, weight fractions) and ceramic (Al 40% and O 60%). The vacuum vessel was assigned Al alloy antikorrodal (Al 95% , Si 1.1%, Mg 0.9% and traces of Cu, Mn, Zn, Be, Ti and Ni).

The production rate of radioisotopes was calculated per region and per primary proton. The results were then normalized to the actual number of primary protons and treated off-line for the build-up and the decay of radioactivity. In order to obtain the specific activity from the scored total activity in a FLUKA region, the volume and density of the regions were calculated and included in the normalization process.

The results from the FLUKA simulations are given in table 5.1 for Cu, for targets 70, 71, 82, 141 and 146. The specific activities refer to the 1^{st} of January 2007 and are normalized to 1 Bq g^{-1} of ^{60}Co. This nuclide was chosen because of its important contribution to the measured dose rate. The recommended sorting criterion for the definition of classes is the waiting time or year of irradiation. The fingerprints in table 5.1 are partial as they do not include the contribution from gamma spectroscopy - they are given only to show the dependence on the waiting time.

In the estimate of the activity of 3H no diffusion was taken into account, because diffusion is not simulated in FLUKA. If no correction is made, the estimate is rather conservative.

It should be noted that the proton beam is relatively high energy and therefore the spectra of secondary particles which are responsible for the activation is not much affected by the target material. This is why the target material has little impact on the fingerprint. In addition, the core thickness is too short to develop a full hadronic shower at 1.4 GeV and for this reason different core thicknesses produce different levels of total activity but not different fingerprints.

The waiting time was the only criterion adopted to define the fingerprint classes for the ISOLDE targets. As a consequence, there are small fiuctuations within the same class among targets of different core material, number of primary protons and target thickness. These fiuctuations, quantified as standard deviation in Table 5.1, are not an indication of the error of the Monte Carlo simulations but of the impact of different core materials on the activation process. They are a physical property of the ISOLDE targets and a result of the category selection. The only way to reduce these fiuctuations would be to increase the number of different categories.

Category	**1995-1996**				**1997-1998**			
Target	70	71	76	**Average**	82	141	146	**Average**
Year	1995	1995	1995		1998	1998	1998	
Protons $\cdot 10^{18}$	2.4	2.19	0.02		1.36	0.028	1.2	
Core material	Nb	La	Sn		Nb	Ti	La	
Core thichness (g cm^{-2})	50	123	115		54	28	139	
H3	1.4	1.5	1.46	**1.45 ±0.05**	1.13	1.38	1.2	**1.24 ±0.13**
V49	-	-	-	**-**	0.007	0.011	0.006	**0.008**
								0.0026
Mn54	-	-	-	**-**	0.015	0.019	0.012	**0.015 ±0.0035**
Fe55	0.43	0.37	0.39	**0.4 ±0.03**	0.62	0.82	0.54	**0.66 ±0.14**
Co57	-	-	-	**-**	0.015	0.018	0.013	**0.015 ±0.0025**
Co60	1	1	1	**1**	1	1	1	**1**
Ni63	0.63	0.77	0.72	**0.71 ±0.07**	0.43	0.35	0.53	**0.44 ±0.09**

Table 5.1: Results from FLUKA simulations for Cu, targets 70, 71, 82 and 146. The specific activities are normalized to 1 Bq g^{-1} of ^{60}Co.

5.3.4 Calculation of the fingerprints

A second set of FLUKA simulations was run to calculate the fingerprints according to the classes defined in Section 5.3.3. All components of the same material are merged into one single representative region to obtain the average specific activity. The results are the average over four targets which differ in core material and thickness. The specific activity per material of this *hybrid* target calculated for a reference irradiation cycle (10^{18} primary protons, 3 year waiting time) represents the generic fingerprints to be used for the characterization. The actual fingerprints for a given target are obtained by normalizing these values to the real waiting time with an off-line program.

The radionuclide inventory is then obtained by

1. scaling the fingerprints to the number of primary protons or to the measured activity in the samples;

2. combining the fingerprints of different materials with the appropriate weight fractions, using the formulae given in the next sections.

Different normalization procedures are used for different material categories, as described in the next sections. The fingerprints are entirely based on FLUKA simulations and therefore the expressions *fingerprint* values and *FLUKA* values will be used with equivalent meaning.

5.3.5 Induced radioactivity in the Al components

The entire vacuum vessel of the ISOLDE targets is made of aluminium, which is therefore the most massive material (about 13 kg per target). A large fraction of the induced radioactivity is concentrated in the two points of the vessel where the proton beam passes through. The rest of the vessel is activated by the secondary radiation. The induced radioactivity is not uniform and depends on the position with respect to the target core. The average activity $S_{b,Al}$ is different from the one of the Al sample $s_{b,Al}$. Following Expression 5.4 and choosing Na-22 as reference gamma emitter, the fingerprints are scaled to the sample activity by means of the coefficient ϵ_{Al} (Table 5.2), which is the average ratio of the measured $S_{Al,Na-22}$ over $s_{Al,Na-22}$:

$$\epsilon_{Al} = \left\langle \frac{S^I_{Al,Na-22}}{s^I_{Al,Na-22}} \right\rangle_{Selected\,targets} \tag{5.12}$$

The average ratio ϵ_{Al} can be used to predict the specific activity ($s^F_{Al,Na-22}$) in any of the Al samples from the predicted average activity ($S^F_{Al,Na-22}$): $s^F_{Al,Na-22} = \frac{S^F_{Al,Na-22}}{\epsilon_{Al}}$.

The ratio $k_1 = \frac{S^F_{Al,Na-22}}{\epsilon_{Al} s^I_{Al,Na-22}}$ gives an evaluation of the accuracy of both the FLUKA predictions and the available information on the radiological history, on

Target	47	111	112	264	
$S_{Al,Na-22}$ (Bq/g)	42.2	19.8	243	320	
$s_{Al,Na-22}$ (Bq/g)	47.3	23.8	372	348	Average
ϵ_{Al}	0.892	0.832	0.653	0.92	0.824

Table 5.2: Specific activity (Na-22) of all the Al elements with respect to the Al samples for a selection of target. Average ratio ϵ_{Al} to be used for the normalization.

which the predictions depend. The average ratio k_1 calculated for about 60 targets is 0.90, which suggests that the average predictions of the dominant gamma emitter in Al are accurate within 10% error even prior to any normalization. From Expression 5.4 we obtain the radiological characterization:

$$\overrightarrow{A_{Al}} = \overrightarrow{S^F_{Al}} \frac{s^I_{Al,Na-22}}{S^F_{Al,Na-22}} \epsilon_{Al} M_{Al} \tag{5.13}$$

where A is the total activity and M is the weight. The radionuclide inventory of the Al in target 146 is compared to the ISOCS measurement in Section 5.4.2. The inventory also includes the activity of extraneous bodies in the category "aluminium" as explained in Section 5.3.9.

5.3.6 Induced radioactivity in categories "Other Metals" and "Ceramics"

The induced radioactivity in the metal components and ceramics inside the vessel is calculated by scaling the FLUKA fingerprints to the measured activity of a copper sample. Copper is chosen as reference material because it has a well known material composition and the dominant radioactive nuclide (Co-60) is a gamma emitter, which can be easily detected even if the total activity in copper is as low as a few Bq/g. In order to estimate the activity distribution among Cu components, the ratio ϵ_{Cu} between measured activity of all Cu components and measured activity of the sample is calculated for four different targets:

$$\epsilon_{Cu} = \left\langle \frac{S^I_{Cu,Co-60}}{s^I_{Cu,Co-60}} \right\rangle_{Selected targets} \tag{5.14}$$

5.3 shows the measured activity and the corresponding ratio ϵ_{Cu}.

As for the case of aluminium, the average ratio ϵ_{Cu} can be used to predict $s^F_{Cu,Co-60}$ from $S^F_{Cu,Co-60}$: $s^F_{Cu,Co-60} = \frac{S^F_{Cu,Co-60}}{\epsilon_{Cu}}$. The ratio $k_2 = \frac{S^F_{Cu,Co-60}}{\epsilon_{Cu} s^I_{Cu,Co-60}}$ calculated for about 60 targets is 0.83. Therefore the average discrepancy between direct FLUKA predictions and measurements for Cu is about 20%. It should be noted that k_2 varies by a factor of 2 from one target to the other and in one case (target 62) the error is as high as a factor of 13. The exception of target 62 suggests that the discrepancy is due to errors on the radiological history. With this

Target	173	225	247	264	
$S_{Cu,Co-60}$ (Bq/g)	398	669	537	1200	
$s_{Cu,Co-60}$ (Bq/g)	690	1200	906	1550	**Average**
ϵ_{Cu}	0.577	0.558	0.593	0.787	**0.629**

Table 5.3: Specific activity (Co-60) of all the Cu elements with respect to the Cu samples for a selection of target. Average ratio ϵ_{Cu} to be used for the normalization.

respect, the normalization procedure allows correcting errors in the available information about the waste. For comparison, the average ratio $S^F_{Cu,Co-60}/S^I_{Cu,Co-60}$ for targets 173, 225, 247 and 264 is 1.02. This value alone (2% discrepancy between measurement and prediction) does not validate the method because it is viciously infiuenced by the fact that ϵ_{Cu} - which appears in $S^F_{Cu,Co-60}$ - is calculated using the very same targets. It nevertheless shows that the normalization procedure leads to an overall improvement of the radiological characterization. The radionuclide inventory of any material a in the category "Other Metals" can be obtained with the formula:

$$\overrightarrow{A_a} = \overrightarrow{S^F_a}\frac{s^I_{Cu,Co-60}}{S^F_{Cu,Co-60}}\epsilon_{Cu}M_a \tag{5.15}$$

The complete inventory is:

$$\overrightarrow{S^F_{OtherMetals}} = \frac{\epsilon_{Cu}}{M_{OtherMetals}}\sum_a\left(\overrightarrow{S^F_a}\frac{s^I_{Cu,Co-60}}{S^F_{Cu,Co-60}}M_a\right) \tag{5.16}$$

The items "Other Metals" of target 146 were measured with ISOCS and compared to the radionuclide inventory obtained with the above formula (Table 5.4). The results are not satisfactory because most of the gamma emitters are overestimated, which might be due to a systematic error in the FLUKA model of the target. In particular, better accuracy is expected for the prediction of Co-60, which is the reference nuclide. Furthermore, the characterization underestimates the activity of Na-22. The model was therefore improved as follows.

	ISOCS measurements (Bq/g)	Radiological Characterization (Bq/g)
Na-22	4.32	0.98
Ti-44	1.6	7.2
Mn-54	11.9	34.2
Co-60	304	346

Table 5.4: Comparison between the specific activity in "Other Metals" as measured by ISOCS and calculated with the preliminary fingerprint method.

Copper and steel represent more than 90% of the weight of the "Other Metals". As previous measurements have shown that the scaled predictions of activity in copper are reliable, the main source of error in the characterization of the "Other Metals" is supposed to come from steel. Both the steel and the Cu samples were located in an arbitrary position inside the hybrid target, which is the situation described in Section 5.2.4. The radiation intensity (to which the activity of all nuclides is linearly proportional) varies with location because of distance and self-absorption. This leads to the violation of Condition 5.6. In the case of steel, ϵ_{Cu} is not appropriate and a correction factor ϵ_{corr} is calculated as follows. According to Expression 5.11 the specific activity in steel is:

$$S_{b,Steel} = F_{b,Steel}\epsilon_{Cu}\epsilon_{corr}s_{Cu,Co-60} \tag{5.17}$$

Using the definition of ϵ_{corr} (Expression 5.9) and with $F_{b,Steel} = S_{b,Steel}/S_{Co-60,Cu}$ (from Section 5.2.4) we obtain:

$$\overrightarrow{S_{Steel}} = \overrightarrow{S^F_{Steel}}\frac{s^I_{Cu,Co-60}}{S^F_{Steel,Co-60}}\epsilon_{Steel} \tag{5.18}$$

where $\epsilon_{Steel} = S_{Steel,Co-60}/s_{Cu,Co-60}$. The specific activity of Co-60 in steel can be inferred from the measurement of target 146 under the hypotheses that the prediction of Co-60 in Cu is relatively accurate and that the contribution from small Al and Ta components is negligible:

$$S_{Steel,Co-60} = \frac{A^I_{AllMetals,Co-60} - A^F_{Cu,Co-60}}{M_{AllMetals}} \tag{5.19}$$

The inferred specific activity of Co-60 in steel is 70 Bq/g for target 146. From the activity of the Cu sample we obtain:

$$\epsilon_{Steel} = \frac{S_{Steel,Co-60}}{s^I_{Cu,Co-60}} \approx 0.1 \tag{5.20}$$

If we also include the contribution from small Al and Ta components left with the "Other Metals" to account for the presence of Na-22 (cf. Section 5.3.9), the formula for the radiological characterization becomes:

$$\overrightarrow{A_{AllMetals}} = \sum_{a=Cu,Al,Ta} \overrightarrow{S^F_a}\frac{s^I_{Cu,Co-60}}{S^F_{Cu,Co-60}}\epsilon_{Cu}M_a + \overrightarrow{S^F_{Steel}}\frac{s^I_{Cu,Co-60}}{S^F_{Steel,Co-60}}\epsilon_{Steel}M_{Steel} \tag{5.21}$$

This formula is validated by comparison with the measurement of target 47 (which has never been used to determine any of the above parameters). The results are given in Section 5.4.2 (together with the other benchmark measurements) and show excellent agreement.

5.3.7 Induced radioactivity in the target core and container

The target core (or target converter) can be made of different elements from C to U, depending on the ion which is required. The 60 targets which have been dismantled have about 20 different core compositions. In addition, none of them has the same target core in terms of both composition and weight. The material activation strongly depends on the composition but it is impractical to run one set of simulation per target. As the nuclear interactions depend on the nature of the nuclei and not on the atomic structure of the material, FLUKA simulations are performed to estimate the nuclide production in pure elements. The actual radionuclide inventory is the sum of contributions from the single core elements weighted over their respective mass fractions. In the FLUKA simulations a 9 cm long and 0.8 cm radius core is sliced into 5 adjacent modules, all modules being identical and 1.8 cm long. Each module is further divided into 9 samples of different pure elements, 2 mm in thickness. All samples of the same element are defined as one single FLUKA region: one region is therefore the union of 5 samples, one sample per module. The volume of one region is $2.01cm^3$ [1].

In the simulations all the samples are irradiated by the same number of primary protons. However, the interaction probability - and therefore the number of histories required to attain statistical significance - depends on the element density. In order to obtain comparable interaction probability for all samples, all elements are assigned a reference density of $5g/cm^3$. The weight of each region is $2.01cm^3 \times 5g/cm^3$. It should be noted that also in reality, as in the simulations, the core density is different from the natural density of the pure elements. The core is surrounded by a 0.06 cm thick layer of Ta (representing the container) and irradiated by 1.4 GeV protons. The spectrum of protons, neutrons and pions - and with it the nuclide production - changes along the target. However, each FLUKA region is the union of samples located at different places in the core. The region activation is thus representative of a homogenous, pure, thick target. With this method it is possible to score the induced radioactivity in 9 pure elements with one single set of simulations. Several sets of simulations were performed to score the induced radioactivity in the following pure elements: Ag, Al, Be, B, C, Ca, Ce, Cl, Cs, In, Li, Mg, Na, Nb, N, O, Pb, P, Rb, S, Si, Sn, Sr, Ta, Ti, U, W and Zr. At present the information on residual nuclei from La is not available in FLUKA. The element La is therefore assigned the same induced radioactivity as Ce. The results from FLUKA (specific activity) are scaled to 10^{18} primary protons and 3 year waiting time to obtain the generic fingerprints. The values of specific activity are not normalized to any dominant gamma emitter because the characterization is not based on normalization with a sample. Every core is made of 3 different elements at maximum. The specific activity is calculated with the following formula:

[1] Volume of one sample:$(0.8cm)^2 \times 0.2cm$. Volume of one region: $5\times$ volume of one sample.

$$A_{Core} = M_{Core} \sum_{e=1}^{3} \left(\frac{T_e m_e}{\sum_{k=1}^{3} T_k m_k} S_e^F \right) \tag{5.22}$$

where M_{Core} is the core mass, T_e is the stoichiometric coefficient of the element e, m_e is the atomic mass and is the fingerprint for the element e normalized to the actual number of primary protons and waiting time. The characterization is based only on FLUKA simulations because the core is activated by the primary protons. The Cu and Al samples are activated by secondary radiation and are not representative of the core activity. However, if there is no information on the radiological history the fingerprints are scaled to the measured activity of the samples. The values M_{Core} and T_e are given by the user, together with the number of protons and year of irradiation. If M_{Core} is not specified, a default value of 140 g is taken which is the average over the 60 target cores. The container is mostly made of Ta. In addition to the radiological history, the activation of the container also depends on the core material. The fingerprints are therefore calculated as the average over 4 different targets cores. The radiological characterization is given by:

$$\overrightarrow{A_{Container}} = \overrightarrow{S^F_{Container}} (M_{Container} - M_{Core}) \tag{5.23}$$

where $M_{Container}$ is the weight of the category "container", which includes the weight of the target core.

5.3.8 Induced radioactivity in the source

There are different families of target source depending on the technology for ionization (plasma, laser, surface ionization...). The most common sources are W-surface, MKIII, MKV and MKVII and are mainly composed of 6 different materials (C, Cu, steel, Nb, Ta and W). The weight fractions of the materials are given in Table 5.3.8.

Source family	Weight fraction $W_{Source,e}$					
	C	Cu	steel	Nb	Ta	W
W-surf	0	0	0	0	0	1
Ta	0	0	0	0	1	0
MKIII	0.05	0	0.847	0	0.103	0
MKV	0.34	0	0	0.41	0.25	0
MKVII	0	0.911	0	0.014	0.075	0

Table 5.5: Weight fraction of elements in different sources. The sum over all fractions is 1.0 for every source family.

The source is activated by secondary radiation and therefore the radiological characterization is normalized to the activity of the Cu sample:

$$A_{Source} = M_{Source} \frac{s^I_{Cu,Co-60}}{S^F_{Cu,Co-60}} \epsilon_{Cu} \sum_e W_{Source,e} S^F_e \tag{5.24}$$

where M_{Source} is the weight of the materials in the category "source", W_{Source}, e is the weight fraction of the element e for the given source family (see Table 5.3.8) and S^F_e is the fingerprint of the element e (independent from the source family). If the coefficient ϵ_{Cu} is not available either the fingerprints are normalized to ϵ_{Al} or the absolute values from FLUKA are taken.

5.3.9 Corrections for the presence of extraneous bodies

Although great care has been given in sorting the target components, a small number of components has unavoidably fallen in the improper category, mainly because they are firmly attached to other components of different material composition. The contribution to the total activity depends on their specific activity (which is known) and on their weight. The weight of extraneous bodies cannot be directly measured. It is however possible to infer a realistic estimate via the gamma spectroscopy analysis. For example, the production of Na-22 in copper and steel via multifragmentation (the only possible production channel) is very little. On the other hand, Na-22 is the dominant gamma emitter in aluminium. It is good approximation to attribute the activity of Na-22 in "Other Metals" to the extraneous Al bodies and assume they have the same specific activity as the aluminium sample:

$$M_{Extr\,Al} = \frac{A_{ExtrAl,Na-22}}{s_{ExtrAl,Na-22}} \approx \frac{S^I_{a,Na-22}}{s^I_{Al,Na-22}} M_a \tag{5.25}$$

The above calculation leads to $M_{Extr\,Al} = 71g$ for target 146. A conservative value of 100 g is used for all targets. The same reasoning applied to extraneous steel bodies in the category "aluminium" (dominant gamma emitter in steel: Co-60) gives $M_{ExtrSteel} = 18.7g$ for target 146. This approximates to 50 g of steel components in the category "aluminium" per target. No radioactive nuclide generated in Ta was detected by ISOCS in the items "Other Metals": the Ta bodies should not weigh more than 10 g. The contribution from small pieces of ceramics, which are relatively light, is negligible.

5.3.10 Off-line calculation of the radionuclide inventory

The calculation of the radionuclide inventory is performed by a specifically written program in Python. The program reads an input file with the following information:

1. target number;
2. years from last irradiation;

3. number of primary protons;
4. activity of the Al sample;
5. activity of Cu sample;
6. weight of the items in the category "Aluminium";
7. weight of Cu components;
8. weight of the "Other Metal";
9. weight of "Ceramics";
10. weight of the container;
11. weight of the source;
12. type of source;
13. weight of the target core;
14. chemical formula of the target core material.

Depending on the source type and core material, the program reads the generic fingerprints and applies the formulae given in the previous sections. It then creates one file per material and per target with the radionuclide inventory and the corresponding fraction of LE, which are the Swiss Exemption limits [7].

5.4 Validation

The aim of the present study is to validate the fingerprint method, which is based on FLUKA simulations. It should be noted that any discrepancy between experimental values and predictions should not be imputed to the FLUKA code only. Errors are also due to the lack of precise information about the material and the simplifications used in the method. The accuracy of FLUKA in the treatment of material activation has been verified in previous studies [8] with dedicated experiments involving samples of well known material composition, precise irradiation conditions and exact implementation of the geometry in FLUKA - all conditions which are seldom met by historic waste.

5.4.1 Direct prediction: activity in the target container

As described in the previous sections, the radiological characterization of the target container is based on the absolute predictions of FLUKA. This method was validated by comparison of the radionuclide inventories predicted by FLUKA and by gamma measurements for the core of target 183.

The core of target 183 consists of a Tantalum bar and UC pellets. The bar has a length of 215 mm, a diameter of 10 mm and a mass of 277 g. For comparison, the hybrid target core in FLUKA is 90 mm in length and 16 mm in diameter.

In 2000, the target was irradiated with a total of 5.5×10^{18} protons. Since then and until 2002, the target has been stored in the intermediate storage facility at CERN.

In 2002, the target was dismantled and samples were taken from the Ta wires holding the bar in the target assembly. The wires, which are thought to be representative for the activity levels of the bar, were analysed by gamma-spectrometry with a hpGe detector. As the induced radioactivity varies largely among different samples, only the maximum values of specific activity were retained. Dose rate measurement at 1 m distance and comparison with the inferred activity suggest that the average specific activity should be up to 2.5 times lower than the maximum activity [9].

The gamma-spectroscopy measurement was performed two years after irradiation. In order to compare the results with FLUKA predictions, the FLUKA fingerprints at 3-year waiting time are scaled to 2-year waiting time and normalized to 5.5×10^{18} protons. Table 5.6 shows the maximum specific activity measured with gamma spectroscopy, the estimated average specific activity (calculated by dividing the maximum specific activity by 2.5) and the radionuclide inventory calculated with the fingerprint method (FLUKA predictions).

The specific activity obtained with the fingerprint method always lies within the maximum and average value measured by gamma spectroscopy. The only exceptions are Gd-153 and Lu-174, for which the prediction is conservative with respect to the measurement. On average, the FLUKA predictions are close to the measured maximum activity and therefore provide a conservative radionuclide inventory. One reason for the overestimate is that only half of the primary protons actually hit the converter, whilst in the simulations it is the totality of the primary protons. Additional reasons for discrepancy are the different target size (in FLUKA it is smaller than in reality) and the treatment of radioactive decay which is tailored for waiting times longer than 3 years (for target 183 it was only two years). The latter reason might explain the absence of Te-127m (108 day half-life) in the FLUKA inventory.

The Ta-bar contains a series of isotopes which are not detected by gamma spectroscopy but which are predicted by FLUKA. One of them is the low energy alpha emitter Gd-148 ($E_\alpha = 3MeV$). Its concentration can be inferred from the proton fiux and the published cross section data to $A_s = 45kBq/g$. This estimate is in excellent agreement with the prediction of FLUKA ($A_s = 43.9kBq/g$).

5.4.2 Scaled prediction: Activity in the Al, Cu and other metals

The radiological characterization of the entire target, with the only exception of the container, is based on FLUKA predictions scaled to the measured sample

Nuclide	Estimated average, gamma spectroscopy (kBq/g)	FLUKA predictions (kBq/g)	Measured maximum, gamma spectroscopy
H-3	-	3200	-
Te-127m	114	-	285
Ba-133	-	85	-
Ce-139	69.6	114.9	174
Pm-143	346.4	492.5	866
Pm-145	-	140.9	-
Sm-145	-	719.3	-
Gd-148	-	43.9	-
Gd-151	178.8	226	447
Gd-153	113.2	570	283
Tb-157	-	42	-
Dy-159	-	367.3	-
Hf-172	708	1739	1770
Lu-173	992	2199	2480
Lu-174	74	209.5	185
Hf-178	-	33.9	-
Ta-179	-	3072	-
Ta-182	97.2	117.4	243

Table 5.6: Specific activity (kBq/g) of the Ta bar in target 183 as measured with gamma spectroscopy (average and maximum values) and estimated with FLUKA.

activity. Tables 5.7 and 5.8 show the comparison between measured (ISOCS) and predicted (FLUKA) activity for "Aluminium" and "Other Metals". All discrepancies are within the error bars.

Nuclide	ISOCS (Bq/g)	FLUKA (Bq/g)	Nuclide	ISOCS (Bq/g)	FLUKA (Bq/g)
H-3	no */gamma*	914	*C-14*	no */gamma*	0.19
Na-22	320 (11%)	285.7	*Ni-63*	no */gamma*	0.17
Fe-55	no */gamma*	8.3	*Ti-44*	-	0.13
Co-60	0.43 (35%)	0.63	*Ar-39*	-	0.06
Mn-54	0.72 (118%)	0.46	*Ar-42*	-	0.02
V-49	-	0.23	*Co-57*	-	0.02

Table 5.7: Specific activity (Bq/g) of "aluminium" of target 146 as measured with gamma spectroscopy (ISOCS) and estimated with FLUKA. The symbol "-" means that the activity is below the detection threshold.

Nuclide	ISOCS (Bq/g)	FLUKA (Bq/g)	Nuclide	ISOCS (Bq/g)	FLUKA (Bq/g)
H-3	no */gamma*	159	*Mn-54*	-	0.14
Fe-55	no */gamma*	119	*Nb-91*	-	0.13
Co-60	43.3 (10%)	45.8	*V-49*	-	0.12
Ni-63	no */gamma*	38.2	*Ar-42*	-	0.04
Na-22	0.72 (18%)	0.74	*Hf-172*	-	0.04
Ti-44	0.6 (25%)	0.7	*Ni-59*	-	0.03 Bq/g
Nb-93	-	0.49	*Co-57*	-	0.02 Bq/g
Ar-39	-	0.2	*Hf-178*	-	0.01 Bq/g
Ta-179	-	0.15	*Lu-173*	-	0.01 Bq/g

Table 5.8: Specific activity (Bq/g) of "Other Metals" of target 47 as measured with gamma spectroscopy (ISOCS) and estimated with FLUKA. The symbol "-" means that the activity is below the detection threshold.

5.5 Conclusions on the fingerprint method

The fingerprint method calculates the induced radioactivity by scaling the predictions from Monte Carlo simulations with the measured activity of a trace nuclide in reference samples. This method requires a preliminary study to assess the number of classes and the number and position of reference samples. In addition, it entails gamma spectroscopy measurements of the samples and extensive Monte

Carlo simulations to calculate the fingerprints. A specifically written program is recommended to perform the necessary normalizations.

This method can be applied to a large fraction of radioactive waste from particle accelerators, namely the items which have been exposed to a space dependent radiation field (e.g., on the beam line) with a complex irradiation cycle and which are made of several subcomponents: it is therefore complementary to the matrix method [1].

The fingerprint method involves a case-specific study to define classes and calculate fingerprints. Although the subsequent application is very fast, any new category of waste would still require a new study and investment in time and simulations. By contrast, the matrix method involves an important initial study to calculate the cross sections and representative spectra, which can then be applied to a very large spectrum of waste.

Among the disadvantages of the fingerprint method, it is mentioned that it is neither applicable to future machines (there is no sample available) nor to items with unknown radiological history.

Chapter 6

The matrix method

The items of radioactive waste from particle accelerators are very different from each other in terms of material composition, irradiation conditions, criteria under which they have been sorted and available information. It is therefore ambitious to characterize them all with one practical and possibly mathematically-elegant method. Nevertheless the following method can be applied to a large fraction of the CERN radioactive waste, namely the waste from present and future machines, the main components of the past machines and the radioactive electronic devices.

The matrix method is similar to the one developed and used at the Paul Scherrer Institute to characterize items irradiated in secondary particle fields, which is briefly summarized in section 3.3 and described in the papers [40, 41, 42, 106, 37, 107]. It is based on the calculation of nuclide production yields for selected target materials and particle spectra, which are representative of the accelerator. At first glance one could imagine applying the PSI method to CERN waste by simply extending the selection of materials and spectra. In reality it implicitly imposes strict requirements which are commonly met by the present PSI waste but not by historic radioactive waste in general.

In order to clearly define the field of validity and the requirements, the matrix method is for the first time here formally developed from the activation formula to the complete calculation of the radionuclide inventory [34]. The underlying hypotheses are explicitly stated, together with possible corrections to extend the field of validity of the method.

6.1 Hypotheses

The matrix method can be applied to any item of waste which fulfils the following requirements.

6.1.1 Uniform irradiation profile

It is assumed that the physical processes which are responsible for the activation are uniform in time. In the case of particle accelerators the induced radioactivity

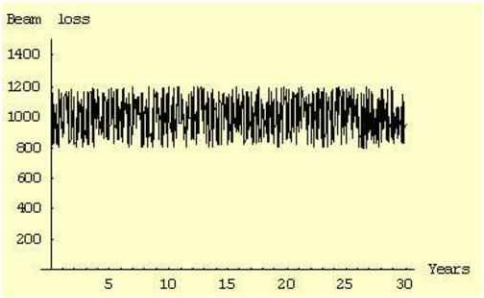

Figure 6.1: Example of constant irradiation profile.

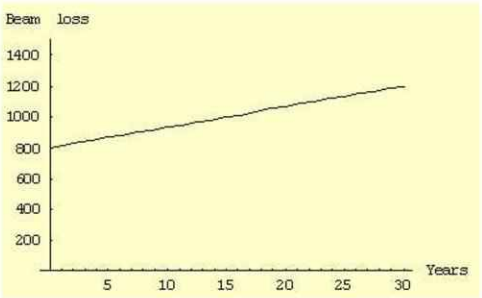

Figure 6.2: Example of irregular irradiation profile.

is due to beam losses and the beam loss profile should be constant over the irradiation time. The irradiation profile $I(t)$ is considered as constant if, for any time t,

$$\int_{t}^{t+T_{min}} I(\tau)\, d\tau \approx Const \cdot T_{min} \tag{6.1}$$

where T_{min} is the half life of the most short-lived nuclide of interest, which for the present study is about one year. Examples of constant and irregular irradiation profile are given in figures 6.1 and 6.2, respectively.

The beam loss in figure 6.1 is in arbitrary units and takes random values in the range from 800 to 1200. The average beam loss over any one-year period is about 1000: it is therefore constant for the purposes of this study. As long as it is constant, it is not necessary to know the value of the irradiation profile. This is because the radionuclide inventory is normalized to the measured dose rate, which is directly proportional to the irradiation intensity.

6.1.2 Known irradiation cycle

The irradiation time and the waiting time should be known with an uncertainty which is equal to or better than T_{min}, i.e. smaller than one year.

6.1.3 Uniform particle spectrum

By *uniform spectrum* it is meant that during the irradiation time the spectrum of activating particles is the same in every point inside the item of waste. This requirement is rather restrictive but it is certainly met by small objects and by subcomponents of large machine elements.

6.1.4 Known particle spectrum

In the matrix method the radionuclide inventory is explicitly calculated from the particle spectra, which must be known. It is not necessary to know the absolute values of the spectra: they should be normalized to one particle per unit surface per unit time.

6.1.5 Uniform material composition

The radionuclide inventory is calculated for a given material composition, which must be uniform within the item of waste. In particular, if one item is composed by several pieces of different materials each piece must be characterized separately.

6.1.6 Known material composition

The material composition must be known, including trace elements and impurities. It is very important to correctly evaluate the presence of elements from which γ emitters are produced. This is because the matrix method relies on a dose rate measurement. An error on the estimate of γ emitters will affect the prediction of all the other nuclides.

6.1.7 Absence of heavy (Z>82) elements

The Bateman equations for radioactive series are not included in the matrix method, as they play a minor role for the production of artificial long-lived nuclides. Moreover, in radioactive series the presence of a nuclide is a time-dependent function of the presence of the parent nuclides. In order to take such non-linearity into account, the matrix method would require important modification which is not justified by the little gain in accuracy. Nevertheless, it is possible to predict the nuclides which are in secular equilibrium with their parents or whose parents have a half life shorter than T_{min}. This hypothesis only slightly reduces the field of validity of the matrix method because the accelerator components contain negligible amounts of heavy ($Z > 82$) elements. In addition, most of the nuclides of interest are directly produced by nuclear interactions.

6.1.8 No contamination

The matrix method cannot estimate the contamination, which requires separate measurements (e.g., smear tests). However, the method can still be applied to contaminated waste to predict only the induced radioactivity, provided that the contamination does not affect the dose rate measurements.

6.1.9 Representative dose rate measurement

It should be possible to accurately measure the dose rate in contact with the item of waste, and the dose rate should be representative of the waste. This requirement is satisfied in the majority but not the totality of real cases. For example, certain components must be taken apart in order to be measured, which is not always feasible. If a container is filled with different items of waste (e.g., objects irradiated in different machine locations), the dose rate in contact with the container is of no use for the matrix method as the waste does not meet the requirement of uniform particle spectrum.

6.2 Activation formula and additive rule

The matrix method is based on the calculation of the activation formula. The number of radioactive nuclei of isotope b per gram of target element e produced per unit time by I primary particles per second is:

$$n_b = I\frac{N_{Av}}{M_e}\sum_{i=p,n,\pi,pho}\int \Phi_i(E)\sigma_{i,e,b}(E)\,dE \tag{6.2}$$

where N_{Av} is Avogadro's number, M_e is the atomic weight of the target element e, $\Phi_i(E)$ is the spectrum of particle i (proton, neutron, pion or photon) generated by one primary particle and $\sigma_{i,e,b}(E)$ is the particular cross-section for the projectile i leading from the target nucleus e to the desired isotope b.

The specific activity A_b per gram of material expected after an irradiation time t_{irr} and a waiting time t_{wait} is:

$$A_b = I\frac{N_{Av}}{M_e}x_b\sum_{i=p,n,\pi,pho}\int \Phi_i(E)\sigma_{i,e,b}(E)\,dE\,(1-e^{-\lambda_b\,t_{irr}})\,e^{-\lambda_b\,t_{wait}} \tag{6.3}$$

where λ_b is the decay constant of the isotope b and x_b is the weight fraction of the element e. In order to obtain the specific activity of all nuclides produced in an item of waste, this calculation should be extended to all the elements e of which the material consists. If a nuclide b_2 is produced by the decay of b_1, in 6.3 we have $A_b = A_{b_2}$ and $\sigma_{i,e,b} = \sigma_{i,e,b_1}$; the decay constant λ_b is set equal to λ_{b_2} if $\lambda_{b_1} >> \lambda_{b_2}$ and to λ_{b_1} if $\lambda_{b_1} << \lambda_{b_2}$.

When it comes to classify a material on the basis of its radioactivity, the value of total activity alone is seldom an appropriate indicator. In fact, for a given level of activity the radiological hazard depends on the type and energy of particles emitted, in addition to the chemical properties of the nuclides. In order to take these properties into account, each radioactive nuclide should be associated one reference limit of specific activity. Depending on the purpose of the classification (e.g., transport, final repository etc) the specific activities should be compared with the appropriate set of reference limits, which we will call L_b. The comparison is done with the so-called additive rule:

$$RAD = \sum\frac{A_b}{L_b} \tag{6.4}$$

where the non-dimensional parameter RAD is an absolute level of induced radioactivity. For example, for an item of waste to be free-released its specific activity A_b should be such that $RAD < 1$ for the appropriate set of L_b values.

If we combine 6.3 and 6.4, we obtain a formula which gives the global parameter RAD for a given item of waste:

$$RAD = \sum_b\frac{1}{L_b}\sum_e x_e I\frac{N_{Av}}{M_e}\sum_{i=p,n,\pi,pho}\int \Phi_i(E)\sigma_{i,e,b}(E)\,dE\,(1-e^{-\lambda_b\,t_{irr}})\,e^{-\lambda_b\,t_{wait}} \tag{6.5}$$

where x_e is the weight fraction of the element e.

6.3 Definition of activation matrix

In this section we define the elemental weight w_e as the number of atoms of the target element e per gram of material: $w_e = \sum x_e N_{Av} M_e$. The set of elements composing the target material is represented by the vector $\overrightarrow{W(material)}$, which has as many components as the stable isotopes which can be found in accelerator materials. We also define a unitary spectrum $\phi_i(E)$ as:

$$\phi_i(E) = \frac{\Phi_i(E)}{\sum_i \int \Phi_i(E)\, dE} = \frac{\Phi_i(E)}{\Psi} \tag{6.6}$$

where Ψ is the radiation intensity as a result of one primary particle impinging on the target. The time dependence of the activity can be represented by the function $g_b(t_{irr}, t_{wait})$:

$$g_b(t_{irr}, t_{wait}) = \frac{(1 - e^{-\lambda_b\, t_{irr}})\, e^{-\lambda_b\, t_{wait}}}{t_{irr}} \tag{6.7}$$

We introduce the normalization factor $K = I_{tot}\, \Psi$, where I_{tot} is the total number of primary particles lost near the item of waste over the irradiation time t_{irr}. The integral inside 6.3, which is a function of both e and b, can be written as:

$$f_{e,b}(\phi) = \sum_i \int \sigma_{i,e,b}(E) \phi_i(E)\, dE \tag{6.8}$$

The set of functions f calculated for a given spectrum are represented by the activation matrix $[M(spectra)]$, which has as many rows as the nuclides b and as many columns as the target elements e.

The reference limit and the time dependence of the activity can be coupled to obtain a time-dependent parameter specific of the isotope b: $D_b(t_{irr}, t_{wait}) = g_b(t_{irr}, t_{wait}) \div L_b$. The set of specific parameters D_b is represented by the vector $\overrightarrow{D(irr.cycle)}$, which depends on the irradiation cycle and has as many elements as the nuclides of interest.

In 6.3 we can now separate the elements which depend on the chemical composition e from those which depend on the radioactive nuclides b:

$$\begin{bmatrix} \frac{A_{b_1}}{g_{b_1}(t_{irr},t_{wait})} \\ \cdots \\ \cdots \\ \cdots \\ \frac{A_{b_n}}{g_{b_n}(t_{irr},t_{wait})} \end{bmatrix} = K \begin{bmatrix} f_{b_1,e_1}(\phi) & \cdots & \cdots & \cdots & f_{b_1,e_n}(\phi) \\ \cdots & \cdots & & & \\ \cdots & & \cdots & & \\ \cdots & & & \cdots & \\ f_{b_1,e_n}(\phi) & \cdots & \cdots & \cdots & f_{b_n,e_n}(\phi) \end{bmatrix} \begin{bmatrix} w_{e_1} \\ \cdots \\ \cdots \\ \cdots \\ w_{e_n} \end{bmatrix} \tag{6.9}$$

The global parameter RAD is given by:

$$RAD = K \begin{bmatrix} \frac{g_{b_1}(t_{irr},t_{wait})}{L_{b_1}} & \cdots & \cdots & \cdots & \frac{g_{b_n}(t_{irr},t_{wait})}{L_{b_n}} \end{bmatrix} \times$$

$$\times \begin{bmatrix} f_{b_1,e_1}(\phi) & \cdots & \cdots & \cdots & f_{b_1,e_n}(\phi) \\ \cdots & \cdots & & & \cdots \\ \cdots & & \cdots & & \cdots \\ \cdots & & & \cdots & \cdots \\ f_{b_1,e_n}(\phi) & \cdots & \cdots & \cdots & f_{b_n,e_n}(\phi) \end{bmatrix} \begin{bmatrix} w_{e_1} \\ \cdots \\ \cdots \\ \cdots \\ w_{e_n} \end{bmatrix} \tag{6.10}$$

or according to the proposed notation:

$$RAD = K(normalization)\overrightarrow{D(irr.cycle)}\,[M(spectra)]\,\overrightarrow{W(material)} \tag{6.11}$$

6.4 Normalization with dose rate measurement

The parameter RAD is proportional to a normalization factor K, which depends on the beam loss and distance from the source and which can be estimated by measuring the dose rate near the radioactive material.

The dose rate measured by a detector is given by the activity of each nuclide multiplied by a response coefficient r_b, which depends on the material attenuation as well as on the energy and emission rate of γ- and β-particles. The set of response coefficients, multiplied by the function $g_b(t_{irr}, t_{wait})$, is represented by the vector $\overrightarrow{G(irr.cycle)} = \begin{bmatrix} g_{b_1} r_{b_1} & \cdots & g_{b_n} r_{b_n} \end{bmatrix}$. The dose rate $\dot{D}$ is therefore:

$$\dot{D} = K \begin{bmatrix} g_{b_1}(t_{irr}, t_{wait})\, r_{b_1} & \cdots & g_{b_n}(t_{irr}, t_{wait})\, r_{b_n} \end{bmatrix} \times \times \begin{bmatrix} f_{b_1,e_1}(\phi) & \cdots & \cdots & \cdots & f_{b_1,e_n}(\phi) \\ \cdots & & \cdots & & \cdots \\ f_{b_1,e_n}(\phi) & \cdots & \cdots & \cdots & f_{b_n,e_n}(\phi) \end{bmatrix} \begin{bmatrix} w_{e_1} \\ \cdots \\ \cdots \\ \cdots \\ w_{e_n} \end{bmatrix} \tag{6.12}$$

It is now possible to calculate the parameter RAD without using the normalization factor K, which is replaced by a measure of the dose rate:

$$RAD = \frac{\overrightarrow{D(irr.cycle)}\,[M(spectra)]\,\overrightarrow{W(material)}}{\overrightarrow{G(irr.cycle)}\,[M(spectra)]\,\overrightarrow{W(material)}} \tag{6.13}$$

This formula shows that the parameter RAD is proportional to the dose rate near the object.

6.5 Requirements for the implementation of the matrix method

The calculation of the matrix itself requires tabulated cross-sections for all particles, energies and reactions of interest. For the specific case of CERN, the activating particles are neutrons, protons, pions and photons and the energy ranges

from fractions of eV to a few TeV. Only part of the required cross sections exists in literature. When experimental data are not available, the cross sections can be calculated with the Monte Carlo code FLUKA [78, 102]. In addition, representative spectra should be either calculated via Monte Carlo or measured.

The accuracy of the characterization depends on the precision with which the material composition is known. Radiochemical analysis should be performed to assess in detail the elemental composition of the most frequently used materials.

In the case of particle accelerators, in order to correctly define the irradiation cycle the radiological history of the machine must be well documented. The documentation at CERN includes indirect information like yearly radiation surveys, measurements of high energy dosimetry and previous studies of induced radioactivity. For a limited number of cases, the exact number of primary particles lost per year and per location is also available.

The dose rate normalization requires an appropriate detector (e.g., scintillation detector), which ideally can give a quantitative estimate of the contribution of different radioactive nuclides to the measured dose rate. In addition to this, a Ge detector is advisable to validate the radiological characterization via spectroscopy analysis of samples.

The calculation of the factor RAD can only be done if a set of reference limits exists. Otherwise, the matrix method is limited to the estimate of the specific activity of each single radioactive nuclide.

6.6 Fields of application

The method uses the activation formula without any simplification and is therefore very precise. It requires the calculation of the activation matrix, which can be calculated once and for all and applied to any uniformly activated item of waste. The dependence on the material composition only appears in the vector $\vec{W}$, whilst the time dependence only appears in vectors $\vec{D}$ and $\vec{G}$. This separation allows investigating the impact of having a different material composition or irradiation time at a given location. It is not required to know the number of primary particles lost in the accelerator because the inventory can be normalized by a simple dose rate measurement.

If we limit our study to a few representative materials and if we define an irradiation time to be applied by default to all objects coming from a certain location or belonging to the same category the calculation can be tabulated for a limited number of cases. In the end, for a given item of waste, the parameter RAD is given by a tabulated coefficient (which depends on the machine where it has been irradiated and the material composition) and the dose rate.

Provided that all hypotheses described in 6.1 are fulfilled, the matrix method can be applied to any item of waste. However, there are special cases where this method is particularly convenient and which are here presented.

6.6.1 Waste from large areas with uniform spectrum

The application of the matrix method to an item of waste requires the initial effort of calculating the representative spectrum. This effort is fully justified when the same spectrum can be applied to a large collection of items of waste.

6.6.2 Small-size waste

There is no inferior limit in the size of the waste that can be characterized with this method. In a Monte Carlo calculation, for example, it is difficult to obtain statistically relevant results in tiny regions or in low-density materials. This could be the case of irradiated electronic devices waste, where even very small parts of Ni and Ag are of relevance for the radiological characterization. The same reasoning holds valid for the activation of impurities, which is almost unpredictable with Monte Carlo methods and difficult to measure. In the matrix method the values in the vector $\vec{W}$ can be arbitrarily small without affecting the accuracy of the result.

6.6.3 Components with well known radiological history

In an accelerator environment like the one at CERN, the concept of radiological history is related to the one of *traceability*, that is the knowledge of the movements and changes in the machine components along the years. The traceability of components in a machine is of utter importance for the definition of the irradiation cycle, which is one of the requirements of the matrix method.

6.6.4 Future machines

The matrix method requires a dose rate measurement for the final normalization and cannot be directly applied to future machines. Nevertheless, expression 6.11 can be calculated for predicted values of I_{tot} and Ψ. The matrix method allows estimating the amount and level of radioactive waste to be expected from a future machine for a set of possible scenarios. This method could be used in the feasibility study and in the cost estimate of a new project. In fact, different elemental compositions can be tested and alternative materials can be proposed on the basis of the estimated cost of disposal.

6.7 Corrections and extensions

There are few possible simplifications which extend the applicability of the matrix method to items of waste which only meet part of the requirements of 6.1. As diffusion of volatile nuclides and contamination are not assessed by this method, the characterization should be corrected and completed accordingly.

6.7.1 Extension to waste with non-uniform radiation intensity

If the spectrum of activating particles inside an extended item of waste is uniform in space but the radiation intensity Ψ varies from one point to another, it is still possible to apply the matrix method. The quantity RAD will vary in space but will always be proportional to the dose rate. It is therefore possible to calculate the average and maximum RAD in the item of waste by calculating expression 6.13 for the average and maximum dose rate. However, it is required that the object is made of one single material and that it is far enough from the source of radiation as to have an equilibrium spectrum.

6.7.2 Extension to waste with non-uniform material composition

An item of waste which is composed of sub-components of different materials can be characterized as long as it is possible to measure the dose rate of at least one single sub-component and the activating spectrum is the same for all sub-components. The characterization is first performed on the measured sub-component with 6.13. 6.11 is then applied to the same sub-component in order to estimate the coefficient K, which is the same for all sub-components. The radiological characterization of the remaining sub-components is inferred from 6.11 by using the estimated coefficient K and the appropriate material composition $\vec{W}$.

6.7.3 Completion with contamination assessment

The radiological characterization should be completed by a separate estimate of the contamination, which cannot be calculated directly with the matrix method. The contamination can be quantified by measurements of samples before and after decontamination and by smear tests. The evaluation can be completed with the matrix method only if the material composition of the source of contamination is known. However, even in this case the method is not accurate because the contamination is rarely uniform and is affected by the characteristics of the surface, the chemical properties of the radioactive nuclides and by the geometrical shape of the item of waste.

6.7.4 Correction for volatile nuclides

Attention should be paid to those radioactive nuclides which can escape the item of waste via diffusion. Indeed, the matrix method does not include diffusion in the predictions. Corrective factors should be applied to the activity of the volatile nuclides; alternatively the matrix method will provide a rather conservative estimate of induced radioactivity.

6.8 Disadvantages

Apart from the limits in applicability, there are a few intrinsic disadvantages in the matrix method. Such weak points are of no consequence in the ideal case where all the requirements are satisfied and our knowledge of material composition and radiological history is very accurate. In the real cases, the impact of these disadvantages should be weighted and, if necessary, compensated.

The first disadvantage is that this method is sensibly affected by uncertainty in key input paramters. In the general case, a small uncertainty on one input value will have a small impact on the result. However, the result is proportional to the dose rate and, to a certain extent, to the activity of the dominant γ emitter. In the worst case, the dominant γ emitter is produced by thermal neutrons interacting with traces of one specific element. Any error on the estimate of this trace, which is difficult to measure, will lead to an equivalent error on the final result via the dose rate normalization. In addition, the estimate of the activity of all the radioactive nuclides depends on our knowledge about this trace.

The second disadvantage is that the result depends on a large number of parameters (i.e., energy dependent cross-sections, materials etc). If there is a discrepancy between predicted and measured values of specific activity it is almost impossible to understand the source of error in the calculation, which could be limited to a specific parameter (e.g., our knowledge on the material composition of trace elements in a certain item of waste) or systematic (e.g., errors in the cross sections of positive pions for certain reactions). The matrix method can be validated but not improved by simply applying it to different items of waste. One way to improve it would be to systematically replace predicted cross-sections with newly measured cross-sections or with dedicated activation experiments under well-defined conditions. For items of historic waste which have already been sorted on the basis of their material composition and which are therefore mixed in terms of irradiation time and location in the accelerator, a different method is needed.

Chapter 7

Dependence of induced radioactivity on the irradiation cycle

In the Matrix method presented in chapter 6 the induced radioactivity is calculated analytically and it is normalized to the measured dose rate. This method requires the estimation of the dependence of activity on the radiological history (time build-up). The radiological history, here also referred to as *irradiation cycle*, is defined as the succession of periods of irradiation and waiting, including the time elapsed after the end of the last irradiation. If the irradiation cycle is well known, the time build-up can be calculated exactly. However, there are at least two cases where this is not possible:

a) the radiological history of the material is only partially known,

b) the material consists of a collection of items, each item with a different radiological history.

In case a) we do not know the radiological history but we can use the information available (e.g., production year of the object, year of decommissioning of the machine etc) to infer a probability distribution which reflects our state of knowledge. By collecting additional information it is possible to reshape the distribution. More information on the probability distributions can be found in section 8.3.2.

In case b) we do not know the radiological history of one single object but we know the frequency distribution of all the possible irradiation cycles. Both cases can be addressed with the same mathematical approach. The only difference is that in case a) the probability distribution reflects the present state of knowledge whilst in case b) the frequency distribution is a physical property which depends on how heterogeneous the items are.

In this chapter it is described an original method to calculate the average and maximum time build-up for a given machine and per nuclide. Whenever a simplified formula is used to approximate the exact analytical expression, an estimate of the error introduced is provided. The simplified formulae can be used as the

basis for a reverse calculation, i.e. the estimate of the most probable irradiation cycle for a given measured activity.

7.1 The activation formula

The material activation can be calculated analytically with the activation formula: the specific activity A expected after an irradiation time t_{irr} and a waiting time t_{wait} is:

$$A = I_{Av}\frac{N_{Av}}{M_e}\sum_{i=p,n,\pi}\int \Phi_i(E)\sigma_{i,e,b}(E)\,dE(1-e^{-\lambda_b t_{irr}})e^{-\lambda_b t_{wait}} \tag{7.1}$$

where N_{Av} is Avogadro's number, M_e is the atomic weight of the target material e, $\Phi_i(E)$ is the spectrum of particle i generated by one primary particle, $\sigma_{i,e,b}(E)$ is the particular cross-section for the projectile i leading from the target nucleus e to the desired isotope b and I is the number of primary particles per second. The exponential terms inside the integral represent the time build-up and will be referred to as f_b:

$$f_b(t_{irr}, t_{wait}) = (1-e^{-\lambda_b t_{irr}})e^{-\lambda_b t_{wait}} \tag{7.2}$$

Expression 7.1 is valid only if the beam intensity I is constant during t_{irr}. However, in the operation of particle accelerators the intensity changes in time with the requirements of the different experiments. In terms of radiological characterization, it is very good approximation to assume that the beam loss is constant at least over one year of operation. Corrections for a beam loss which changes every year are presented in section 7.6.

From the activation formula 7.1 we can infer that the induced radioactivity is proportional to the time build-up and to the average number of primary particles per second I_{av}:

$$A \propto I_{av} f_b(t_{irr}, t_{wait}) = I_{tot} g_b(t_{irr}, t_{wait}) \tag{7.3}$$

where A is the activity, I_{tot} is the total number of particles lost during the irradiation time and $g_b = f_b/t_{irr}$.

7.2 Definition of time variables

We define t_{start} as the year when a particle accelerator starts operation, t_{end} as the year when it is decommissioned, t_{in} as the year when the object of interest is introduced in the machine, t_{out} as the year when it is removed and t as the present, or the time when the radiological characterization is calculated (Figure 7.1). The following variables can be deduced from those mentioned above: t_{on} is the machine lifetime ($t_{on} = t_{end} - t_{start}$, typical figures for CERN are from 5 to 30 years), t_{off} is the time from the shutdown ($t_{off} = t - t_{end}$, from 5 to 30

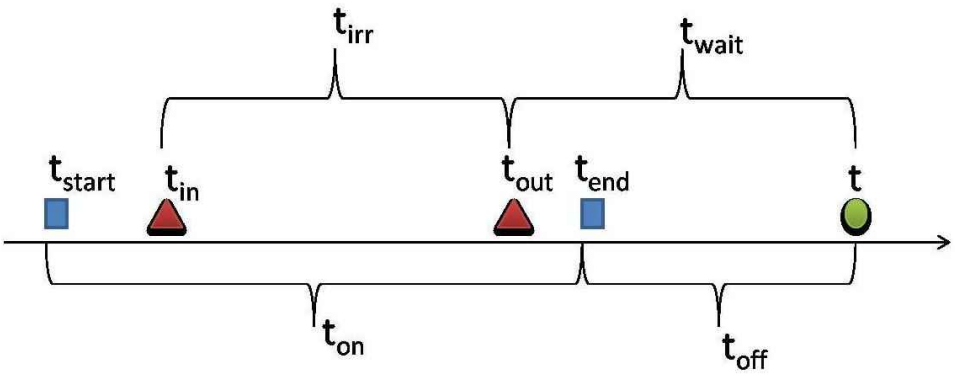

Figure 7.1: Line of time with start and end of the machine operation (squares), introduction and removal of the object (triangles) and present (circle).

years), t_{irr} is the irradiation time ($t_{irr} = t_{out} - t_{in}$, minimum one year) and t_{wait} is the waiting time ($t_{wait} = t - t_{out}$, from 5 to 40 years). For the purposes of radiological characterization, the calculations can be performed just for a limited number of reference t (e.g., t=Jan 2005, Jan 2010, Jan 2015...). Indeed, for most nuclides of interest the calculated activity at t=T* can be conservatively applied to T*<t<T*+5 with very little error.

It is here assumed that t_{on} and t_{off} (and therefore t_{start} and t_{end}) are always known. t_{irr} and t_{wait} are referred to the component, t_{on} and t_{off} to the machine operation. All the time variables are expressed in years.

7.3 Information available on the radiological history

The exact calculation of the time build-up f_b and g_b requires the knowledge of both t_{in} and t_{out}. It is possible to calculate an average (F_b, G_b) and maximum ($F_{b,Max}$, $G_{b,Max}$) time build-up if only one of these parameters is known, as long as there is a probability distribution for the remaining one. The main advantage of these average time build-up is that they no longer depend on unknown parameters.

In the next sections we will calculate the exact formulae of the average time build-up for any nuclide b and for the three following scenarios:

a- t_{in} is known, t_{out} is unknown,

b- t_{in} is unknown, t_{out} is known,

c- $t_{irr} = t_{out} - t_{in}$ is known, both t_{in} and t_{out} are unknown.

In section 7.5 the exact formulae will be simplified depending on the half-life of the nuclide.

There are objects which are exposed to radiation until they break and need to be replaced. In these cases the expected t_{irr} is simply equal to their expected lifetime, which will be called μ For most electric and mechanical devices, it is good

approximation to assume a constant failure rate, which leads to an exponential probability distribution (pdf) for the variable t_{irr}. As a specific example, the exponential distribution represents very well the lifetime of neon lamps.

7.3.1 Scenario a: t_{in} is known, t_{out} is unknown

From the knowledge of t_{in} and t_{end} it is possible to evaluate the maximum irradiation time $T = t_{end} - t_{in}$. The unknown parameter is t_{out}, which can be related to the random variable $x = t_{out} - t_{in}$. The variable x admits an exponential distribution with average irradiation time μ:

$$p_{\mu,T}(x) = \frac{e^{-x/\mu}}{\int_0^T e^{-w/\mu} dw} = \frac{e^{-x/\mu}}{\mu(1 - e^{-T/\mu})} \tag{7.4}$$

The average time build-up is calculated by weighting all possible time build-up with the probability distribution:

$$F_b(\mu, T, t_{off}) = \int_0^T f_b(T, x) p_{\mu,T}(x) dx = \int_0^T (1 - e^{-\lambda_b x}) e^{\lambda_b (T - x + t_{off})} \frac{e^{-x/\mu}}{\mu(1 - e^{-T/\mu})} \tag{7.5}$$

$$F_b(\mu, T, t_{off}) = \frac{\left[\lambda_b \mu - e^{-(1-\lambda_b \mu)T/\mu} + e^{-T/\mu}(1 - \lambda_b \mu)\right]}{(1 - \lambda_b \mu)(1 - e^{-T/\mu})} e^{-\lambda_b (T + t_{off})} \tag{7.6}$$

The maximum time build-up corresponds to continuous irradiation until t_{end}:

$$F_{b,Max}(T, t_{off}) = (1 - e^{-\lambda_b T}) e^{-\lambda_b t_{off}} \tag{7.7}$$

7.3.2 Scenario b: t_{out} is known, t_{in} is unknown

The maximum possible irradiation time T is determined by t_{out}, which is known: $T = t_{out} - t_{start}$. In the random variable $x = t_{out} - t_{in}$, the unknown parameter is t_{in}. As for scenario a, the variable x admits an exponential distribution with average irradiation time μ:

$$p_{\mu,T}(x) = \frac{e^{-x/\mu}}{\int_0^T e^{-w/\mu} dw} = \frac{e^{-x/\mu}}{\mu(1 - e^{-T/\mu})} \tag{7.8}$$

In addition, from t_{out} we can evaluate the time elapsed from the end of irradiation $t_{wait} = t - t_{out}$. The average time build-up is calculated by weighting all possible time build-up with the probability distribution:

$$F_b(\mu, T, t_{wait}) = \int_0^T f_b(T_{wait}, x) p_{\mu,T}(x) dx = \int_0^T (1 - e^{-\lambda_b x}) e^{-\lambda_b t_{wait}} \frac{e^{-x/\mu}}{\mu(1 - e^{-T/\mu})} \tag{7.9}$$

$$F_b(\mu, T, t_{wait}) = \frac{\left[\lambda_b\mu + e^{-(\lambda_b\mu+1)T/\mu} + e^{-T/\mu}(\lambda_b\mu+1)\right]}{(\lambda_b\mu+1)(1-e^{-T/\mu})} e^{-\lambda_b(T+t_{wait})} \tag{7.10}$$

The maximum time build-up corresponds to continuous irradiation from t_{start}:

$$F_{b,Max}(T, t_{wait}) = (1-e^{-\lambda_b T})e^{-\lambda_b t_{wait}} \tag{7.11}$$

7.3.3 Scenario C: $t_{irr} = \mu$ is known, t_{in} and t_{start} are unknown

Although we do not know t_{in}, we can infer from μ that the object has started irradiation at latest μ years before t_{end}. Therefore the maximum time elapsed from t_{start} until t_{in} is $T = t_{end} - t_{start} - \mu$. Within this period, the object may have been introduced in the machine in any time with equal probability. The probability distribution of $x = t_{end} - t_{out}$ is thus linear:

$$p_T(x) = \frac{1}{T} \tag{7.12}$$

The average time build-up is:

$$F_b(\mu, T, t_{off}) = \int_0^T f_b(t_{off}, x) p_T(x) dx = \int_0^T (1-e^{-\lambda_b\mu})e^{-\lambda_b(x+t_{off}} \frac{1}{T} dx \tag{7.13}$$

$$F_b(\mu, T, t_{off}) = \frac{(1-e^{-\lambda_b\mu})(1-e^{-\lambda_b T})}{\lambda_b T} e^{-\lambda_b t_{off}} \tag{7.14}$$

The maximum time build-up is obtained by taking the limit of T to 0, which corresponds to an irradiation time $t_{irr} = \mu$ followed by the waiting time $t_{wait} = t_{off}$, i.e. $t_{out} = t_{end}$:

$$F_{b,Max}(\mu, t_{off}) = \lim_{T\to 0} \frac{(1-e^{-\lambda_b\mu})(1-e^{-\lambda_b T})}{\lambda_b T} e^{-\lambda_b t_{off}} = (1-e^{-\lambda_b\mu}e^{-\lambda_b t_{off}} \tag{7.15}$$

7.4 Calculation of the uncertainty of the time build-up

In addition to the average and maximum values, it is useful to associate an uncertainty to the evaluation of the time build-up. The same uncertainty on the radiological history has different impact on F_b depending on the half-life of the nuclide b. In order to quantify the impact we define an error $\epsilon_b(n)$ as:

$$\epsilon_b(\tau) = \frac{f_b(t_{irr}+\tau, t_{wait}-\tau) - f_b(t_{irr}, t_{wait})}{f_b(t_{irr}, t_{wait})} \tag{7.16}$$

where τ is the number (or fraction) of years of uncertainty on t_{out}. The higher τ, the longer the irradiation time and the shorter the waiting time.

By substituting Expression 7.2 in Expression 7.16:

$$\epsilon_b(\tau) = \frac{e^{\lambda_b \tau} - 1}{1 - e^{-\lambda_b t_{irr}}} \tag{7.17}$$

Expression 7.17 is exact and valid for both positive and negative τ. For long-lived nuclides ($T_{1/2}$>33 years) it reduces to $\epsilon_b(\tau) \approx \tau / t_{irr}$. For short-lived nuclides ($T_{1/2}$<1 year) it approximates to $\epsilon_b(\tau) \approx \sqrt[T_{1/2}]{2^\tau} - 1$. For example, if t_{irr} is expected to be 20 years with one year uncertainty, the uncertainty on the time build-up would be 5% for 137-Cs ($T_{1/2}$=30 years) and 150% for 57-Co ($T_{1/2}$=272 days). The uncertainty on the time build-up does not depend on t_{wait}.

7.5 Categories of nuclides

The formulae presented in section 7.3 can be actually simplified in different ways depending on the half-life of the nuclide, which can be sorted in four categories:

1. nuclides with $T_{1/2} < 1$ year;
2. nuclides with 1 year $< T_{1/2} <$ 30 years;
3. nuclides with 30 years $< T_{1/2} <$ 100 years;
4. nuclides with $T_{1/2} >$ 100 years.

For the first category, only the last few years of the irradiation cycle are relevant for the time build-up. The second category requires the most complex calculation because the time build-up varies with the machine lifetime, which is comparable to $T_{1/2}$. For the third category this dependence is less important and the calculation can be further simplified. For the last category only the total number of nuclear reactions is relevant and not their time distribution over the irradiation cycle. The choice of 1, 30 and 100 years as limits between the categories is based on the validity of the proposed methods.

7.5.1 Time build-up for nuclides with $T_{1/2} < 1$ year

There are few nuclides with half-life shorter than one year and which are of interest for elimination in the final repositories, namely: 49V, 54Mn, 57Co and 65Zn. The activity of these nuclides is likely to be close to saturation by the end of operation. The error introduced by the assumption would be 0.1% for nuclides with $T_{1/2}$=1 year and t_{irr}=10 years.

Scenario a

By setting in Expression 7.5, the time build-up for scenario a (cf. Section 7.3.1) becomes:

$$F_b(\mu, T, t_{off}) = \int_0^T f_b(T, x) p_{\mu,T}(x) dx \leq \int_0^T e^{\lambda_b(T-x+t_{off})} \frac{e^{-x/\mu}}{\mu(1-e^{-T/\mu})} dx \quad (7.18)$$

$$F_b(\mu, T, t_{off}) = \frac{e^{-\lambda_b \mu} - e^{-\lambda_b T}}{(\lambda_b \mu - 1)(1-e^{-T/\mu})} e^{-\lambda_b t_{off}} = \frac{(e^{-\lambda_b T} - e^{-\lambda_b \mu}) e^{-\lambda_b t_{off}}}{(1-e^{-T/\mu})(1+\lambda_b \mu)} \quad (7.19)$$

Expression 7.19 can be further simplified depending on whether the object has long or short lifetime μ:

$$\mu < 1/\lambda_b \Rightarrow F_b(\mu, T, t_{off}) \approx \frac{e^{-lambda_b T}}{(1-\lambda_b \mu)} e^{-\lambda_b t_{off}} \quad (7.20)$$

$$\mu > 1/\lambda_b \Rightarrow F_b(\mu, T, t_{off}) \approx \frac{e^{-T/\mu}}{(\lambda_b \mu - 1)(1-e^{-\lambda_b t_{off}})} e^{-\lambda_b t_{off}} \quad (7.21)$$

Scenario b

In the calculations for scenario b (cf. Section 7.3.2), the probability distribution decreases with increasing t_{irr}. The term has higher probability weight for small values of t_{irr} and therefore it cannot be set to 1 as for scenario a. Expression 7.10 should be used without any simplification.

Scenario c

The simplification applied to Expression 7.14 leads to:

$$F_b(T, t_{off}) = \int_0^T f_b(t_{off}, x) p_T(x) dx \leq \int_0^T e^{-\lambda_b(x+t_{off})} \frac{1}{T} dx \quad (7.22)$$

$$F_b(T, t_{off}) = \frac{(1-e^{-\lambda_b T})}{\lambda_b T} e^{-\lambda_b t_{off}} \approx \frac{e^{-(\lambda_b t_{off})}}{\lambda_b T} \quad (7.23)$$

7.5.2 Time build-up for nuclides with 1 year $< T_{1/2} <$ 30 years

These nuclides have a half life which is comparable to the irradiation time and the waiting time, typical for most items of waste at CERN (the average lifetime of an accelerator is about twenty-five years). The function f_b is therefore very sensitive to the exact irradiation cycle. The formulae 7.4-7.5 can be simplified only in the special case where the expected irradiation time is much shorter than the maximum possible irradiation time: $T > 5\mu$.

Scenario a, T>5μ

The time build-up for the scenario a can be simplified in different ways depending on how long the lifetime μ of the object is with respect to the decay time of the nuclide b.

If $\mu > 1/\lambda_b$:

$$\begin{aligned} F_b(\mu, T, t_{off}) &= \lim_{T/\mu \to 0} \frac{\left[\lambda_b\mu + e^{-(1-\lambda_b\mu)T/\mu} + e^{-T/\mu}(1-\lambda_b\mu)\right]}{(1-\lambda_b\mu)(1-e^{-}T/\mu)} e^{-\lambda_b(T+t_{off})} \\ &= \frac{e^{-T/\mu}}{(\lambda_b\mu - 1)} e^{-\lambda_b t_{off}} \end{aligned} \tag{7.24}$$

If $\mu < 1/\lambda_b$:

$$\begin{aligned} F_b(\mu, T, t_{off}) &= \lim_{T/\mu \to 0} \frac{\left[\lambda_b\mu + e^{-(1-\lambda_b\mu)T/\mu} + e^{-T/\mu}(1-\lambda_b\mu)\right]}{(1-\lambda_b\mu)(1-e^{-}T/\mu)} e^{-\lambda_b(T+t_{off})} \\ &= \frac{\lambda_b\mu}{(1-\lambda_b\mu)} e^{-\lambda_b(T+t_{off})} \end{aligned} \tag{7.25}$$

Scenario b, T>5μ

In the build-up for scenario b the term $(\lambda_b\mu - 1)$ does not appear and therefore there is one single simplified formula for any value of μ:

$$\begin{aligned} F_b(\mu, T, t_{wait}) &= \lim_{T/\mu \to 0} \frac{\left[\lambda_b\mu + e^{(\lambda_b\mu+1)T/\mu} + e^{-T/\mu}(\lambda_b\mu+1)\right]}{(\lambda_b\mu+1)(1-e^{-}T/\mu)} e^{-\lambda_b t_{wait}} \\ &= \frac{\lambda_b\mu}{(1+\lambda_b\mu)} e^{-\lambda_b t_{wait}} \end{aligned} \tag{7.26}$$

Scenario c

The time build-up for scenario c cannot be simplified and Expression 7.14 must be used even under the hypothesis $T > 5\mu$.

7.5.3 Time build-up for nuclides with 30 years $< T_{1/2} <$ 100 years

In this case the half life is so long that it is not necessary to average the time build-up over all the possible irradiation times. The proposed formula is:

$$g_b(t_{wait}) = \frac{f_b(t_{irr}, t_{wait})}{t_{irr}} \approx \lambda_b(1 - \lambda_b t_{wait}) = G_b(t_{wait}) \tag{7.27}$$

Expression 7.27 is composed by two terms:

$$\lambda_b \geq \frac{(1 - e^{-\lambda_b t_{irr}})}{t_{irr}} \tag{7.28}$$

, and

$$(1 - \lambda_b t_{wait}) \leq e^{-\lambda_b t_{wait}} \tag{7.29}$$

The overestimate in the first term partially compensates for the underestimate in the second term. The error introduced by this simplification $[(g_b - G_b)/g_b]$ is always lower than 1% in the time scale of interest ($33 < T_{1/2} < 100$ years, $t_{irr} > 5$ years, $1 < t_{wait} < 40$ years). The waiting time t_{wait} can be replaced with the time t_{off} from the shutdown of the facility (which is equal or shorter than the time t_{wait} from the removal of the item) with negligible effects on the G_b.

The average time build-up depends on the expected lifetime μ of the object but not on t_{in} or t_{out}:

$$F_b(\mu, t_{wait}) = \mu g_b t_{wait} = \lambda_b \mu (1 - \lambda_b t_{wait}) \tag{7.30}$$

The maximum time build-up is:

$$F_{b,Max}(t_{on}, t_{wait}) = t_{on} g_b t_{wait} = \lambda_b t_{on} (1 - \lambda_b t_{wait}) \tag{7.31}$$

7.5.4 Time build-up for nuclides with $T_{1/2} > 100$ years

A large number of nuclides of interest for the radiological characterization fall in this category. The half life is so long that only a negligible fraction of radioactive nuclides decay during the waiting time. For the same reason, the activity at the end of the irradiation time is so far from saturation that the dependence of f_b on t_{irr} is almost linear. The scenarios a-c thus lead to the same formula for the time build-up:

$$g_b = \frac{f_b(t_{irr}, t_{wait})}{t_{irr}} = \frac{(1 - e^{-\lambda_b t_{irr}})(e^{-\lambda_b t_{wait}})}{t_{irr}} \approx \lambda_b \tag{7.32}$$

This formula does not depend on the machine but only on the nuclide and it is accurate within 1% error for the irradiation cycles of interest. The time build-up therefore depends on the total number of particles I_{tot} and its error is equal to our uncertainty on I_{tot}.

The average and maximum time build-up are:

$$F_b(\mu) = \mu \lambda_b \tag{7.33}$$

$$F_{b,Max}(T) = T \lambda_b \tag{7.34}$$

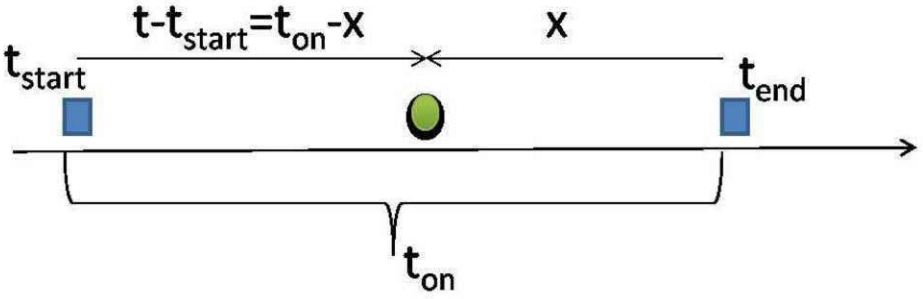

Figure 7.2: Line of time with start and end of the machine operation (squares), and integrating variable x (circle).

7.6 Correction for non-uniform irradiation cycles

The above analysis was performed for the case of a uniform beam loss rate I_{av}, in which case the activity is proportional to $I_{av,b}F_b$ (Expression 7.3). For an arbitrary beam loss rate $I(t-t_{start})$ which is a function of the time $t-t_{start}$ from the beginning of the machine operation, Expression 7.3 is not valid unless $I_{av,b}$ is calculated appropriately and takes into account the half life of the nuclide. Indeed, for the time build-up of short lived nuclides it is mainly the beam losses at the end of the irradiation which play a role. The activity of a nuclide decreases exponentially with time. It is therefore intuitive that also the contribution of beam losses to the time build-up should be weighted with an exponential function of time. The following analysis, which is in principle valid for any nuclide, is particularly important for nuclides with half life shorter than 30 years. For the other nuclides only I_{tot} is of relevance for the characterization and no correction is needed.

If the beam loss rate I(t) is not constant the exact time build-up is:

$$\int_0^{t_{on}} \lambda_b e^{-\lambda_b x} I(t_{on}-x)dx \tag{7.35}$$

where t_{on} is the irradiation time and we have set $t-t_{start}=t_{on}-x$. Figure 7.2 shows the line of time with the variables used in Expression 7.35.

By setting Expression 7.3 equal to Expression 7.35 we obtain the definition of the average $I_{av,b}$:

$$I_{av,b}=\frac{\int_0^{t_{on}} \lambda_b e^{-\lambda_b x} I(t_{on}-x)dx}{1-e^{-\lambda_b t_{on}}} \tag{7.36}$$

For the special case $I(t-t_{start})=I$, constant over $0<t-t_{start}<t_{on}$, we obtain $I_{av,b}=I$ as it should be. The integral in Expression 7.36 can be transformed into a sum under the hypothesis that $I(t-t_{start})=I(t_{on}-x)$ be constant during one year, i.e. $I(t_{on}-k-x)=I(t_{on}-k)$ for 0<x<1 year and k=0,1,2,...,t_{on} years. This leads to:

$$\int_k^{k+1} \lambda_b e^{-\lambda_b x} I(t_{on}-x)dx = \int_k^{k+1} \lambda_b e^{-\lambda_b x} I(t_{on}-k)dx = I(t_{on}-k)(1-e^{-\lambda_b})e^{-\lambda_b l} \tag{7.37}$$

$$\Rightarrow \int_0^{t_{on}} \lambda_b e^{-\lambda_b x} I(t_{on}-x)dx = \sum_{k=0}^{t_{on}-1} (1-e^{\lambda_b})e^{-\lambda_b k} I(t_{on}-k) \tag{7.38}$$

After some algebra we obtain the value of I_{av} from Expressions 7.36 and 7.38:

$$I_{av,b} = \frac{e^{\lambda_b}-1}{e^{\lambda_b t_{on}}-1} \sum_{m=0}^{t_{on}-1} e^{\lambda_b m} I(m) \tag{7.39}$$

The average $I_{av,b}$ must be calculated for every machine and is nuclide dependent (i.e. it is a function lf λ).

Expression 7.39 should be used as it is for nuclides with half life between 1 and 33 years and can be simplified for the case of nuclides with half life shorter than one year in the following way. We first define the new variable and we substitute it in Expression 7.39. The sum over the years of operation can be reduced to include only the last three years of operation because the contribution from the previous years is in general lower than 2% (error calculated for a representative nuclide with $T_{1/2}$=0.5 year and beam intensity constant over t_{irr}). After substitution we obtain:

$$I_{av,b} = /frac1-\alpha_b 1-\alpha_b^3 \left[I(t_{on}) + \alpha_b I(t_{on}-1) + \alpha_b^2 I(t_{on}-2)\right] \tag{7.40}$$

Expression 7.40 might seem complex, but this is only because the dependence on α_b has been left in evidence. If we apply it to the specific case of V49 and Mn54 we obtain:

$$A \propto I_{av,b} f_b = \frac{0.24 I_0 + 0.12 I_1 + 0.06 I_2'}{2_{t_{off}}} \tag{7.41}$$

where I_0 is the beam loss during the last year of operation, I_1 refers to the previous year etc.

As an example of the analysis that these simplified formulae allow, from Expression 7.41 we learn that to improve the accuracy of our predictions on the activity of Mn54 we should first improve our knowledge of t_{off} rather than the one of the beam loss I_1 and I_2. Indeed, an error of one year on t_{off} has the same impact as an error of a factor of 6 on I_2. For comparison, in the case of Ni63 an error of one year on t_{off} has an impact of 0.67% on the activity of Ni63, whilst an error of a factor of 6 on I_2 corresponds to $500 \cdot (I_2/I_{tot})$% (values calculated from Expression 7.27).

7.7 Conclusions

The present chapter assesses the dependence of induced radioactivity on the irradiation cycle. It is found that in most cases the complete analytical expression which describes the time build-up can be considerably simplified without introducing significant errors in the estimate. Certain simplifications require at least some knowledge on the machine history, whilst others are of general validity. Uncertainties on the radiological history of an item were converted into statistical errors on the activity. Simplifications and uncertainties are very much nuclide-dependent and can be classified on the basis of the nuclide half-life and on the object lifetime.

As soon as the parameters are calculated for the machine and object of interest, the formulae allow estimating the time build-up of any nuclide with a rather simple mathematical expression.

All information that is strictly required is relative to the machine and to the average lifetime of the objects to be characterized. If the results refer to objects with the same radiological history, further information on the irradiation conditions will reduce the uncertainty on the estimated activity. If the results refer to an entire class of objects with different radiological histories, the activity distribution will be a physical property of the objects which cannot be reduced.

The idea of performing calculations with probability distributions rather than single values is further developed in section 8.3. The method can indeed be applied to material composition and particle spectrum in the same way it has been applied to the time build-up.

Chapter 8

Further methods for the radiological characterization

8.1 The direct FLUKA calculation

If the radiological history and the material composition are well known, the induced radioactivity can be calculated directly with the Monte Carlo code FLUKA [78, 102]. In particular, the latest version of FLUKA (2006) has an improved evaporation and multi-fragmentation model which allows for a more accurate prediction of induced radioactivity. Recent experiments in the CERN-EU High-Energy Reference Field (CERF) facility [108] have shown that most nuclides produced in materials commonly used in accelerators are predicted within 20% accuracy [26].

8.1.1 Relevant settings

Although most FLUKA commands are optional, there are a few which are nearly always needed in order to provide a meaningful definition of the problem to be studied. In general, the following elements need to be defined:

- the radiation source;
- the geometrical layout;
- the materials;
- the requested results;
- setting of parameters and technical directives.

Some physical effects are automatically activated, but others can be switched off or on by the user with appropriate commands. For example, the transport of the electromagnetic shower can be disactivated for studies of induced radioactivity in hadron accelerators and activated for electron accelerators.

The most recent evaporation model with heavy fragment evaporation is not activated by default and must be switched on with the card PHYSICS EVAPORAT. This physics effect is of uttermost importance in prediction of induced radioactivity because the evaporation of fragments determines the type of radioactive nuclide produced in a reaction. In addition to the option EVAPORAT, also the option COALESCE must be requested in order to include the coalescence effect in the nuclear model. Evaporation of fragments and coalescence are not automatically activated because they are CPU time consuming and do not have any impact on most of FLUKA applications.

The photonuclear reactions are requested by the card PHOTONUC. These reactions have very small cross-sections with respect to other electromagnetic interactions with atoms and electrons. They become very important for electron accelerators like LEP and are negligible in hadron accelerators. In the latter case, the electromagnetic cascade is often not transported for an efficient use of CPU time and the photnuclear reactions are discarded. The same reasoning applies to muon photonuclear interactions, which are included with the card MUPHOTON.

The scoring of induced radioactivity can be done in different ways. The first method is to score the production rate of radioactive nuclides per primary particle and to do the analysis off-line. The second method is to request FLUKA to go further in the calculations and predict the specific activity expected after a given irradiation cycle. The irradiation cycle is defined via the cards RADDECAY, DCYTIMES and DCYSCORE.

The geometry to be studied is always defined according to the rules of combinatorial geometry and consists of several regions, where each region is assigned a material. The scoring of induced radioactivity can be done per region or in a regular spatial structure which is independent from the geometry.

Due to anavoidable simplifications introduced in the geometry definition,some regions may be relatively large and correspond in reality to a group of components with finer structures. Scoring per region can only provide the average value of activity in the whole volume without any information on the distribution within the region. This has the unfavorable effect that hot spots cannot be detected by this method. On the other hand, scoring in large regions offers the advantage of better statistics.

8.1.2 Off-line treatment of time build-up

As mentioned above, FLUKA can be requested to produce formatted files, which contain estimates of the production rate of radioisotopes per region and per primary particle. The production rate is then multiplied by the time build-up, which is calculated with an off-line routine called *usrsuw*. This routine solves the Bateman equations up to the third generation.

With this method, the scoring can only be performed on a region basis. In order to calculate the specific activity per region, the region volumes must be calculated by the user. A special Monte Carlo technique has been developed

for this purpose. All regions are assigned vacuum and are enclosed in a virtual spherical isotropic source of neutrons. The track-length of these neutrons inside a region is proportional to its volume. The normalization coeffient can be calculated by comparison with the track-length in a region of known volume.

8.1.3 On-line treatment of time build-up

An online treatment with the exact analytical solution of the Bateman equations has been recently implemented in FLUKA [109]. This treatment provides a more accurate approach to the production and time evolution of residual nuclei because it considers all possible successive decays down to the last stable decay product. In addition, it allows FLUKA to simulate complex irradiation conditions consisting of several periods of irradiation and intermittent cooling times. Furthermore, it records the exact position where every nuclide was produced and therefore provides the user with the induced radioactivity distribution. On-line treatment of the time build-up can make use of these latest implementations.

Scoring can be requested on a region-independent geometrical mesh encompassing the whole geometry. The advantage of this method is that the bins can be of arbitrary size and it is possible to study the distribution of induced radioactivity within any single region. On the other hand, one bin could lay on the border between two different regions and lead to unphysical results. The size of the bin is a balance between the probability of including two regions (large bins) and the difficulty of obtaining low statistical errors (small bins).

From the physics point of view the greatest difference between the off-line and the on-line time treatment lies in the accuracy with which the build-up and decay of radioactivity are calculated.

8.1.4 General considerations on the FLUKA method

The direct FLUKA calculation is particularly appropriate for large and complex items, as shown in radiological studies performed for the ATLAS detector of the future Large Hadron Collider (LHC) at CERN [4]. Monte Carlo allows transporting particles through complex geometries and predicting induced radioactivity even in those cases where the radiation field changes dramatically with position. The price for these capabilities is that each specific study requires on average months of work in terms of geometry implementation, computational time and data analysis. Moreover, the results are valid for the specific case studied but, as a general rule, cannot be extended to other cases without important investements in time.

Due to the above considerations, independently of the specific time-treatment used, there are cases where the full Monte Carlo calculation is not efficient for the radiological characterization. For example, it is not efficient to run one entire simulation per item of waste only because of different details in the geometry or to account for slightly different material composition. A different method,

specifically developed for such cases, is described in chapter 5.

An important limitation of direct Monte Carlo calculations, especially for on-line time treatment, is the fact that all input parameters must be known before launching the simulations, because they must be implemented in the input code in order to be taken into account. It is technically impossible to make a parametric study.

Experimental validation of the calculations is recommendable because the uncertainties associated to nuclear models and simplifications in the geometry. Uncertainties on irradiation conditions or trace elements can be reduced with gamma spectroscopy and radiochemical analysis.

8.2 Gamma spectroscopy measurements

The radiological characterization can be entirely based on gamma-spectroscopy measurements, in a way similar to the approach of the Ispra Laboratory. A description of the detectors available on the market is given in a dedicated section of this study. In this section, attention is paid to the benefit of such a system for CERN requirements.

A system for gamma-spectroscopy is an important investment (in the order of 1 M euros), which can be justified only if it can be used continuously over the years. This is equivalent to say that the amount of waste which can be characterized by such a system must be large enough to pay back the investment.

The characterization requires the calculation or the measurement of a calibration factor. One calibration factor is needed per kind of waste and per type of radionuclide inventory. There is also a limit on the size and weight of the item of waste because:

- an item which is too big cannot enter the counting chamber;
- it is impossible to detect the presence of a source inside an item which is too massive.

The selection of candidate waste for this kind of characterization requires a preliminary study about the impact of size and weight on the calibration factor, with a view to characterize the largest fraction of waste with the least number of factors required.

In addition to the characterization for final elimination, such a system can be used during the operation of LHC to distinguish between materials which can be handled in a normal workshop and those which require a special workshop for handling of radioactivity. The combined use of the system for radioactive waste management and operational radiation protection is an interesting option for optimization of resources.

An alternative - if the amount of candidate waste does not justify the purchase - is to rent such a system for a certain number of months.

As a last remark, it is not recommended to postpone the measurements and wait for decay below the limits, especially when the free-release conditions are not fulfilled because of long-lived nuclides. In this case the waiting time would be unduly long. Moreover, the later decision measurement will be more difficult due to the decay of nuclides which are easibly measurable, like 60-Co.

8.3 The statistical method

The radiological characterization must incorporate sufficient safeguards to provide what is called *defence in depth* [110]. Such safeguards compensate - to a certain extent - for the uncertainties associated with the input parameters and the models used for the characterization. It is common practice to require that the key parameters are set with a certain degree of conservatism.

All of the models used in the characterization, as well as the input data, have associated uncertainties. These uncertainties arise through assumptions made about the irradiation conditions and through the lack of knowledge about material composition. In order to account for these uncertainties, one can develop distributions of values for the parameters rather than use simple values, in a way which is similar to the one presented in chapter 7. The probability distribution of the input parameters can be assigned specific shapes that reflect the likelihood that any one value in the distribution will occur. The likelihood takes into account the state of knowledge (i.e. the experience) prior to any measurement (cf. section 8.3.1).

The uncertainties of the input values are propagated through the model and lead to uncertainties in the output values (cf. section 8.3.3). This method will be referred to as *statistical*.

To a certain extent, the statistical method has already been applied to the calculation of the time build-up. However, if the application to one single input parameter is relatively straightforward, the extension to a set of input parameters is rather complex and requires careful analysis.

The statistical method represents the natural development of the matrix method from the domain of single values to the one of probability distributions. As such, it cannot be developed until the matrix method is fully operative and experience has been gained from its first applications. The goal of the present study is to describe the underlying philosophy and to provide guidelines for its implementation.

8.3.1 Bayes

The statistical method is based on Bayesian statistics. The main difference between Bayesian and conventional statistics lies in the different use of the term probability. The object of conventional statistics is the probability distribution $f(x|\hat{x})$, which is the probability distribution of estimates x for a given true value $\hat{x}$. The task of the experiment is actually to make statements about $\hat{x}$, which is

unknown. In addition to $f(x|\hat{x})$, the Bayesian statistics also allows calculating the probability distribution $f(\hat{x}|x)$, which is the conditional distribution of the true value $\hat{x}$ given the measured estimate x.

The so-called *posterior* distribution $f(\hat{x}|x)$ is calculated by weighting the information from the experiment with the prior information:

$$f(\hat{x}|x) = K f_0(\hat{x}|x) f(\hat{x}) \tag{8.1}$$

where K is a normalization constant, the ***likelihood*** $f_0(\hat{x}|x)$ is the probability distribution that the measurand has the true value $\hat{x}$ if only the measured value x is given, and the *model prior* $f(\hat{x})$ represents the information about the measurand prior to the measurement.

The conditional distribution of the true value $f(\hat{x}|x)$ can be calculated with the principle of maximum information entropy S [111]:

$$S = -\int f_0(\hat{x}|x) f(\hat{x}) ln\left(f_0(\hat{x}|x)\right) d\hat{x} \tag{8.2}$$

The solution of equation 8.2 can be obtained with the multiplicators of Lagrange [112]:

$$f(\hat{x}|x) = K f(\hat{x}) e^{-\frac{(\hat{x}-x)^2}{(2u^2(x))}} \tag{8.3}$$

where u(x) is the uncertainty on the experimental value x.

An application of expression 8.3 is described in [113] and is here reported as an example. In the measurand is the activity of a radiation source, there exists the meaningful information that the measurand is non-negative before the measurement is carried out. This is to say:

$$f(\hat{x}) = \begin{cases} const & \text{if } \hat{x} \geq 0 \\ 0 & \text{if } \hat{x} < 0 \end{cases} \tag{8.4}$$

In this example it is assumed that there is no other information available before the experiment and therefore all positive values of $\hat{x}$ have the same probability. The distribution $f(\hat{x}|x)$ is a product of the model prior $f(\hat{x})$ and a truncated gaussian (see Figure 8.1, which is taken from [114]). The important difference of the guassian distribution in equation 8.3 with respect to conventional statistics is that it is not an approximation of the distribution of measured values from repeated measurements. Instead, it expresses the state of knowledge about the measurand x and is the explicit result of the maximisation of information entropy [113].

Further applications to count-rate measuring systems and spectrometric measurements can be found in [114].

8.3.2 Probability distributions

The choice of the appropriate probability density function certainly depends on the judgement of the expert. In particular, it is the expert who should use her

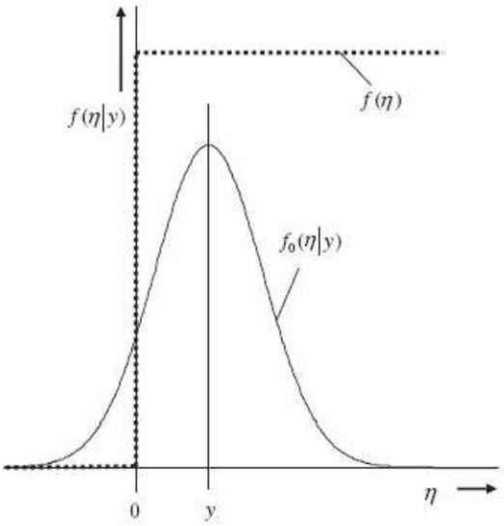

Figure 8.1: Probability distribution of the true value η ($\hat{x}$ in the text) given in equation 8.3 for a non-negative measurand y (x in the text).

experience to convert the available information into mathematical uncertainties. In this sections the most frequent distributions are presented.

The probability density function for a continuous uniform distribution on the interval [a,b] is:

$$f(x) = \begin{cases} 0 & \text{for } x < a \\ \frac{1}{b-a} & \text{for } a \leq x \leq b \\ 0 & \text{for } x > b \end{cases} \tag{8.5}$$

This function is also referred to as *rectangular* distribution. It is used in section 7.3.3 to calculate the time build-up for an object with known life time.

The sum of two quantities, each being assigned a rectangular distribution, is best represented by a triangular distribution like the one given in Figure 8.2. This distribution is described by the following set of conditions:

$$f(x) = \begin{cases} \frac{2(x-a)}{(b-a)(c-a)} & \text{for } a \leq x \leq c \\ \frac{2(b-x)}{(b-a)(b-c)} & \text{for } c \leq x \leq b \end{cases} \tag{8.6}$$

The principle of maximum entropy can be applied to a measurand which is known to lie between the values $a \pm d$ and $b \pm d$. This is the case of a uniform distribution but with limits which are prescribed inexactly. The principle of maximum entropy leads to a *curvilinear trapezoid* [113] like the one shown in Figure 8.3.

The implementation of the statistical method for the radiological characterization requires more probability distributions than those described in this section. The most important ones are the exponential (cf. section 7.3.1) and the gaussian distributions.

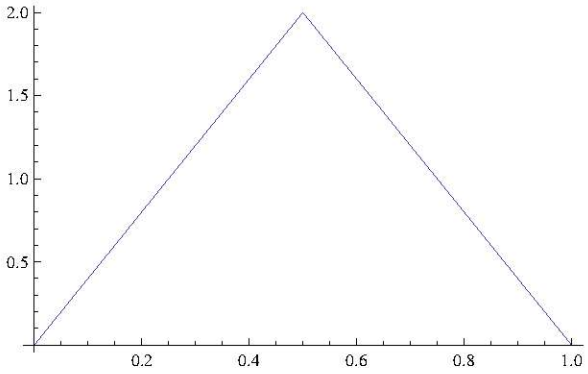

Figure 8.2: Triangular probability distribution with a=0, c=0.5 and b=1.0.

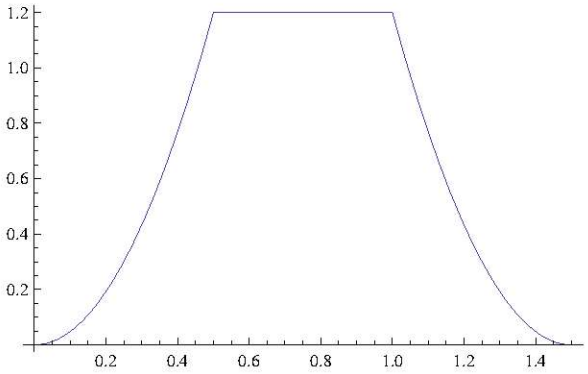

Figure 8.3: Curvilinear trapezoid, probability distribution with inexact lower and upper limits.

8.3.3 Uncertainty propagation

The radionuclide inventory inherits the uncertainties associated to the input values and described by the probability distributions above. The law of propagation of uncertainty evaluates the standard uncertainty associated with an estimate of the output quantity, given the estimates and uncertainties of the input quantities and the degrees of freedom associated with them.

There are several ways to implement the propagation of distributions.

- numerical methods;
- exact analytical methods;
- approximated analytical methods, where the model is replaced by Taylor series.

The analytical methods can be easily applied in simple cases and become very complex with the real cases. They have the advantage of evaluating the propagation exactly without any approximation [115] [116]. However, due to the complexity of the calculations involved only the first- or higher-order Taylor series approximation are of practical use. As an alternative, numerical methods are an effective way to estimate the propagation by providing a numerical representation of the distribution for the output quantity.

8.3.4 Detection limit and decision threshold

Depending on the purpose of the radiological characterization, there are activity limits or constraints to which the radionuclide inventory must be compared (cf. sections 1.3 and 1.2), which in this section will be referred to as guideline values. In the general case, the elimination pathway of the radioactive waste is decided based on whether the activity is above or below the guidelinevalues. The activity is estimated via calculations or measurements. At this point, it is important to distinguish between detection limits and decision threshold, as recommended by the International Organization for Standardization [113].

The decision threshold y^* allows a decision to be made as to whether the registered pulses in a measurement include a contribution by the sample. The detection limit η^* is the lowest amount of activity that can be distinguished from the absence of activity within a stated confidence limit. For non-negative measurands it is always true that $0 < y^* < \eta^*$. The difference between using the detection limit and the decision threshold is that measured values are to be compared with the decision threshold while the detection limit is to be compared with the guideline value. In practice, this means that if the measurand is below the decision threshold, it can be concluded that the true value of the measurand is below the guideline with a probability of error of $< \beta$. If the measurand is above the decision threshold, there is a probability $< \alpha$ that the true value is zero. The errors α and β are decided by the user and determine - together with

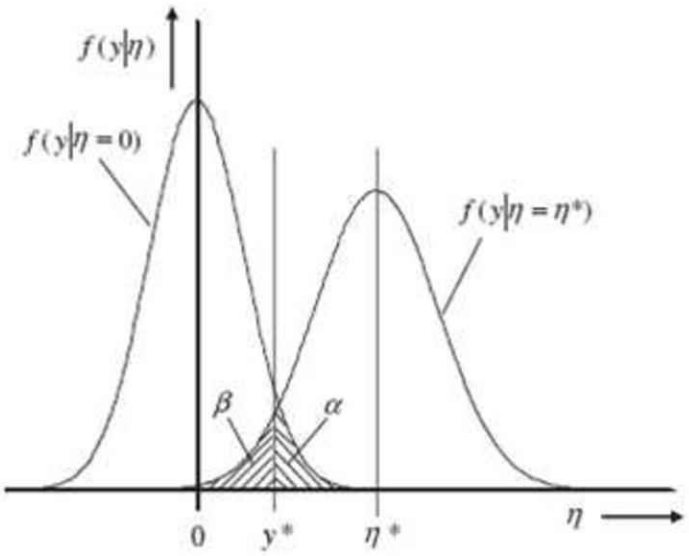

Figure 8.4: Illustration of the decision threshold y^* and the detection limit η^*.

the measurement or calculation uncertainty and the guideline value - the decision threshold.

It is evident that if there are large uncertainties in the measurements, the decision threshold is relatively small and it becomes difficult to prove that the item of waste is below the guideline values. The uncertainty is affected by the quality of the detector but also by the availability of information and by the accuracy of the calculations for the uncertainty propagation.

A detailed mathematical foundation of Bayesian characteristic limits can be found in [111]. The above concepts are illustrated in Figure 8.4- which is taken from [114]- where $f(y|\eta)$ is the conditional probability of obtaining y in the measurement when the true value is η.

8.3.5 Considerations on the statistical method

The application of the Bayesian theory to measurements of induced radioactivity has found its way in Germany - at least in the form of guidelines. German are indeed most of the articles available in literature on this subject. In the final repository of the Aube (cf. section 1.4.2) in France, proof of fullfillment of the acceptance criteria can be based on statistical considerations. However, no precise guideline is given concerning the recommended statistical techniques nor the Bayesian method is mentioned. The application of the statistical method to Monte Carlo predictions of induced radioactivity is still an unexplored domain.

The method here proposed can be summarized as follows:

- collection of the available information and choice of the probability distributions for the input values;

- calculations with Monte Carlo, measurements, application of the Matrix or the Fingerprint method to predict the induced radioactivity;
- calculation of the propagation of uncertainty and estimate of the error associated to the output values;
- comparison with the decision threshold, to be calculated based on the guideline values and the uncertainties above.

If the result is close to the decision threshold and if the financial impact of the decision is worth investing additional resources, the procedure can be repeated to reduce the uncertainty and set the decision threshold at a higher level.

Chapter 9

Conclusions

9.1 A challenging task

The operation of particle accelerators leads to the unavoidable production of radioactive waste. The radioactivity induced in the accelerator components consists of beta and gamma emitters, and in exceptional cases might contain alpha emitters. The situation is therefore rather different than for nuclear reactors, where most of the radiological hazard lies in contamination and fissile materials.

The elimination of an item of radioactive waste towards final repositories requires the radionuclide inventory, i.e. a list of nuclides with their specific activity. At present there is no single method for the radiological characterization which can be applied to all items of waste from any particle accelerator, because the material activation strongly depends on the irradiation conditions which are specific to each machine. The approaches adopted by other laboratories in Europe span from analytical calculations like at PSI, which are the result of a 15-year study, to high-technology measurement systems like at JNRC in Ispra, which require a multi-million budget. The development of a method to meet the needs of CERN - the largest accelerator's complex in Europe - with a limited budget and on a few-year time scale is, to say the least, a challenging task.

The characterization of CERN waste shall take into account a number of factors, which were covered in the present study. From the legal point of view, depending on the origin of the waste it is either the Swiss or the French legislation which applies. A part for the different sets of radioactivity limits, also the underlying philosophy is different from one legislation to the other. The most remarkable difference is the possibility of free-release for the Swiss waste. Moreover, every Country has its own elimination pathways with specific requirements for waste acceptance.

Until now, the radiological characterization at CERN was made on a case-by-case basis by means of gamma-measurements, semiempirical formulae and Monte Carlo simulations. Part of this study is devoted to a description of these techniques and to a short presentation of the CERN historic waste, pre-conditioning, storage facilities and waste management.

From the physical point of view, the induced radiactivity is the result of nuclear interactions. The Monte Carlo code FLUKA is chosen as the best tool to simulate nuclear interactions induced by high energy neutrons, pions and protons. The choice of this code is motivated by a careful study of the relevant nuclear models and the way they have been implemented on various codes.

The analytical prediction of the radionuclide inventory also requires the calculation of representative spectra. The machines which compose the CERN accelerator complex are presented with their beam energy and specificities. Special attention is paid to the beam loss-mechanisms, which are responsible for the presence of secondary-particle radiation fields.

Although the radioactive waste management is a necessary practice for virtually any nuclear facility, there are actually few laboratories which share the complexity of CERN. The study of the state of the art in radiological characterization is therefore limited to the cases of the JNRC Ispra and PSI.

The initial aim of this study was the establishment of one method for the characterization of radioactive waste at CERN. The complexity of the project actually suggested that several methods are needed to deal with the specific problems of each category of waste. In addition to the successful development and application of the fingerprint method, this study has lead to the definition of a number of short-term and long-term objectives.

9.2 Methods for radiological characterization

Radioactive waste which has uniform irradiation profile, particle spectrum and material composition can be characterized by the matrix method (cf. section 9.2.1). The matrix method has been initially conceived and developed by the PSI Institute. It is here presented for the first time with a complete mathematical formulation and with a clear statement of the limits of validity.

If the irradiation profile, the particle spectrum and the material composition are known but not uniform, the waste can be characterized with the fingerprint method (cf. section 9.2.2). In particular, the fingerprint method is most appropriate for components on the beam line (where the radiation field is strongly space dependent), as long as it is possible to extract a sample for the gamma-ray normalization.

If all the above parameters are not uniform - but known - and the item of waste is a *single-case*, it is not justified to invest time on the preliminary study required by the fingerprint method, beacuse such a study would serve for one item only. It is recommended to predict the induced radioactivity with direct Monte Carlo simulations.

Two alternative methods are here proposed for items of waste which fullfil at least one of the following conditions:

- they have been sorted on a material basis (they are mixed in terms of radiological history);

- they have unknown radiological history;
- they consists of small objects with different and uncertain material composition (e.g., electronic boards, neon lamps).

These items can be characterized by a gamma-spectroscopy measurement system if they are not too massive (<1 ton) and if the size is small enough to enter the detection chamber. The result of the gamma-spectroscopy measurement shall be completed by radiochemical analysis to quantify the presence of pure beta emitters. This method is particularly appropriate in case of unknown radiological history because the measurements do not require any prior knowledge about the waste. The second method is based on the Bayes theory. A tentative radionuclide inventory is first proposed, based on experience or preliminary calculations with FLUKA and the matrix method. The inventory is made more accurate by increasing the number of sample measurements and reducing the uncertainty on the input parameters. The statistical method is effective for mixed waste, as both the uncertainty on the input parameters and the variance of the activity distribution are taken into account for the radiological characterization.

9.2.1 The matrix method

The matrix method calculates the induced radioactivity from values of irradiation cycle, material composition, particle spectra and dose rate measurements under the assumption that these values are known, that the chemical composition and the activity distribution are fairly homogeneous over the item of waste and that the irradiation is continuous and constant. It can be applied to a large fraction of the CERN radioactive waste, namely the waste from present and future machines, the main components of the past machines and electronic devices.

The matrix method requires the calculation of all relevant cross-sections, which can be performed with the Monte Carlo code FLUKA, and the selection of representative materials and spectra. It uses the activation formula without any simplification and is therefore very precise. It separates the dependence on the material composition and the irradiation time. This separation allows investigating the impact of uncertainties on these parameters. It is not required to know the number of primary particles lost in the accelerator because the inventory can be normalized by a simple dose rate measurement.

For items of historic waste which have already been sorted on the basis of their material composition and which are therefore mixed in terms of irradiation time and location in the accelerator, this method cannot be applied.

9.2.2 The fingerprint method

The so-called fingerprint method is one of the methods for the radiological characterization presently under study at CERN and was applied for the first time on a set of irradiated targets from the ISOLDE facility.

Extensive Monte Carlo simulations allowed selecting categories of targets with similar mixtures of radioactive nuclides. The fingerprint of each category was calculated both with Monte Carlo and with gamma spectroscopy. Measurements and simulations were in good agreement and together could provide information on trace elements and difficult-to-detect nuclides.

Because of the well-known irradiation conditions and material composition it was relatively straightforward to apply the fingerprint methods to the ISOLDE targets. Thanks to the excess of information it was possible to validate the FLUKA predictions (particle transport, cross sections...) by comparing predictions and measurements. In a certain sense, part of the available information was used to characterize the targets and part of it to validate the characterization. In the future, this method can be applied to more complex cases for which the direct validation is, as a general rule, not possible and all the available information is needed for the characterization.

9.3 Project planning

The present study has covered all relevant aspects of material activation and allows defining the next steps and priorities in such a challenging project.

Classification of the waste

The historic waste presently stored at CERN must be classified in terms of availability of information, area in the machine where it has been activated, material composition, distance from the beam line, the way it has been conditioned, elimination pathway and radiological history. These criteria allow choosing the appropriate method for the radiological characterization: matrix, fingerprints, direct FLUKA simulations or full gamma-spectroscopy. Depending on the required accuracy, the uncertainty can be reduced with the Bayes method.

The classification of waste according on the method to be used is an important step towards the definition of priorities, inasmuch as the justification of the effort in implementing a method lies in the amount of waste which can be characterized with it.

Computer cluster

The calculation of representative spectra, the FLUKA simulations for direct prediction of induced radioactivity and, most of all, the calculation of cross-sections with Monte Carlo nuclear models require several months of CPU time. The Radiation Protection Group is now equipped with a new set of 7 Linux machines, including one machine which hosts the database for radiological characterization. This set of machines, which is also used for calculations of operational radiation protection, is being transformed in a beowulf cluster for optimization of resources.

Database

The calculation of induced radioactivity relies on a large number of input values. In order to reduce the risk of loss of information and redundacy, it is recommended to store the data in a database. A preliminary study has lead to the creation of a Postgresql database. The database can be accessed with Python scripts for the extraction, insertion and modification of values.

The implementation of a database is the first step towards a user-friendly system, where different users are entitled different privileges in the handling of data, including visualization and modification. All these operations, including the actual calculations, are performed with the programming language Python.

Activity limits

The required accuracy of the radionuclide inventory depends on the elimination pathway. France and Switzerland apply different activity limits for the classification of radioactive waste. These limits are implemented in the database for immediate comparison with the predicted inventory.

Cross-sections

The neutron cross-sections below 20 MeV are taken from the JEFF library. A program has been specifically written to analyze the data and convert the ENDF format into a standard format.

The Monte Carlo code FLUKA is used to calculate the neutron cross-sections from 20 MeV to 10 TeV, the pion and proton cross-sections from 1 MeV to 10 TeV, and the ion cross-sections.

Particle spectra

The representative spectra are calculated with the code FLUKA for pions, protons and neutrons. The number of spectra to be calculated is a compromise between accuracy and complexity. Only the spectra which differ considerably in terms of production rates are implemented in the method. The priority shall be given to the areas in the accelerator complex from which most of the historic waste comes (i.e., the SPS accelerator).

The representative spectra are inclued in the database, which should contain the date of the calculation and a reference to the full documentation of the simulations.

Impact of material composition

The material composition influences the radiological characterization in terms of material cross-sections and in terms of neutron moderation. The representative spectra are always calculated at equilibrium, i.e. the shape of the spectrum does not vary with space. A specific study is needed to assess the material thickness

required to reach the equilibrium spectrum in order to investigate the distribution of induced radioactivity in massive objects.

Selection of representative material compositions

On the basis of the production rate per element - to be calculated by folding representative spectra with cross-sections - the most important elements are selected. These elements can be divided into two major groups: those which are relevant in spallation reactions and those in neutron capture. A careful analysis of all possible reaction channels and a comparison with the activity limits determines the criteria for the required accuracy of material composition.

The representative materials are then implemented in the database.

Libraries for gamma-spectroscopy

The semi-automated identification of radioactive nuclides in gamma-spectroscopy is performed by means of user-defined libraries, which contain the gamma-rays of the expected nuclides. Failure to include a relevant nuclide or inclusion of irrelevant nuclides in the library might lead to wrong conclusions about the detected radionuclide inventory. It is important to create one library per category of waste after studying the dominant reaction channels (see above).

The libraries must be included in the database for the characterization and shall be accessible from the software Genie2000.

Time development

Due to the relatively long time-scale of the irradiation cycle, there is no need to solve the complete set of Bateman equations. It is recommended to consider cumulative cross-sections and calculate the time build-up with the simplified formulae presented in chapter 7.

Geometry factors

The normalization of the radionuclide inventory with the measurement of dose rate can be performed by means of a geometry factor, which expresses the gamma-attenuation properties of the item of waste. This dependence of this coefficient with size and material composition can be assessed with a general study, partially based on similar studies available in literature.

FLUKA can transport the secondary particles emitted during nuclei decay and estimate the energy deposited in the detector. In order to calculate the geometry factor for an arbitrary geometry and radionuclide inventory, a specifically-written routine must be created. This routine shall convert the list of nuclides with their activity into a source file which FLUKA can use for further transport in the geometry.

Probability distributions

As a general rule, the amount of trace elements and the irradiation conditions are not known exactly. The probability distribution of these parameters must be assigned by performing radiochemical analyses of samples and by studying the operation history of the machines.

The probability distributions are used in the matrix method for the calculation of the uncertainty of the predictions.

Inventory of radioactive waste

All the available information on the material composition and radiological history of radioactive waste is presently stored in the database ISRAM. An interface must be created to exchange information between ISRAM and the database for the characterization. The two databases are written with the language SPQL, which makes the interface technically easy to develop. Each item of waste must be assigned a representative spectrum and a representative material composition, as well as a probability distribution for trace elements and for the irradiation cycle.

Implementation of the matrix method

As soon as the points described above are finished, a Python [1] program can be written to perform the calculations. The program allows the user to select the machine area (i.e., the representative spectrum), the material composition, the probability distributions for trace elements and radiological history and the item of waste from ISRAM.

The predicted radionuclide inventory is stored in the Postgresql database and it is tranferred to ISRAM after validation.

Error propagation in the characterization

Among the requirements of the final repositories, there is an estimate of the error associated to the radiological characterization. The error can be calculated with extensive measurements of samples and by analytical calculations. In the latter case, the uncertainties in the input parameters are propagated through the matrix method with the standard rules of statistics. The errors can be further reduced with repeated measurements by means of the Bayes method.

Calculations of the fingerprints

The calculation of the fingerprints needs a preliminary study, which is specific to the family of waste to be characterized. This study is aimed at defining the classes and establishing the normalization factors and the choice of samples.

[1] Although any scripting language would be adequate, in the case of CERN it is recommended to use Python for compatibility with other analysis tools.

The number of families of waste to be studied is defined during the classification of waste (see above).

Choice of gamma-spectroscopy system

The choice of a system for full gamma-spectroscopy measurements depends on the amount and kind of candidate waste at CERN and on the requirements of operational radiation protection.

The installation of the detector shall comply with the requirements of waste traceability, namely to avoid mixing potentially radioactive material with conventional material. In addition, the detector must be installed in an area with sufficiently low radiation background. In the case of purchase and use for free-release, a quality assurance programme must be implemented to obtain the license from the Authorities.

9.4 Final considerations

With few remarkable exceptions, a complex problem cannot be solved but with a complex solution. In the case of characterization, the following *apparently* simple solution could be proposed: to make all predictions with the existing code FLUKA. In this case the complex task is left entirely to the user, who should find all the relevant information about the waste (which is simply unrealistic for historic waste) and perform one set of simulations per item of waste (which is unbearably expensive in terms of CPU and analysis time). Another simple solution is to base the characterization on measurements only. Here the complexity is transferred to the need of high technology, with the associated high costs and difficulties to assure a constant quality of measurement. As an alternative, it can be required that the solution is simple for the user: the characterization is done by using a user-friendly software and one single dose-rate measurement. In this case it is the development of the method which is extremely complex. Advanced mathematics, probability theory, feasibility studies and sophisticated nuclear models are required to justify all the decisions which are taken and hidden to the user, for whom the software is a blackbox. There is no such a thing as a simple method for both the user and the developer. The optimization lies in the equilibrium between the number of measurements to be performed, the effort in programming, the amount of waste to be charaterized per year, the CPU time for the simulations, the information needed about the waste, the budget constraints, the level of competence of the user and the accuracy of the predictions. It is with this philosophy in mind that the combined use of the methods here proposed is intended.

The activation formula can be calculated exactly if the input data are known exactly. As this is never the case, the input data shall be assigned a probability distribution, whose error propagation can then be calculated exactly. Very surprisingly, this basic concept has found very little application in radiological

characterization sofar and - to the knowledge of the author - is limited to a few pioneering studies in Germany. The introduction of this concept in the context of CERN is an original contribution.

The implementation of the matrix method implies a large effort for the calculation of the relevant cross-sections and the representative spectra. On the other hand, the same representative spectra can be used for operational radiation protection and the same cross-sections are useful for other laboratories. It is clear that this work can only be the result of a collaboration between members of the Radiation Protection Group at CERN and physicists from other laboratories.

In the so-called *standard* statistics it is assumed that there is no prior knowledge about the statistical variable. Its mean value and variance is estimated via a (possibly infinite) number of measurements. In the case of radioactive waste, the situation is rather the opposite. Experience suggests a prior probability distribution of the induced radioactivity, and the number of measurements available to confirm or modify this distribution is limited. It is interesting to note that until now the large majority of estimates of errors in characterization are calculated in the standard way - namely those provided by detectors and Monte Carlo simulations. The introduction of the Bayes method in this field opens the door to new possibilities of optimization.

It is common practice in radiation protection to adopt conservative values in case of uncertainty. In the case of radiological characterization, it is not obvious to decide which values are more or less conservative. For example, it is conservative to assume a larger content in terms of a trace element if the element leads to a long-lived radioactive nuclide. However, this is no longer valid if the same radioactive nuclide is the dominant gamma emitter on which the normalization is based. As a last example, the induced radioactivity decreases with increasing waiting time. Nevertheless, the *predicted* induced activity of long-lived nuclides is higher if the assumed waiting time is longer, as long as the normalization is based on a dose-rate measurement.

In the past years, the radioactive waste from CERN machines was pre-conditioned and sorted according to material composition. This sorting has the clear advantage of including in a waste package all material which has the same radioactive nuclides. However, in spite of the homogeneity in terms of kind of nuclides, this waste must be considered as mixed because the items may have a different radiological history. The consequence is that although the nuclides are the same, the relative presence of the nuclides is different. It is therefore not possible to predict one single fingeprint and perform a normalization measurements near the whole package. This situation has suggested the technique of the Bayes method and sample measurements.

The amount of radioactive waste Swizterland and France could expect to receive from CERN in the next century will depend on the efficiency of the free-release process, on the accuracy of the nuclear waste zoning and on the design choices of future accelerators. With this respect, it is clear that the understanding of activation mechanisms and the development of methods for the radiological

characterization play a dominant role. The present study represents a step further in this direction.

Appendix A

Comparison between two scintillators for gamma ray spectroscopy

The Radiation Protection Group at CERN is considering buying a new scintillator for gamma ray spectroscopy. The new detector should perform dose rate measurements and identification of radioactive nuclides. Among the most important requirements:

- data transfer to computer for analysis;
- quantitative analysis for a given source geometry;
- immediate identification of the main radioactive nuclides, without data transfer to computer;
- simple and intuitive usage;
- compact and easy to carry in confined areas;
- proved reliability and efficient after-sale service.

Two detectors have been tested in February 2007: the BNC 935 (Berkeley Nucleonics) and the Inspector1000 (Canberra). The technical specifications of the two detectors are given in table A.1.

The information is taken from the respective instructions and based on measurement performed on an accelerator component (namely a cavity from the machine LEP).

The plus points are highlighted in bold types. It goes without saying that such comparison is bound to be subjective and based on the needs of the group. Both the detectors fulfill the basic requirements, namely in terms of resolution, energy range, identification of the radioactive nuclides, data transfer onto a computer and intuitive use.

	BNC SAM935	INSPECTOR1000
Detector	3x3 NaI	1.5x1.5 LaBr3
Performance		
Resolution	7%	3.50%
Calibration	Int. Cs source	Ext. source,periodic
Technical aspects		
Probe connection	Fragile	Robust
Display	Monochrome	Touch-sensitive, polychrome
Connection to PC	RS 232	USB
Weight	5.8 kg	1 kg
Size	Cumbersome	Compact
Battery	8 hours	4-12 hours, depends on usage
Software		
In situ analysis	**Simple and fast**	Fast
Data processing	BNC software	Genie2000 and Windows
Quantitative analysis	Point sources only	Any geometry (Genie2000)
Library	128 radionuclides	Library from Genie2000
Usage		
Start of detector	1.5 minutes	3 minutes
Interface	Buttons	Buttons or display
Usage	**Intuitive**	Experience needed
Supplier	New to CERN	CANBERRA
Origin	USA	Europe
After-sale service	Acceptable	Satisfactory
Price of detector	15355 $	16000 euros
Price of software	1500 $	Installation of Genie2000

Table A.1: Direct comparison of Inspector1000 and BNC935

The BNC935 detector is designed for simple and intuitive use. On the one hand, the data analysis is fast and straightforward. On the other hand, the detector itself is cumbersome and relies on fragile connections. Moreover, the analysis of the measured spectra is only qualitative.

The Inspector1000 is compatible with the Windows environment and namely with the software Genie2000. This software allows quantitative analysis of the measured spectra, including the implementation of the source geometry and the usage of extensive libraries of gamma emitters. At CERN, the software Genie2000 is already used to analyze the data of the portable gamma-detector ISOCS (CANBERRA) and of a laboratory Ge detector. Therefore measurements with the three detectors can be easily compared and the analysis environment (e.g., library and geometry) can be shared. However, some experience is needed to fully exploit the functionality of the Inspector1000.

At CERN the main use of the detector would be related to the radiological characterization of radioactive material for elimination and shipping, qualitative measurement of potentially radioactive objects and the identification of unknown sources and samples. If the measurement environment is appropriate, it could be used for in-situ radiological characterization of stored material. The detector could also be used to localize lost sources, for measurements in case of emergency and for benchmark measurements in experiments. However, these uses are considered as exceptional. Concerning the requirements for the radiological characterization, priority was given to the compatibility with the software Genie2000 in order to benefit from the existing experience. Moreover, the usage of one software for analysis of all spectroscopy measurements allows reliable storage and management of the files, which is part of the quality assurance. The detector Inspector1000 is therefore considered as the most appropriate.

Among the weak points of the Inspector1000, it should be mentioned that its use requires a minimum of experience. However, this initial effort is negligible with respect to the competence required by any gamma spectroscopy measurement and it is justified by the wide range of functionalities. The probe LaBr3 is preferred to the one of NaI because of its better energy resolution, which is an asset for the identification of nuclides. In addition, the detector could be used for monitoring in high-level radiation environments because of the relatively little efficiency. This is of no hindrance for measurement of items with low-level activity, because the data capture time can be extended at will. Furthermore, the detector is very compact and can be used to characterize items which are out of reach of a Germanium detector.

The Inspector1000 with LaBr3 probe is on the market since Mai 2007.

Bibliography

[1] U. Amaldi. The importance of particle accelerators. In *Proceedings of the seventh European Particle Accelerator Conference, EPAC*, 2000.

[2] M. Hoefert and D.Forkel-Wirth. On the release of radioactive material produced at high-energy accelerators. In *Proceedings of the 10th congress of the IRPA*, page 317, May 2000.

[3] CERN. *Safety code 42, Radiation Protection*, 2006.

[4] V. Hedberg, M. Magistris, M.N. Morev, M. Silari, and Z. Zajacová. Radioactive waste study of the ATLAS detector. In *Proceedings of the Eight Meeting on Shielding Aspects of Accelerators, Targets and Irradiation Facilities (SATIF-8)*, Pohang, Republic of Korea, 22-24 May 2006.

[5] ASN. *Guide d'Elaboration des études déchets ind 2.* ASN, 2002. SD3-D-01.

[6] OECD Nuclear Energy Agency. *Removal of reglatory controls for materials and sites.* NEA, 2004. NEA/RWM/RF(2004)6.

[7] OECD Nuclear Energy Agency. *Regulatory and institutional framework for nuclear activities, France.* NEA, 2003. ISSN 1727-3854.

[8] Ordonnance du 22 juin 1994 sur la radioprotection (ORaP). http://www.suva.ch.

[9] IAEA. *Principles for the Exemption of Radiation Sources and Practices from Regulatory Control.* Number 89 in Safety. IAEA, 1988.

[10] OECD Nuclear Energy Agency. *Radioactivity Measurements at Regulatory Release Levels.* NEA, 2006. ISBN 92-64-02319-4.

[11] Ordonnance fédérale n. 76-65 concernant la protection contre les radiations. Switzerland, june 1976.

[12] OECD Nuclear Energy Agency. *Regulatory and institutional framework for nuclear activities, Switzerland.* NEA, 2003. ISSN 1727-3854.

[13] W. Heep. The ZWILAG plasma facility, technology for treating nuclear waste. In *Proceedings of KONTEC 2007, Conditioning of Radioactive Operational & Decommissioning Wastes*, Dresden, Germany, 2007.

[14] HSK. *Central interim storage facility, Wuerenlingen*, 2002. annual report.

[15] H. Hoefert. Categorization and treatment of solid material with low specific radioactivity from the high-energy accelerator environment. Technical note, CERN, 1998. CERN/TIS/RP/98-15.

[16] M. Magistris and Y. Algoet. Caractérisation radiologique du module lep entreposé en ISR7 à destination de l'INDE. Technical note sc-2006-055-rp-sn, CERN, 2006. EDMS 801680.

[17] M. Buckley and Z.K. Hillis. Summary of the workshop on the potential application of metal melting in the UK nuclear sector. Technical report, NNC, 2004. Report 11426/TR/002.

[18] S. V. Adamenko and V. I. Vysotskii. Laboratory collapse of electron-nuclear plasma and full-range nucleosynthesis of stable usual and superheavy nuclei. In *Frontiers of Nonlinear Physics*, pages 511–516, 2005.

[19] S. Myers. Rapport provisoire de surêté du SPS/CNGS et LHC, description succinte des installations environnantes dans l'etablissement d'accueil. Document d'exploitation, CERN, 2006. EDMS 684067, http://ab-dep-op-sps.web.cern.ch/ab-dep-op-sps/.

[20] H. Vincke and Graham R. Stevenson. Radiation levels in LHC points 2 and 8 due to beam dumping on the TEDs at the bottom of TI2 and TI8. Cern-tis-2003-013-rp-tn, CERN, 2003. EDMS 399784.

[21] L. Ulrici. General procedure for the establishment of the waste study for the LHC experiments. Technical note cern-sc-2005-085-rp-tn, CERN, 2005. EDMS 678189.

[22] CERN. *CAS - CERN Accelerator School: basic course on general accelerator physics*, Geneva, 2005. CERN. Selected contributions.

[23] G. Arduini. Cern, private communication.

[24] A.H. Sullivan. *A guide to radiation and radioactivity levels near high energy particle accelerators*. Nuclear Technology Publishing, 1992.

[25] D.M. Skyrme. The evaporation of neutrons from nuclei bombarded with high energy protons. *Nuclear Phys.*, 35:177, 1962.

[26] S. Roesler L. Ulrici M. Brugger, A. Ferrari and J. Vollaire. Calculation of radioactive isotope production cross-sections in fluka and their application to radiological studies. In *Shielding Aspects of Accelerators, Targets and Irradiation Facilities Eighth Meeting (SATIF-8)*, May 2008.

[27] A. Ferrari and P. R. Sala. Physics of showers induced by accelerator beams. In *"F. Joliot" Summer School in Reactor Physics*, volume 1, pages 1154–1159. CEA, August 1995.

[28] H. Sugita T. Ishikawa and T. Nakamura. Thermalisation of accelerator produced neutrons in concrete. *Health Physics*, 209(2)(60), 1991.

[29] J.W. Tuyn and C. Lamberet. Radioactive waste managament at CERN. Technical Note TIS/RP/TM/98-04, CERN, 1998.

[30] L. Ulrici and R. Menendez. Radioactive waste project - budget review 2007. Technical report, CERN, 2008. SC-2008-008-RP-SN, EMDS 893788.

[31] E. Neukaeter I. Auler, F. Helk and F. Zimmermann. *Messverfahren zum Nachweis der Unterschreitung niedriger Grenzwerte fuer grosse freizugebende Massen aus dem Kontrollbereich.* European Commission, 1991. EUR 13 438.

[32] M. Franz I. Auler, E. Neukater and B. Krebs. Release measurements for materials out of controlled areas. *Applied Radiation and Isotopes*, 53, 1-2:331–336, July 2000.

[33] Canberra Industries, inc, 800 Research Parkway, Meriden, CT 06450, US. *Genie2000 Spectroscopy System - Operations*, 2001.

[34] M. Magistris. Radiological considerations on multi-MW targets. Part II: after-heat and temperature distribution in packed Ta spheres. *NIM A*, 545:822–839, 2005.

[35] Y. Donjoux. Etalonnage et utilisation d'un détecteur de radiation microspec-2. Technical report, Ecole d'Ingénieurs de Genève, 1995. Diplome de Physique Nucléaire.

[36] F. Atchison. PWWMBS: a computer based book-keeping system for radioactive waste from the PSI-West accelerator complex. Technical report, PSI, 2001. AN-96-01-20.

[37] F. Atchison. Inventories for active-waste from accelerator facilities. Scientific and Technical Report 90, PSI, 2002. ISSN 1423-7650.

[38] F. Atchison and H. Schaal. *ORIHET3 - Version 1.1.* PSI, 2001. A guide for users.

[39] J. Blachot G. Audia, O. Bersillon and A.A. Wapstra. The nubase evaluation of nuclear and decay properties. *Nuclear Physics*, A624, 1997.

[40] F. Atchison. The PSIMECX medium-energy neutron activation cross-section library. Part I: Description and procedures for use. Technical Report 98-09, PSI, 1998. ISSN 1019-0643.

[41] F. Atchison. The PSIMECX medium-energy neutron activation cross-section library. Part II: Calculational methods for light to medium mass nuclei. Technical Report 98-10, PSI, 1998. ISSN 1019-0643.

[42] F. Atchison. The PSIMECX medium-energy neutron activation cross-section library. Part III: Calculational methods for heavy nuclei. Technical Report 98-11, PSI, 1998. ISSN 1019-0643.

[43] F. Atchison and J. Duvoisin. Copper activation in various neutron spectra, august 1994. Technical report, PSI, 1999. AN-96-99-55.

[44] J. Stepanek and C.E. Higgs. A general description of AARE: a modular system for advanced analysis or reactor engineering. In *Proceedings of the 1998 In. Reactor Physics Conf.*, Jackson Hole, Wyoming, 1988.

[45] F. Atchison. Spectra for use with PWWMBS to represent the 72 MeV regions of the PSI-West accelerator complex. Technical report, PSI, 2004. TM-85-04-03.

[46] F. Atchison. Parameters for classification and characterization of radioactive waste from the 72 MeV regions of the PSI-West accelerator complex. Technical report, PSI, 2004. TM-85-04-04.

[47] D. Schumann F. Atchison and R. Weinreich. Comparison of PWWMBS calculated inventories with sample analysis results. Technical report, PSI, 2004. TM-85-04-16.

[48] P. Feynman. *QED: The Strange Theory of Light and Matter.* Princeton University Press, 1988.

[49] R. Serber. Nuclear reactions at high energies. *Phys. Rev.*, 72:1114, 1947.

[50] M. Goldberger. The interaction of high energy neutrons and heavy nuclei. *Phys. Rev.*, 74:1269, 1948.

[51] V.S. Barashenkov et al. Intranuclear cascades with many-particle interactions. *Nuc. Phys. B*, 6:11–31, 2002.

[52] K. Chen et al. Vegas: A monte carlo simulation of intranuclear cascades. *Phys. Rev.*, 166:949, 1968.

[53] J.R. Glauber. Cross sections in deuterium at high energies. *Phys. Rev.*, 100:242, 1955.

[54] K. Zalewski. Hadron nucleus collisions at very high energies. *Ann. Rev. Nucl. Part. Sci.*, 55:55, 1985.

[55] A. Capella and A. Krzywicki. Theoretical model of soft hadron-nucleus collisions at high energies. *Phys. Rev. D*, 18(9):3357–3370, Nov 1978.

[56] E. Gadioli and P.E. Hodgson. *Pre-equilibrium Nuclear Reactions*, volume 168/1982. Springer Berlin / Heidelberg, 1982.

[57] A. Kerman H. Feshbach and S. Koonin. The statistical theory of multi-step compound and direct reactions. *Ann. Phys.*, 125/2:429–476, 1980.

[58] V. Weisskopf. Statistics and nuclear reactions. *Phys. Rev.*, 52(4):295–303, Aug 1937.

[59] V. Vandenbosh and J.R. Huizenga. *Nuclear Fission.* Academic Press / New York, 1984.

[60] E. Fermi. High energy nuclear events. *Progr. Theor. Phys.*, 5:570, 1950.

[61] A.S. Botvina and D.H.E. Gross. The effect of large angular momenta on multifragmentation of hot nuclei. *Nuclear Physics A*, 592/2:257–270, sept 1995.

[62] W G Lynch. Nuclear fragmentation in proton- and heavy-ion-induced reactions. *Annual Review of Nuclear and Particle Science*, 37:493–535, Dec 1987.

[63] L.G. Moretto and G.J. Wozniak. Multifragmentation in heavy-ion processes. *Annual Review of Nuclear and Particle Science*, 43:379–455, Dec 1993.

[64] M.W. Zemansky. *Heat and Thermodynamics.* McGraw-Hill Book Company / New York, 1951.

[65] U. Mosel. Fusion and fission of heavy nuclei. *Heavy Ion Collisions*, 2:275, 1980.

[66] A.S. Botvina et al. Statistical simulation of the break-up of highly excited nuclei. *Nuclear Physics A*, 475:663–686, Dec 1987.

[67] H. Haba et al. Recoil properties of radionuclides formed in photospallation reactions on complex nuclei at intermediate energies. In *Proceedings of the 2000 Symposium on Nuclear Data*, Tokai, Japan, Nov 2000.

[68] B. Hiller A.H Blin and A.A. Osipov. On the origin of the vector meson dominance. *Nuclear Physics A*, 589:660–668, 1995.

[69] L. Tiator and L.E. Wright. Delta resonance and nonlocal effects in pion photoproduction from nuclei. *Phys. Rev. C*, 30:989, Sep 1984.

[70] I. Pschorn. The gsi future project : an international accelerator facility for beams of ions and antiprotons. In *7th International Workshop on Accelerator Alignment (IWAA 2002), SPring-8*, Japan, Nov 2002.

[71] L.S. Pinsky et alt. Event generators for simulating heavy ion interactions to evaluate the radiation risks in spaceflight. In *Aerospace, 2005 IEEE Conference*, pages 731–736, Mar 2005.

[72] H. Stocker and W. Greiner. High energy heavy ion collisions–probing the equation of state of highly excited hardronic matter. *Physics Reports*, 137/5-6:277–392, May 1986.

[73] H. Stocker H. Sorge and W. Greiner. Poincare invariant hamiltonian dynamics: Modelling multi-hadronic interactions in a phase space approach. *Annals of Physics*, 192/2:266–306, Jun 1989.

[74] M. Cavinato et al. Monte carlo calculations of heavy ion cross-sections based on the boltzmann master equation theory. *Nuclear Physics A*, 679:753–764, 2001.

[75] L.G. Moretto and G.J. Wozniak. Multifragmentation in heavy-ion processes. *Annual Review of Nuclear and Particle Science*, 43:379–455, 1993.

[76] I. Dostrovsky, P. Rabinowitz, and R. Bivins. Monte carlo calculations of high-energy nuclear interactions. i. systematics of nuclear evaporation. *Phys. Rev.*, 111(6):1659–1676, Sep 1958.

[77] J. Ranft. Dual parton model at cosmic ray energies. *Phys. Rev. D*, 51(1):64–84, Jan 1995.

[78] A. Fassò, A. Ferrari, S. Roesler, P.R. Sala, G. Battistoni, F. Cerutti, E. Gadioli, M.V. Garzelli, F. Ballarini, A. Ottolenghi, A. Empl, and J. Ranft. The physics models of FLUKA: status and recent developments. In *Computing in High Energy and Nuclear Physics 2003 Conference (CHEP2003)*, La Jolla, CA, USA, march 2003.

[79] C.I. Tan A. Capella, U. Sukhatme and J. Tran Thanh Van. Dual parton model. *Physics Reports*, 236/4-5:225–329, Jan 1994.

[80] D.E. Cullen. Prepro 2007, 2007 endf/b pre-processing codes (endf/b-vii tested). Technical report, The Nuclear Data Section, International Atomic Energy Agency, P.O. Box 100, A-1400, Vienna, Austria, Mar 2007. IAEA-NDS-39.

[81] V.V. Kolesov and A.A. Lukyanov. Estimate of doppler broadening of resonances. *Atomic Energy*, 47/3:770–772, Sep 1979.

[82] A. Ferrari E. Cuccoli and G.C. Panini. A group library from jef 1.1 for flux calculations in the lhc machine detectors. Technical report, NEA, 1991. JEFDOC-340.

[83] Moscow Engineering Physics Institute (MEPhI) M. Morev. Private communication, 2007.

[84] G. van Rossum and F. L. Drake. *The Python Language Reference Manual (version 2.5)*, network theory limited; manual edition edition, Nov 2006.

[85] A. J. Koning, S. Hilaire, and M. C. Duijvestijn. TALYS: Comprehensive Nuclear Reaction Modeling. In *AIP Conf. Proc. 769: International Conference on Nuclear Data for Science and Technology*, pages 1154–1159, May 2005.

[86] T. Belgya, O. Bersillon, R. Capote, T. Fukahori, G. Zhigang, S. Goriely, M. Herman, A.V. Ignatyuk, S. Kailas, A. Koning, P. Oblozinsky, V. Plujko, and P. Young. *Handbook for calculations of nuclear reaction data, RIPL-2*. Number 1506 in IAEA-TECDOC. IAEA, 2006. http://www-nds.iaea.org/RIPL-2/.

[87] Tsao Silberberg and Barghouty. Updated partial cross-sections of proton-nucleus reactions. *Ap. J.*, 501, 1998.

[88] H.W. Bertini. Low-energy intranuclear cascade calculation. *Phys. Rev.*, 131/4:1801–1821, Aug 1963.

[89] H.W. Bertini. Reaction cross sections for 30- to 60-mev protons on various elements: Comparison of theoretical results with experiment. *Phys. Rev. C*, 5/6:2118–2119, Jun 1972.

[90] S G Mashnik and V D Toneev. *MODEX: the program for calculation of the energy spectra of particles emitted in the reactions of pre-equilibrium and equilibrium statistical decays*. Dubna, 1974. Communication JINR P4-8417.

[91] K.C. Chandler and T.W. Armstrong. Operating instructions for the high-energy nucleon/meson transport code, hetc. Technical report, Oak Ridge National Laboratory, 1972. ORNL-4744.

[92] S.G. Mashnik K.K. Gudima and V.D. Toneev. Cascade-exciton model of nuclear reactions. *Nucl. Phys. A*, 401/2:329, 1983.

[93] V.S. Barashenkov and V.D. Toneev. Interaction of high energy particle and nuclei with atomic nuclei. Technical report, Atomizdat, Moscow, 1972.

[94] R. E. Prael and M. Bozoian. Adaptation of the multistage pre-equilibrium model for the monte carlo method. Technical report, Los Alamos National Laboratory, Sep 1998. LA-UR-88-3238.

[95] G.A. Ososkov K.K. Gudima and V.D. Toneev. Sov. J. Nucl. Phys. 21 138, 1975.

[96] P. Oblozinsky and I. Ribansky. Emission rate of preformed [alpha] particles in preequilibrium decay. *Physics Letters B*, 74/1:6–8, Mar 1978.

[97] D.J. Brenner and R.E. Prael. Calculated differential secondary-particle production cross sections after nonelastic neutron interactions with carbon and oxygen between 10 and 60 mev. *Atomic and Nuclear Data Tables 41*, pages 71–130, 1989.

[98] J. Ranft and S. Ritter. Rapidity ratios, feynman-x distributions and forward-backward correlations in hadron-nucleus collisions in a dual monte-carlo multi-chain fragmentation model. *Zeitschrift für Physik C Particles and Fields*, 27/4:569–575, 1985.

[99] A. Ferrari G. Battistoni and P.R. Sala. The treatment of nuclear effects for neutrino interactions in the fluka code. *Acta Physica Polonica B*, 37/8, 2006.

[100] F. Ballarini et al. Nuclear models in fluka: present capapabilities, open problems and future improvements. In *AIP Conferene Proceedings*, volume 769, pages 1197–1202, 2005.

[101] R. Engel S. Roesler and J. Ranft. The monte carlo event generator dpmjet-iii. In *Conference Monte Carlo 2000*, Lisbon, Portugal, Oct 2000.

[102] A. Fassò, A. Ferrari, J. Ranft, and P.R. Sala. FLUKA: a multi-particle transport code. Technical note cern-2005-10, CERN, 2005.

[103] S. Roesler. Cern, private communication.

[104] J.W.N. Tuyn H. Hoefert and d. Forkel-Wirth. The decommissioning of accelerators: an exercise in the recycling of radioactive material. Technical note tis-rp/98-18, CERN, 1998.

[105] Th. Otto M. Magistris and L. Ulrici. Radiological characterization of targets from the ISOLDE facility at CERN. In *Proceedings of KONTEC 2007, Conditioning of Radioactive Operational & Decommissioning Wastes*, Dresden, Germany, 2007.

[106] F. Atchison. A revised calculational model for fission. Technical Report 98-12, PSI, 1998. ISSN 1019-0643.

[107] S. Teichmann, M. Wohlmuther, and J. Züllig. Charakterisierung und Klassifizierung radioaktiver Abfälle aus den Beschleunigeranlagen des PSI. In 37. Jahrestagung des Fachverbandes für Strahlenschutz e. V., editor, *Fortschritte im Strahlenschutz: Strahlenschutzaspekte bei der Entsorgung radioaktiver Stoffe*, Basel, Switzerland, 2005. ISSN 1013-4506, 192.

[108] A. Mitaroff and M. Silari. The CERN-EU high-energy reference field (CERF) facility for dosimetry at commercial flight altitudes and in space. *Radiation Protection Dosimetry*, 102:7–22, 2002.

[109] V. Vlachoudis and the FLUKA collaboration. Fluka: new features and a general overview. In *Shielding Aspects of Accelerators, Targets and Irradiation Facilities Eighth Meeting (SATIF-8)*, May 2008.

[110] National Council on Radiation Protection and Measurements. *Managing potentially radioactive scrap material*, ncrp report edition, 2002. 141.

[111] K. Weise. Bayesian-statistical decision threshold, detection limit and confidence interval in nuclear radiation measurement. *Kerntechnik*, 63:214–224, 1998.

[112] K. Weise et al. A bayesian theory of measurement uncertainty. *Meas. Sci. Technol.*, 4:1–11, 1993.

[113] Determination of the characteristic limits (decision threshold, detection limit and limits of the confidence interval) for measurements of ionizing radiation – fundamentals and application. ISO/DIS 11929, 2007.

[114] K. Weise et al. Bayesian decision threshold, detection limit and confidence limits in ionising-radiation measurement. *Radiation Protection Dosimetry*, 2006.

[115] M.G. Cox and P.M. HARRIS. Uncertainty evaluation. Best practice guide 6, National Physical Laboratory, Teddington, UK, 2004.

[116] C.F.Dietrich. *Uncertainty, Calibration and Probability.* Adam Hilger, Bristol, 1991.

Acknowledgements

I would like to express my profound gratitude to my supervisor Luisa Ulrici (CERN) for her amiable supervision and continuous encouragement during my studies.

This thesis has benefited from the experience and guidance of S. Teichmann, M. Wohlmuther and D. Kiselev (PSI), to whom I am deeply indebted.

I owe a particular debt of gratitude to H. Maxeiner and R. Sarrafian (NAGRA) for their precious guidelines; *from the horse's mouth*, one might say.

Special thanks to H. Huhtiniemi (JRC, Ispra) for stimulating discussions and for the material he placed to my disposal.

This thesis would not appear in its present form without the kind assistance and support of my Austrian supervisor H. Böck (TU Wien).
May he live long and famous in the nuclear world.